Copy
RM H57J30

NACA

RESEARCH MEMORANDUM

A SIMULATOR INVESTIGATION OF FACTORS AFFECTING THE DESIGN AND UTILIZATION OF A STICK PUSHER FOR THE PREVENTION OF AIRPLANE PITCH-UP

By Euclid C. Holleman and David L. Boslaugh

High-Speed Flight Station
Edwards, Calif.

NATIONAL ADVISORY COMMITTEE
FOR AERONAUTICS

WASHINGTON

January 22, 1958

NACA RM H57J30

NATIONAL ADVISORY COMMITTEE FOR AERONAUTICS

RESEARCH MEMORANDUM

A SIMULATOR INVESTIGATION OF FACTORS AFFECTING THE DESIGN AND UTILIZATION OF A STICK PUSHER FOR THE PREVENTION OF AIRPLANE PITCH-UP

By Euclid C. Holleman and David L. Boslaugh

SUMMARY

For some current supersonic airplane designs, performance or structural considerations might dictate the use of design features, such as a high horizontal tail, which are susceptible to pitch-up at high angle of attack. This paper presents the results of a simulator study of the factors affecting the design of a device, a stick pusher, for preventing a representative supersonic airplane from entering the pitch-up region. The effects of varying the stick-pusher-activation boundaries, sensing parameters, and magnitude of stick-pusher force on the controllability of the airplane pitch-up were investigated. In addition, the paper deals with the possible tactical importance of the loss in available supersonic maneuverability caused by angle-of-attack limiting in turns and in zoom maneuvers.

A 30-pound stick-pusher force provided positive restorative action and was preferred to a force of either 15 or 45 pounds. It was possible to make peak angle of attack following stick-pusher activation invariant with entry rate by using an activating boundary sensitive to pitching velocity as well as angle of attack. A moderate-authority pitch damper was found to be advantageous in several ways. It greatly reduced recovery transients following activation, decreased the possibility of bothersome multiactivations present in some conditions, and was beneficial when tracking near the stick-pusher boundary.

Considering such factors as speed loss and time-to-change heading, little loss in turn performance need be incurred by stick-pusher operation in the normal operating altitude range of the airplane. During zoom maneuvers to extreme altitudes, the requirements for flight-path correction could represent a condition in which a pilot would be at a tactical disadvantage with angle-of-attack limiting.

INTRODUCTION

Present design trends toward the use of low-aspect-ratio wings and large fuselages have produced undesirable flow fields over a large region of possible horizontal-tail locations. If at some angle of attack the horizontal tail enters into this region, longitudinal instability or pitch-up usually results. The use of a low horizontal tail, which is outside the undesirable flow field through most of the angle-of-attack range of the airplane, has been generally successful in eliminating pitch-up (refs. 1 and 2). However, for some designs, performance or structural consideration may dictate the horizontal-tail location. A high horizontal-tail configuration is susceptible to pitch-up at high angle of attack. To avoid this pitch-up two approaches may be considered: use of a device to stabilize the airplane in the pitch-up region, or use of an automatic device to prevent the airplane from entering this region.

This paper presents the results of a simulator study which evaluated the basic pitch-up problem of an assumed supersonic fighter configuration, including the effects of several linear and nonlinear pitch dampers. However, emphasis was placed on the investigation of factors affecting the design and utilization of a device (stick pusher) which, by automatically applying a sudden push force to the control stick, prevents the airplane from entering the pitch-up region.

The effects of varying the stick-pusher-activation boundaries and the values of the sensing parameters (pitching velocity and angle of attack), magnitude of stick-pusher force, and airplane damping on the controllability of the airplane pitch-up at supersonic speed were investigated.

A final section of the paper deals with the possible tactical importance of the loss in available supersonic maneuverability caused by the use of a stick pusher which limits angle of attack. This analysis considers turns and zoom maneuvers.

SYMBOLS

a_n	normal acceleration, g units
C_D	drag coefficient, Drag/qS
C_L	lift coefficient, Lift/qS

[redacted]

C_m pitching-moment coefficient, $\frac{\text{Pitching moment}}{qS\bar{c}}$

$C_{m_\alpha} = \frac{dC_m}{d\alpha}$

$C_{m_{\dot{\alpha}}} = \frac{dC_m}{d\,\frac{\dot{\alpha}\bar{c}}{2V}}$

$C_{m_{i_t}}$ longitudinal control effectiveness, dC_m/di_t

$C_{m_{\dot{\theta}}} = \frac{dC_m}{d\,\frac{\dot{\theta}\bar{c}}{2V}}$

$\bar{c}$ mean aerodynamic chord, ft

D total drag, lb

F stick force, lb

g acceleration due to gravity, ft/sec^2

h_p pressure altitude, ft

I_Y moment of inertia about airplane Y-axis, slug-ft^2

i_t total incidence of the stabilizer (pilot plus pitch damper), deg

i_{t_D} incidence of the stabilizer due to pitch damper, deg

K_D pitch-damper gain, $i_t/\dot{\theta}$, sec

l_t tail length, ft

M Mach number

m airplane mass, slugs

[redacted]

q	dynamic pressure, lb/sq ft
S	wing area, sq ft
s	Laplacian operator, 1/sec
T	thrust, lb
t	time, sec
t_{45}, t_{90}	time to change heading 45° and 90°, respectively
V	forward velocity, ft/sec
W	airplane weight, lb
α	angle of attack, deg
α^*	angle of attack of stick pusher activation, deg
γ	flight-path angle, deg
Δ	incremental change in a quantity
δ	control-stick deflection, deg
ζ	ratio of actual damping to critical damping
θ	pitch attitude angle, $\alpha + \gamma$, deg
$\dot{\theta}$	pitching velocity, deg/sec or radians/sec
$\dot{\theta}_{eff}$	effective pitching velocity, radians/sec
$\ddot{\theta}$	pitching acceleration, radians/sec^2
τ	washout circuit time constant, sec
φ	phase angle, deg
ψ	angle of yaw, deg
ω	frequency, radians/sec

Subscripts and abbreviations:

max	maximum

[redacted]

min	minimum
0	initial condition
1	second condition
(30-16)	Used to define the stick-pusher-activation boundary. The first number, 30, refers to the pitching velocity in degrees per second for activation at zero angle of attack. The last number, 16, refers to the angle of attack for activation at zero pitching velocity.

A dotted quantity indicates derivative with respect to time.

SIMULATIONS AND CALCULATIONS

Pitch-Up

Test-setup.- An analog computer coupled to a mockup of an airplane control stick by means of a torque servo was used to simulate the longitudinal control characteristics of a maneuvering supersonic fighter. A pilot "flew" the problem by visual reference to an oscilloscope presentation completing the closed-loop simulation.

The control stick, equipped with strain gages to record stick force, operated a torque servo and supplied inputs to the analog. For normal operation, measured stick deflection was converted to proportional stick-force signals by the analog. These signals were transformed into force by the torque servo. A stick-force gradient of 3 pounds per degree was used as a representative value for this investigation. For stick-pusher operation an additional signal from the analog was converted into an abrupt increment of force superimposed on the normal stick force. The stick pusher was activated by an electrical relay when flight variables computed by the analog exceeded predetermined values. The delay between stick-pusher-activation signal and application of the stick force was 0.07 second. The resulting control system was found to be very realistic by pilots who operated it. A schematic diagram describing the system is shown as figure 1(a). The frequency-response characteristics of the system (fig. 1(b)) are representative of current airplane control systems.

The airplane aerodynamics were represented by the following differential equations:

$$\dot{\alpha} = \dot{\theta} + \frac{g}{V} - \frac{g}{V}\frac{qS}{W}\left[C_L(\alpha) - \frac{\bar{c}}{l_t} C_{m_{i_t}}(\alpha)\Delta i_t\right]$$

[redacted]

$$\ddot{\theta} = \frac{qS\bar{c}}{I_Y}\left[\left(C_m(\alpha) + C_{m_{i_t}}(\alpha)\Delta i_t\right) + \frac{\bar{c}}{2V}\left(C_{m_{\dot{\theta}}}(\alpha)\dot{\theta} + C_{m_{\dot{\alpha}}}(\alpha)\dot{\alpha}\right)\right]$$

where

$$\frac{S}{W} = 0.0129$$

$$\frac{S\bar{c}}{I_Y} = 0.033$$

and

$$\frac{\bar{c}}{l_t} = 0.485$$

As indicated, C_m, C_L, $C_{m_{i_t}}$, $C_{m_{\dot{\theta}}}$, and $C_{m_{\dot{\alpha}}}$ were functions of angle of attack (fig. 2). This information was obtained either from unpublished wind-tunnel data or was theoretically estimated for the configuration under consideration. A simple pitch damper ($i_t/\dot{\theta} = K_D$) was assumed for many of the tests. The stabilizer deflection available to the pitch damper was limited to $\pm 1^\circ$ or $\pm 3^\circ$ and the pitch-damper gain K_D was 0.3 second. For some tests a nonlinear pitch damper was used having a gain of $0.3 + 2.5\alpha^2$, with the angle of attack expressed in radians. The stabilizer available to the nonlinear pitch damper was unlimited. For all tests the stabilizer rate was limited to ± 20 degrees per second.

Test procedure.- To obtain the best simulation consistent with simplicity, angle of attack was used as a flight reference for the pilot. A moving target on the oscilloscope was found to be a convenient reference. The target rate was varied from maneuver to maneuver and the pilot referenced his pull-up rate to that of the target. Pull-up maneuvers were made by flying the airplane angle of attack into the pitch-up region. As soon as pitch-up was recognized, by the increase in rate of change of angle of attack, corrective control was applied. The rate and magnitude of corrective control used was entirely at the discretion of the pilot and, as might be expected, varied with the severity of the pitch-up. This test procedure obviated the necessity of assuming and including pilot recognition and reaction time, as was done in the pitch-up investigation of references 3 and 4. For the investigation of the pusher variables the same general test procedure was followed, except that initiation of corrective control was automatic. For most of the stick-pusher firings the pilot attempted to return to the initial trim; however, some attempts were made to override the force of the stick pusher.

[redacted]

Although most of the data were obtained by research engineers, several test pilots (both civilian and military) who had flown current high-performance airplanes flew the problem and were favorably impressed with its realism.

Zoom-Up

Test setup.- Inasmuch as the zoom maneuver was relatively slow (generally 1 to 3 minutes) and short-period dynamics were not of primary interest in this investigation, it was believed that the control-system characteristics would have little, if any, effect on the results obtained. Consequently, a simple spring-restrained stick was used for flight control.

As in the pitch-up investigation, the analog computer solved the airplane aerodynamics which were represented in this instance by three degrees of freedom.

These equations of motion are:

$$\dot{V} = \frac{T}{m} \cos \alpha - g\left(\frac{qS}{W} C_D + \sin \gamma\right)$$

$$\dot{\gamma} = \frac{T}{mV} \sin \alpha + \frac{g}{V}\left(\frac{qS}{W} C_L - \cos \gamma\right)$$

$$\ddot{\theta} = \frac{qS\bar{c}}{I_Y}\left[\left(C_{m_\alpha} \Delta\alpha + C_{m_{i_t}} \Delta i_t\right) + \left(C_{m_{\dot{\theta}}} + C_{m_{\dot{\alpha}}}\right)\frac{\dot{\theta}\bar{c}}{2V}\right]$$

The inclusion of the forward-speed degree of freedom made certain simplifications necessary because of the limitations of the analog equipment. The programmed variables are shown as figure 3. Thrust was programmed as an analytical function of Mach number and altitude and was representative of that produced by a current high-pressure-ratio variable-nozzle turbojet engine with afterburner. Afterburner thrust was assumed to be 40 percent of maximum thrust and was cut off at 65,000 feet during the maneuver. Lift and drag coefficients were obtained from the unpublished wind-tunnel data previously mentioned and were functions of Mach number and angle of attack. The control effectiveness and damping-in-pitch derivatives were functions of Mach number only; the contribution of $C_{m_{\dot{\alpha}}}$ to the longitudinal damping was

[redacted]

combined with $C_{m_{\dot{\theta}}}$. Airplane pitching-moment coefficient varied linearly with angle of attack but was invariant with Mach number, and an ideal moderate-authority pitch damper was used for most tests. Airplane weight decreased as fuel was consumed during the maneuver.

Test procedure.- The simulation of supersonic zoom-up was also piloted. Normal acceleration, Mach number, and pitch angle were used as flight references for the pilot, and zoom profiles of altitude versus range could be observed as a secondary flight reference. This latter reference was not too useful because of the time lag between control input and detectable airplane response.

The zoom maneuver was begun at $M = 2.0$ and an altitude of 50,000 feet. From horizontal flight, zoom entry was made at constant normal acceleration until the desired pitch angle was attained. Constant pitch angle was then flown until round-out was initiated. Round-out was made at constant normal acceleration, and level flight at maximum altitude terminated the maneuver. It was possible for the problem speed to drop below $M = 1.0$, but it was impractical to include the large variation in airplane derivatives which occurred below that speed. Thus, at speeds below $M = 1.0$ the solution was not completely accurate, but it was considered useful in giving orders of magnitude.

Turn Calculations

The turning performance of the airplane under consideration was calculated assuming that the airplane center of gravity moved in a horizontal plane and the airplane instantaneously banked to the proper angle for a balanced turn. Calculations were made for turns at constant angle of attack; consequently, normal acceleration decreased as speed decreased during the maneuver. Maximum thrust was used to minimize the speed loss. The time-to-change heading in the turn was calculated by using

$$\frac{dt}{d\psi} = \frac{971}{57.3g} \frac{M}{\sqrt{(a_n)^2 - 1}}$$

and the speed loss in the turn was calculated by using the relationship

$$\frac{dM}{dt} = \frac{T - D}{m} \frac{1}{971}$$

Step-by-step integration was performed by using Simpson's rule.

[redacted]

PRESENTATION OF RESULTS

DISCUSSION

Controllability of Supersonic Pitch-Up

Basic airplane maneuvers.- Basic airplane maneuvers were made at various rates of pull-up to determine the controllability of the configuration without pitch damper. Representative time histories are shown in figure 4(a) for the flight condition $M = 1.2$, $h_p = 50{,}000$ feet. At low pull-up rate the airplane pitched about 3° in angle of attack and reached an angle of attack of 20° after corrective control was applied by the pilot. At higher rates, however, the airplane reached a peak angle of attack of about 28° after pitching 8°. In attempting to arrest the pitch-up, it was impossible to avoid large undershoots in angle of attack (fig. 4 or 6) during recovery, inasmuch as the basic configuration was lightly damped at this flight condition ($\zeta \approx 0.1$). It is apparent from these maneuvers and from the data of figure 6 that the pitch-up would be uncontrollable. This is particularly true when it is considered that lateral divergence and roll-off would be probable in flight during many of the maneuvers simulated.

Representative time histories for a slightly higher Mach number, $M = 1.4$, are shown in figure 4(b). At low pull-up rates it was possible to recognize and control the pitch-up, but it is doubtful that the pilot could do so if he were preoccupied with any other task. However, at higher entry rates the pitch-up is entirely uncontrollable (figs. 4(b)

[redacted]

and 6(b)). This is the result of the pitching-moment curve not retrimming at high angles of attack (compare C_m for $M = 1.2$ (curve A) and 1.4, fig. 2(b)). Failure to control the pitch-up resulted in extreme angle-of-attack excursions (fig. 6(b)).

Similar tests were made also for an altitude of 40,000 feet. The results indicated, and the pilot concurred, that the pitch-up characteristics were not appreciably affected by the change in altitude.

Linear pitch damper.- Any means of slowing the rate of divergence should aid the pilot materially in controlling pitch-up. Consequently, additional pitch damping was investigated as a means of alleviating the pitch-up. The simple pitch damper previously described was used with a gain of $K_D = 0.3$ second. This provided damping ratios near 0.6 in the linear regime. Calculations were made for pitch damper authority of $\pm 1^\circ$ and of $\pm 3^\circ$. Regardless of authority, neither linear pitch damper proved to be effective in limiting the peak overshoots in angle of attack (figs. 5 and 6). However, the moderate-authority pitch damper ($\pm 3^\circ$) was found to be beneficial in flying below pitch-up and was appreciated by the pilot. In addition, the excursions during the violent recovery transients following pitch-up were quickly damped.

Nonlinear pitch damper.- Because the airplane became unstable in pitch at high angles of attack, it was thought that programming pitch-damper gain as a function of angle of attack might be effective in controlling the airplane pitch-up. A pitch-damper gain of $0.3 + 2.5\alpha^2$ was used with unlimited stabilizer authority. By using a pitch damper of this type at a Mach number of 1.2 and an altitude of 50,000 feet (fig. 7), steady flight was possible in the pitch-up region. Comparison with figure 5(a), for example, shows that for the same entry rate there is no apparent pitch-up with the nonlinear damper, while pitch-up is evident with the linear damper. The nonlinear pitch damper was also tested at the same flight condition with a pitching-moment curve (curve B of fig. 2(b)) which does not retrim. For this condition, also, no developed pitch-up was observed (fig. 7(b)).

Disadvantages for such a pitch damper are immediately apparent. Almost unlimited stabilizer authority would be required by the damper, creating a potentially dangerous condition in the event of a malfunction of the pitch damper.

The airplane maneuverability would be limited by stick control limits, and an increase in stick-force gradient which was evident for the limited-authority damper was even more in evidence for this damper. Moreover, for complete protection against pitch-up a stick pusher might be required in conjunction with the nonlinear pitch damper to prevent

the airplane from reaching an extreme angle of attack where stabilizer control would be incapable of overpowering the combination of unstable pitching moment and airplane momentum.

Considerations in the Design of a Stick-Pusher System

Another means of coping with an intolerable pitch-up of the type under consideration is to prevent the pilot from entering the pitch-up region. This might be accomplished by using a device which automatically applies an abrupt push force to the stick when critical flight variables are exceeded. Such a device, sometimes referred to as a stick pusher, is being used currently on several airplanes. A number of design parameters which influence the design of such a system are considered in the following discussion.

Desired force.- The force of the stick pusher must be capable of preventing the airplane from entering the pitch-up region. With the simulator used in this investigation it was possible to vary the stick-pusher force so that a magnitude could be obtained that was considered acceptable by the pilots. Time histories ($M = 1.2$, $h_p = 50{,}000$ ft without pitch damper) during which the pilot was neither attempting to assist nor override the stick pusher are presented in figure 8. Pull-ups were made with stick-pusher forces of three magnitudes. The lightest force tested, 15 pounds (fig. 8(a)), was considered adequate, but inadvertent overriding by the pilot was possible. The 30-pound stick-pusher force (fig. 8(b)) provided very positive and decisive action for preventing pitch-up. The 45-pound stick-pusher force was generally considered too high by the pilots and could result in violent undershoot maneuvers (fig. 8(c)) should the pilot be taken by surprise. During some maneuvers when the pilot is engrossed in accomplishing a task, he may unintentionally or deliberately override the stick pusher. A series of runs was made in which the pilot deliberately attempted to override the stick pusher at various force levels (fig. 9). The pilot was able to override only the 15-pound stick-pusher force. Again, the highest stick-pusher force resulted in very high stabilizer rates and violent recovery transients.

Summaries of maneuvers using the normal pull-up technique showing the effect of pitch-damping augmentation are presented in figure 10. Although the lowest stick-pusher force was overridden occasionally without pitch damping, the increased controllability of the airplane with pitch damper eliminated the tendency to override the stick pusher. Transients following the stick-pusher activation were decreased also with increased pitch damping. Without pitch damper the undershoots

increased by about 2° with each additional 15-pound increase in stick-pusher force. Little improvement in airplane handling or angle-of-attack excursions was noted with the low-authority pitch damper, but with the moderate-authority pitch damper undershoots were about the same for all three stick-pusher forces.

It was the opinion of all the pilots who "flew" the simulator that the 15-pound force was too light, even with pitch-damper augmentation. The 45-pound force was considered too high, but might be acceptable only with a moderate-authority pitch damper. Of the three stick-pusher forces, the 30-pound force was considered best, and for all subsequent tests the 30-pound stick-pusher force was used.

Overshoots following stick-pusher activation.- Another important consideration in the design of a stick-pusher system is the determination of the factors affecting the required activation point. Excursions in angle of attack for several test conditions and for typical pitching-moment variations were determined for various rates of pull-up and for angles of attack of various stick-pusher activations. A moderate-authority pitch damper was used. These results are summarized in figures 11(a) to 11(d). In each figure the peak angles of attack obtained for the various rates of pull-up are shown, as well as the pitching-moment curves used.

For a Mach number of 1.2 and an altitude of 50,000 feet (fig. 11(a)) stick-pusher activation for low rates of pull-up could be delayed safely to an angle of attack of 15° without excessive excursions in angle of attack. At this angle of attack the airplane is unstable, but the stick pusher can prevent fully developed pitch-up at low entry rates. However, at high entry rates stick-pusher activation must occur by $\alpha = 12°$ if the peak angle of attack is to be limited to 15°. Reducing the altitude to 40,000 feet (fig. 11(b)), slightly decreased the angle-of-attack excursions for all entry rates. The effects of change in C_m characteristics are shown by comparing figures 11(a) and 11(c). The C_m curve used in figure 11(c) had a more gradual transition to instability, but approximately the same initial slope as that used in figure 11(a). For high entry rates α excursions for the two C_m curves were comparable. However, at low pull-up rates to limit the excursion angle to 1°, activation must occur by 14° for the pitching-moment curve with the sharper break (fig. 11(a)), but could be delayed to 17° for the pitching-moment curve of figure 11(c). For a pitching-moment curve with a still more gradual decrease in stability at a slightly higher Mach number (fig. 11(d)), the excursions in angle of attack were greatly reduced throughout the rate of pull-up and angle-of-attack range investigated.

[redacted]

Factors such as control effectiveness, available control rate, and inertia characteristics can greatly influence the overshoot following stick-pusher activation. For the configurations and flight conditions considered, however, it would appear that stick-pusher activation where neutral stability is first encountered would limit overshoot to a relatively small value at low entry rates, but activation considerably below neutral stability might be required at higher entry rates.

Determination of a suitable activation boundary.- As was shown in the previous section, the stick-pusher-activation boundary should be sensitive to entry rate as well as angle of attack. For the present investigation pitching velocity was selected to represent entry rate. From a consideration of the angle-of-attack overshoots, shown in figure 11, it was decided to investigate the combined ($\dot{\theta}$ - α) boundaries[1] shown in figure 12.

A summary of the α excursions obtained for the various boundaries at two flight conditions is presented as figure 13. As would be expected, the higher the activation boundary used, the higher the available normal acceleration and the greater the peak α excursion obtained. Inspection of figure 13 also shows that peak angle of attack was approximately invariant at low and moderate entry rates at the higher boundaries. When using the lowest boundary, activation at needlessly low angle of attack caused overcompensation for entry rate which produced a substantial loss in available maneuverability. Increasing the boundary from (30-16) to (60-16), increased the angle of attack for pusher activation by about 2° at low rates and substantially more at the higher pull-up rates.

As has been discussed, a pitch damper improved the general controllability and reduced the undershoot following stick-pusher activation. However, the pitch damper had no noticeable effect on peak overshoot (figs. 13(a) and (c)).

Some phenomena which occurred during the tests are worthy of note. For low-boundary, low-damping conditions multiactivations of the stick pusher occurred. These repeated stick-pusher "kicks" caused a divergent oscillation which was disconcerting to the pilot while attempting to return to level flight following stick-pusher activation. The addition of pitch damping and the raising of the activation boundary tended to eliminate this phenomenon by quickly damping the airplane motions so that stick-pusher activation occurred only during the pull-up, not during the recovery transient.

---

[1]When the combined signals representing $\dot{\theta}$ and α exceed a boundary value, the stick pusher is activated and remains in operation until the sum of the parameters decreases below the specified boundary.

For some of the tests a buzzer was used to warn the pilot of impending stick-pusher activation. With the buzzer set approximately 1° to 2° below the stick-pusher boundary and with the moderate-authority pitch damper, stick-pusher activation could be avoided at all pull-up rates by terminating the pull-up maneuver at the buzzer signal. However, pull-up without the pitch damper often resulted in stick-pusher activation even though the pilot made every effort after hearing the buzzer to recover without stick-pusher activation.

Attempts at tracking were made just below the stick-pusher boundary (fig. 14). Without the pitch damper, stick-pusher activation resulted in a large attitude change following activation and required breaking off the tracking maneuver; but, with the pitch damper, tracking could be continued except for a momentary disturbance during activation.

Use of a washout circuit.- One disadvantage of using pitching velocity to compensate for entry rate effects is that a substantial portion of the $\dot{\theta}$ stick-pusher-activation signal can be present at $\dot{a}_n = 0$. This may unnecessarily compromise the maneuverability of the airplane unless the additional complexity of Mach number and altitude compensation is introduced. To circumvent this problem a simple resistance-capacitance circuit, sometimes referred to as a washout circuit, can be used (ref. 5). The effect of the washout circuit on the pitch-rate signal can be described in operational notation as

$$\frac{\dot{\theta}_{eff}}{\dot{\theta}} = \frac{\tau s}{1 + \tau s}$$

where $\dot{\theta}$ is the airplane pitching velocity, or input quantity, and $\dot{\theta}_{eff}$ is effective pitching velocity or output to the stick pusher.

It can be shown that at frequencies greater than $1/\tau$ the transfer function approaches unity, but $\dot{\theta}$ signals at low frequencies would be attenuated. Thus $\dot{\theta}_{eff}$ would be relatively large at high $\dot{a}_n$, but would be essentially zero in flight conditions producing steady pitching velocity.

To investigate experimentally the effects of a washout circuit, a series of pull-up maneuvers was made in which systematic variations in washout constant τ were studied at several flight conditions. A typical time history showing the effects of decreasing the value of τ from 5 seconds to 1 second is presented in figure 15 and a summary of the results obtained for the flight condition of $M = 1.4$, $h_p = 40{,}000$ feet is shown in figure 16. In the latter figure, activation points are shown for four values of washout constant at each of three basic boundary conditions. The overshoots were generally small; therefore, to simplify

the summary plot this information is included only for the highest activation condition ($\tau = 0.5$ sec). The results of figure 16 indicate that use of a washout circuit raised the activation boundary by an amount dependent on τ and the $(\dot{\theta} - \alpha)$ boundary. It is evident that the use of a value of $\tau \leqq 1.0$ second raises the activation point to nearly 16° for all cases at low entry rate. Moreover, the slope of the activation boundary with $\dot{a}_n$ can still provide a nearly constant α_{max}.

It is true that the activation point for $\tau = \infty$ (fig. 16) could be raised by using an α intercept greater than 16°. This, however, would result in intolerable overshoot in conditions of 1g flight or low dynamic pressure (fig. 2).

In a practical configuration the activation point would be dependent on the allowable α_{max}. Once the activation point is selected, the desired τ for any $(\dot{\theta} - \alpha)$ boundary can be obtained from simulator studies or by the analytical method of the appendix.

Importance of Restricted Supersonic Maneuverability

It appears that with a stick pusher to prevent entry into the pitch-up region there may be a considerable loss in available maneuverability. Therefore, determining the importance of the development of high lift at supersonic speeds is of interest. If the speed loss associated with the high lift is great, flight in this part of the flight envelope may not be profitable. Yet, to accomplish a mission the utilization of all possible lift may be mandatory. Several tactical situations that might require high-lift maneuverability have been examined and the results included herein.

Turn performance.- The pitching-moment characteristics for the assumed configuration are shown in figure 17 over a rather wide speed range. Based on the analysis of a preceding section, it would appear that stick-pusher activation of about 14° for very low entry-rate maneuvers would satisfactorily prevent pitch-up over the entire speed range. An indication of the loss in maneuverability resulting from such an activation boundary which is invariant with Mach number is presented in figure 18 for two test altitudes. The load factor attainable at $\alpha = 20°$ is presented for reference purposes. At $M = 0.90$ the results indicate very little loss in usable load factor. This is particularly true when it is considered that $\alpha = 14°$ could probably be well into the heavy buffet region. At supersonic speeds where no buffet would be expected, there are indications of significant reductions in maneuverability particularly at $h_p = 50{,}000$ feet. It should be remembered that the results of figure 18 assume zero entry rate, and, therefore, additional losses in available load factor would occur at finite entry rate

[redacted]

and from the pilot's heed of a warning device. It is also evident from figure 18 that it would be necessary for a pilot to maintain constant angle of attack as the speed bleeds off in order to realize maximum maneuverability. If constant g turns were attempted in tight maneuvers, avoiding stick-pusher activation would be impossible.

An important factor that in many instances could determine the usable high-lift maneuverability is the speed loss during an elevated g turn. The results of some simplified calculations relating speed loss and time-to-change heading to normal acceleration and angle of attack are presented in figure 19. In these calculations the angle of attack was held constant at the initial value as the speed decreased, and maximum thrust (fig. 3) was used to minimize speed loss.

Turns initiated at 2g and an altitude of 40,000 feet result in very little loss in speed but require 40 to 50 seconds for a heading change of 90° (fig. 19(a)). As the initial g is increased to 4, the time-to-change heading is decreased more than 50 percent, but an appreciable speed loss is evident. Further increase in initial g to 6 only slightly reduced the time for completion of the turn; however, the speed loss becomes very large. An optimum initial load factor for the conditions under consideration would appear to be of the order of 4g. Similar trends are shown for the 45° heading change. Time-to-turn is a function of g-level, and, therefore, only small effects of altitude are apparent. The speed losses, however, are markedly greater at an altitude of 50,000 feet for comparable turns. The results of figure 19 clearly indicate that an angle-of-attack restriction of 14° would impose little practical penalty in turn performance.

The time to regain speed following a maneuver may also dictate the usable high lift. If the time to accelerate were long, the avoidance of high g turns that result in large losses in speed might be necessary. The calculated time to regain initial Mach numbers of 1.4 and 1.8 for altitudes of 50,000 and 40,000 feet in 1g flight is shown in figure 20; the excess thrust for the airplane considered in this investigation is also shown. It is evident that, because of the limited endurance of this type of aircraft, the extremely long time interval required to regain speed at an altitude of 50,000 feet might further limit the usable load factor at this altitude.

Zoom performance.- Supersonic airplanes may attain altitudes greatly above their normal service ceilings by the simple expedient of converting kinetic energy to potential energy; however, it is not the intent of this paper to explore in detail the tactical uses of the zoom-up maneuver. In certain operations minimum time and horizontal range to extreme altitude might be of utmost importance, whereas in other situations maximum altitude or maximum horizontal range might be desired. A brief analog

investigation has been conducted to determine whether the stick pusher, by limiting angle of attack, would limit the zoom capabilities of the airplane.

From an initial flight condition of $M = 2.0$, $h_p = 50{,}000$ feet, zoom maneuvers to pitch angles of 10° to 50° were made at entry normal acceleration of from 1.5g to 4.0g. Round-out was made at constant normal acceleration (approximately 0.4g) such that maximum altitude was generally attained at about $M = 1.0$.

The effects of pitch-damper augmentation on the response characteristics in typical zooms are shown in figures 21(a) and 21(b). The difficulty in precisely controlling the airplane in the basic condition was quite apparent to the pilot, and most of the maneuvers were made with augmented damping.

Several significant quantities obtained from the zoom records are summarized in figure 22. Maximum angle of attack is presented as a function of entry normal acceleration for a range of pitch angles. The peak altitude and horizontal distance covered from initiation of zoom to attainment of maximum altitude are also presented and have been experimentally corrected to $M = 1.0$ in those instances where $M = 1.0$ and peak altitude were not coincident.

It is evident from the results of figure 22 that $\alpha = 14^\circ$ was exceeded only in steep zooms at low entry rate. For flat zooms the peak angle of attack was a linear function of entry normal acceleration. However, as the zoom becomes steeper, peak angle of attack is relatively large at both very low and high entry normal acceleration with a minimum occurring at about 2.4g. This latter effect is illustrated in figures 23 and 24 for a zoom angle of 50°. At the two higher entry rates, peak angle of attack is attained at the time the desired zoom angle is reached. For $a_n = 1.5$, however, the pilot believed that it would be necessary to initiate recovery prior to attainment of the specified zoom angle if he continued to pull up at the same rate. Therefore, to reach the desired zoom angle additional up-stabilizer was applied at $t = 55$ seconds. Because of the extreme altitude, the increase in normal acceleration was limited, and the desired pitch attitude angle was reached by a combined zoom and snap-up technique. This possible need for flight-path correction at very high altitude represents one flight condition where angle of attack in excess of that afforded with an operating stick pusher might be required. Turn maneuvers at extreme altitude might represent another condition in which a pilot would be at a tactical disadvantage from angle-of-attack limiting.

As a matter of interest, some general observations regarding zooms are included. It is apparent from figure 22 that if maximum horizontal

[redacted]

range is desired, a very low zoom angle combined with low entry normal acceleration would be used; whereas, if maximum altitude is desired, a zoom angle of approximately 30° would be flown, using about a 2g entry. Peak altitudes slightly in excess of 80,000 feet were reached in the latter conditions.

A comparison of the actual altitude attained for several flight conditions with calculations assuming ideal conversion of kinetic to potential energy with zero drag is shown in figure 25. A considerable loss in altitude capability due to drag is evident. Note that the experimental conversion of kinetic to potential energy slightly exceeds the ideal at the lower zoom altitudes, which is attributable to a condition of excess thrust.

The time required to pass through 70,000 feet, together with an indication of the speed loss at this altitude, is summarized in figure 26 for the zooms of figure 22. The data indicate that a zoom angle of about 30° with entry $g = 2.5$ would be optimum from considerations of minimizing the time to zoom to 70,000 feet and the loss in speed.

CONCLUSIONS

A simulator investigation has been undertaken to study the factors affecting the design of a stick-pusher system. This device was used to prevent a representative airplane configuration from experiencing uncontrollable pitch-up at high angles of attack. The results of the investigation, which dealt with basic design parameters of the stick pusher and the possible tactical importance of the loss in available supersonic maneuverability caused by angle-of-attack limiting, indicated that:

1. A 30-pound force provided very positive restorative action for the stick pusher. A 15-pound force was generally considered to be too light and could at times be overridden; whereas, a 45-pound force was generally considered too high, often resulting in violent transients.

2. At low entry rates stick-pusher activation when neutral stability was first encountered limited the angle-of-attack overshoot to a relatively small value, but at higher entry rates considerably earlier activation may be required to avoid large overshoots.

3. It was possible to make peak angle of attack following stick-pusher activation invariant with entry rate by using an activation boundary sensitive to pitching velocity as well as angle of attack.

[redacted]

4. A moderate-authority pitch damper was found to be advantageous in numerous ways when used in conjunction with a stick pusher. It greatly reduced recovery transients following activation, decreased the possibility of bothersome multiactivations present in some conditions, and was very beneficial when tracking near the stick-pusher boundary.

5. The pilots believed that a warning device set to activate slightly before pusher activation was a highly desirable feature. The warning device was more effective when used in conjunction with a pitch damper.

6. A pitch-rate washout circuit was found to be beneficial in reducing the loss in high-lift maneuverability that would result from stick-pusher operation.

7. Little loss in turn performance was incurred by stick-pusher operation in the normal operating altitude range of the airplane, considering such factors as speed loss and time-to-change heading.

8. During zoom maneuvers to very high altitudes, the requirements for flight-path correction could represent a condition in which a pilot would be at a tactical disadvantage with angle-of-attack limiting.

High-Speed Flight Station,
National Advisory Committee for Aeronautics,
Edwards, Calif., October 9, 1957.

[redacted]

APPENDIX

THEORETICAL EFFECTS OF WASHOUT CONSTANT τ ON STICK-PUSHER ACTIVATION BOUNDARY

The effects of τ on the activation of a $(\dot{\theta} - \alpha)$ sensitive stick pusher can easily be calculated theoretically. In operational notation, the ratio of effective pitching velocity to actual airplane pitching velocity can be expressed as

$$\frac{\dot{\theta}_{eff}}{\dot{\theta}} = \frac{\tau s}{1 + \tau s} \tag{1}$$

If a linear lift-curve slope is assumed during the pull-up maneuver, the assumption of constant $\dot{a}_n$ will produce a linear increase in $\dot{\theta}$ with time. For such a ramp $\dot{\theta}$ input, Laplace transform methods can be applied to equation (1) to obtain a time dependent ratio

$$\frac{\dot{\theta}_{eff}}{\dot{\theta}} = \frac{1 - e^{-t/\tau}}{t/\tau} \tag{2}$$

A plot of equation (2) is presented in figure 27, and the means by which these results can be used to calculate the effect of τ on a representative activation boundary at $M = 1.4$, $h_p = 40{,}000$ feet is illustrated.

Assume that constant $\dot{a}_n$ pull-ups are initiated from 1g flight with given values of τ and $\Delta\alpha$. If the substitution

$$t = \Delta\alpha \frac{da_n}{d\alpha} \frac{1}{\dot{a}_n} \tag{3}$$

is made in equation (2), the results shown in figure 28 are readily obtainable. The information of figure 28 can be converted easily into the form of figure 29 at selected values of α^* by using the relationship

$$\dot{\theta}_{eff} = \left(\frac{\dot{\theta}_{eff}}{\dot{\theta}}\right)\left[\frac{(a_n - 1)g}{V} \frac{d\alpha}{da_n} \dot{a}_n\right] \tag{4}$$

The final boundary in the form of figure 30 is then obtained by cross-plotting figure 29. In figure 30 the experimental results of figure 16 have been included for comparison with the theoretical calculations, and it is apparent that good agreement exists.

[redacted]

REFERENCES

1. Weil, Joseph, and Gray, W. H.: Recent Design Studies Directed Toward Elimination of Pitch-Up. NACA RM L53I23c, 1953.

2. Foster, Gerald V., and Griner, Roland F.: A Study of Several Factors Affecting the Stability Contributed by a Horizontal Tail at Various Vertical Positions on a Sweptback-Wing Airplane Model. NACA TN 3848, 1956. (Supersedes NACA RM L9H19.)

3. Campbell, George S., and Weil, Joseph: The Interpretation of Non-linear Pitching Moments in Relation to the Pitch-Up Problem. NACA RM L53I02, 1953.

4. Sadoff, Melvin, Stewart, John D., and Cooper, George E.: Analytical Study of the Comparative Pitch-Up Behavior of Several Airplanes and Correlation With Pilot Opinion. NACA RM A57D04, 1957.

5. Porter, Richard F.: An Analog Computer Study of a Stability Augmentation System for F-86E Aircraft. WADC Tech. Note WCT 54-104, March 1955.

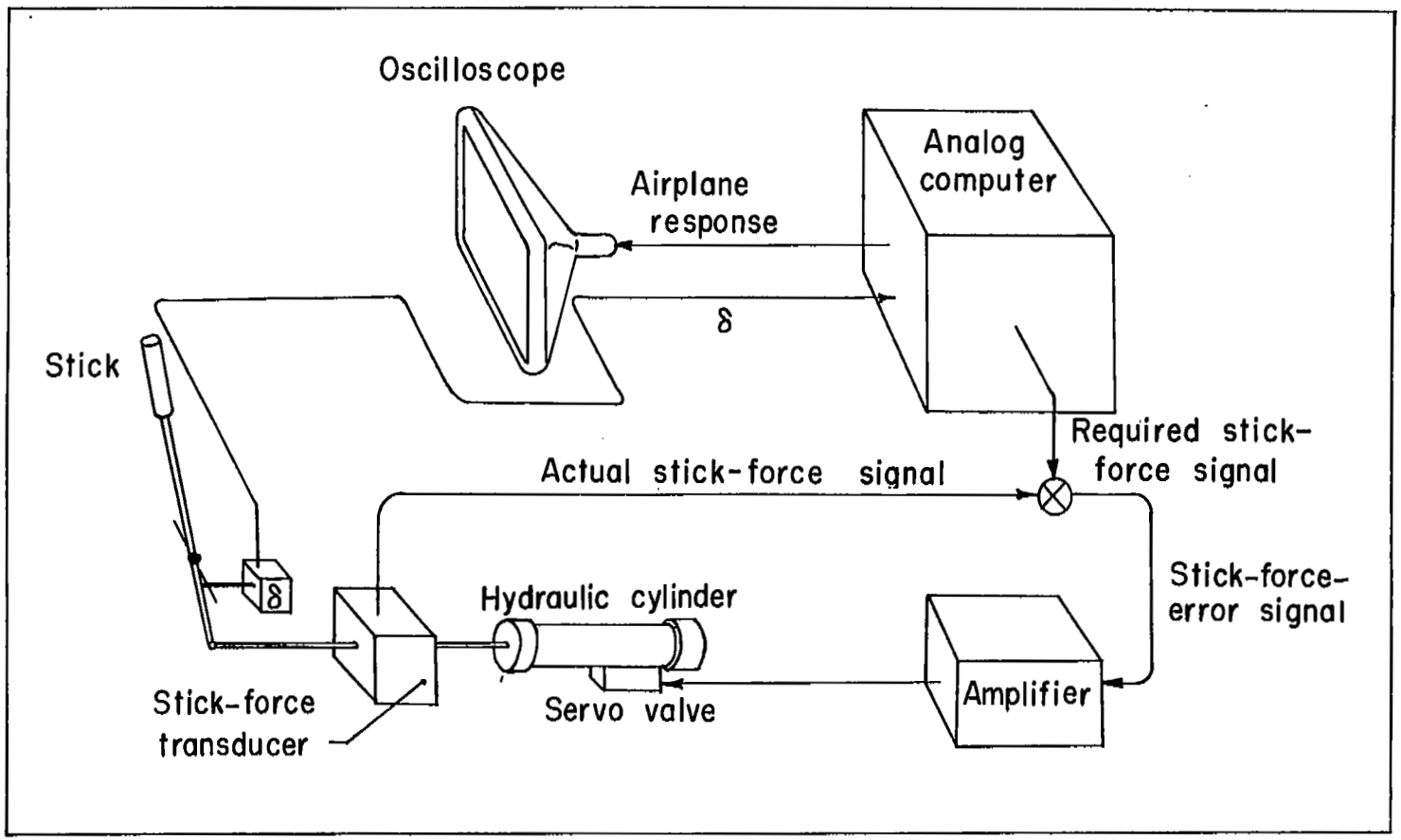

(a) Schematic diagram of the simulator.

Figure 1.- Description and detail characteristics of the control system used in the pitch-up investigation.

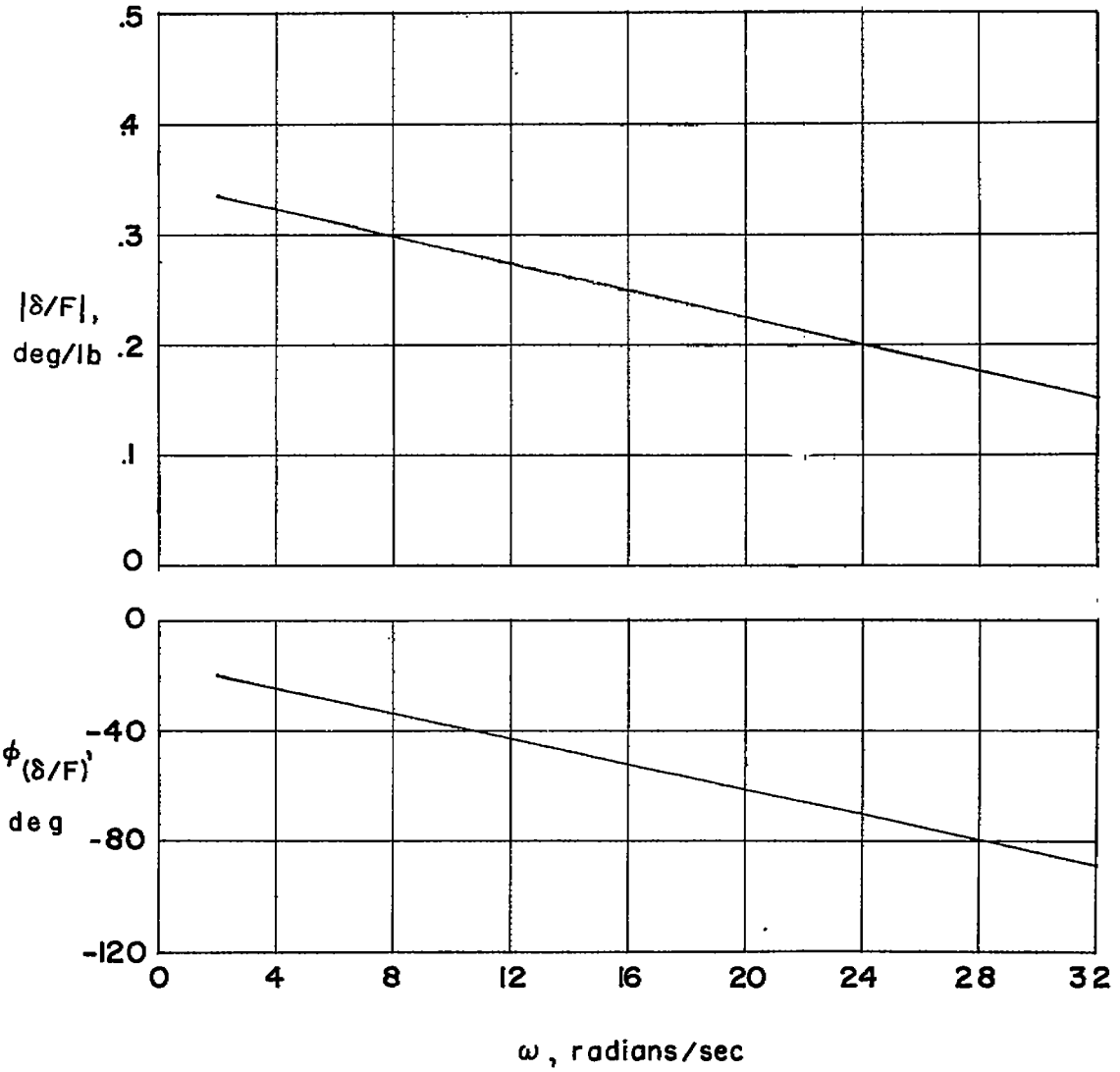

(b) Frequency-response characteristics of the torque servo.

Figure 1.- Concluded.

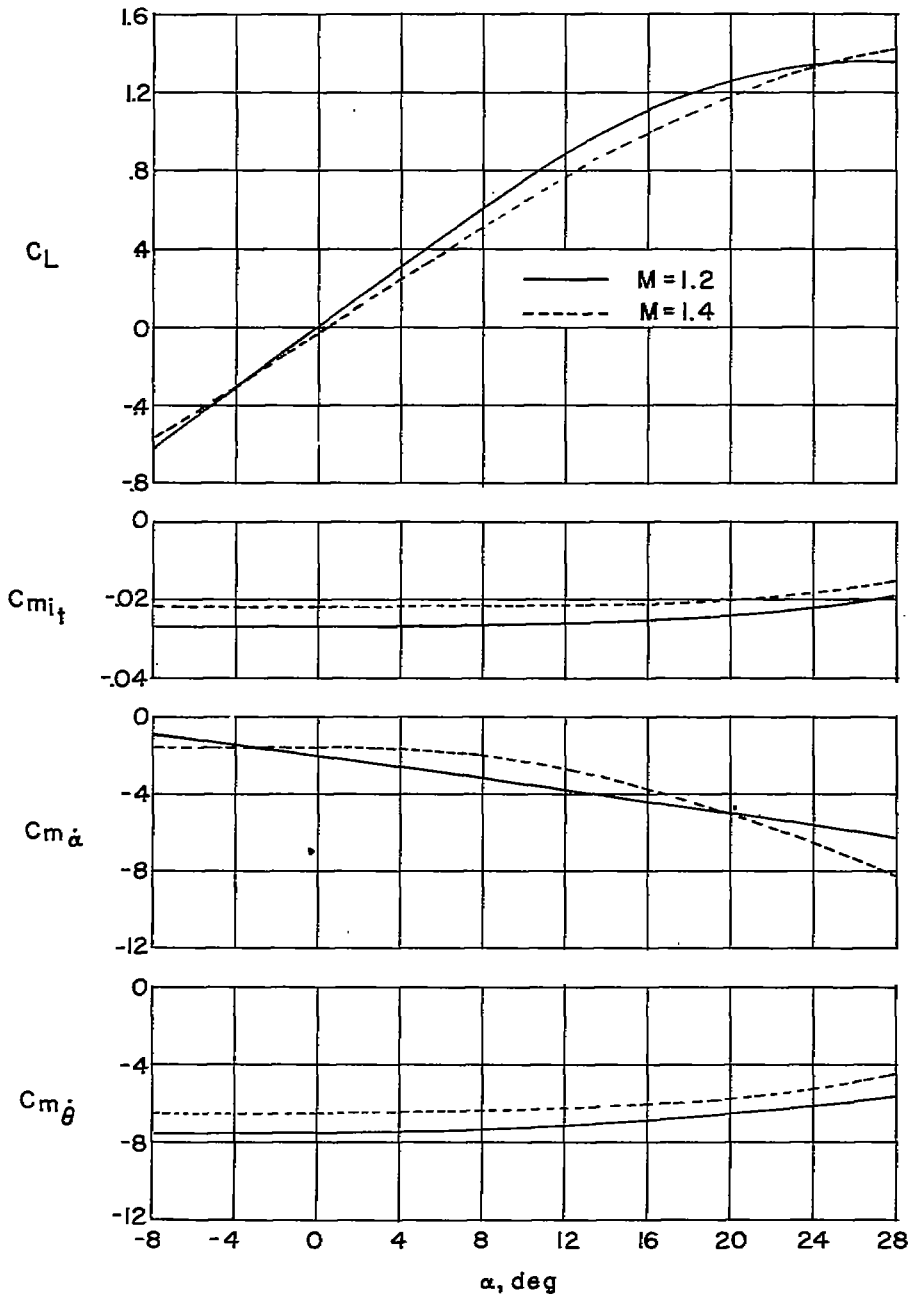

(a) C_L, $C_{m_{i_t}}$, $C_{m_{\dot{\alpha}}}$, and $C_{m_{\dot{\theta}}}$.

Figure 2.- Aerodynamic characteristics used in the pitch-up study.

[redacted]

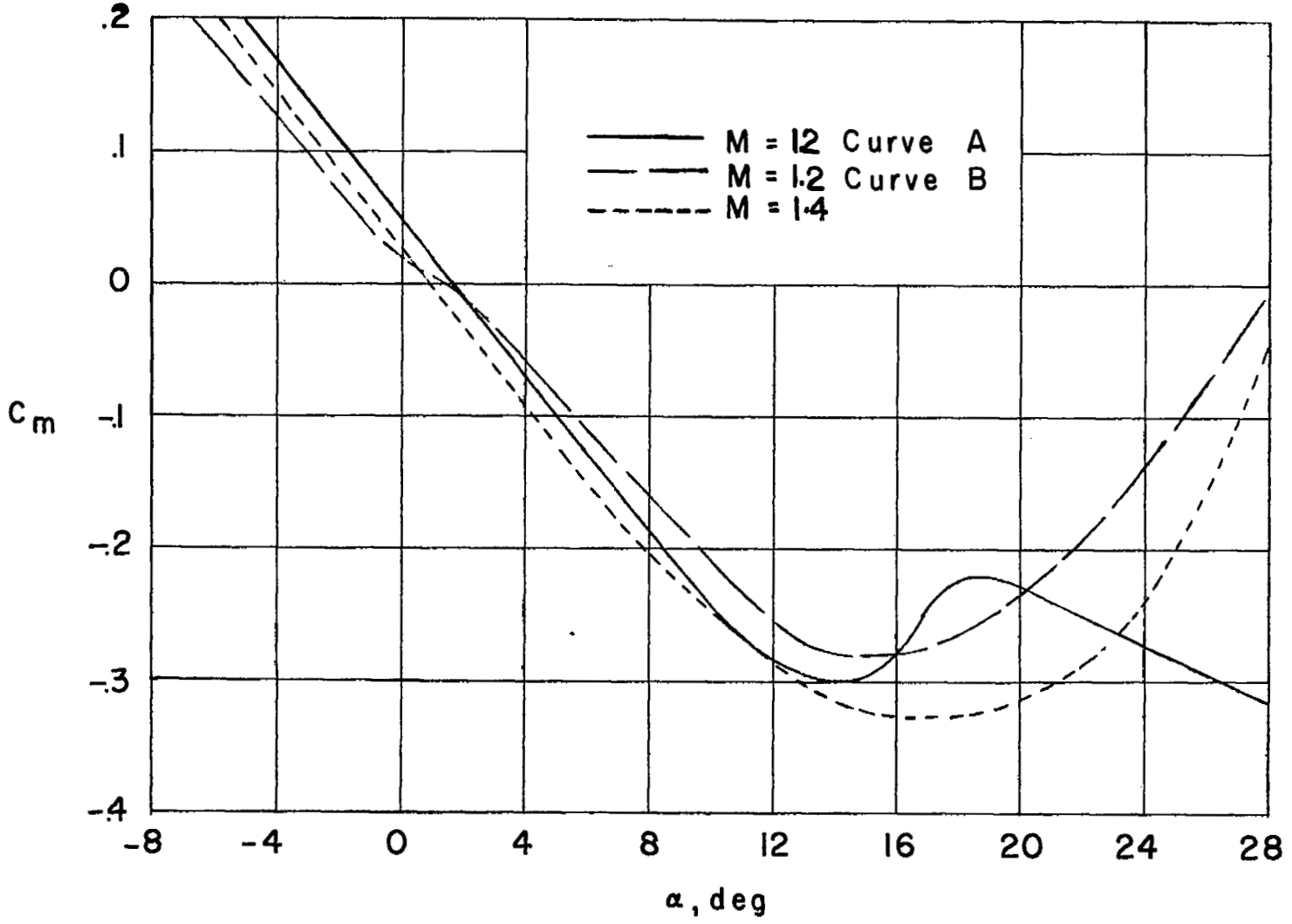

(b) C_m.

Figure 2.- Concluded.

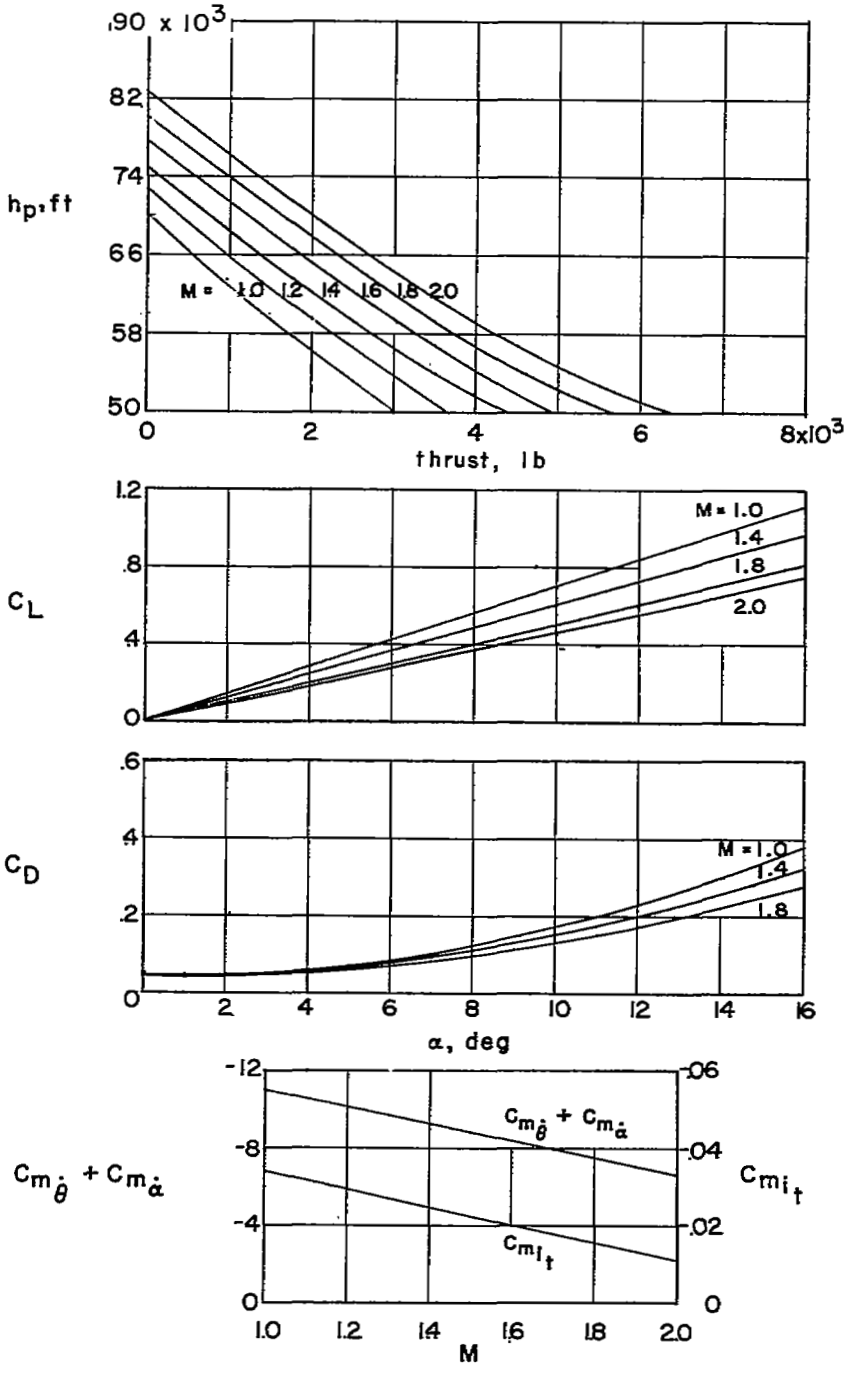

Figure 3.- Aerodynamic characteristics used in the zoom-up study.

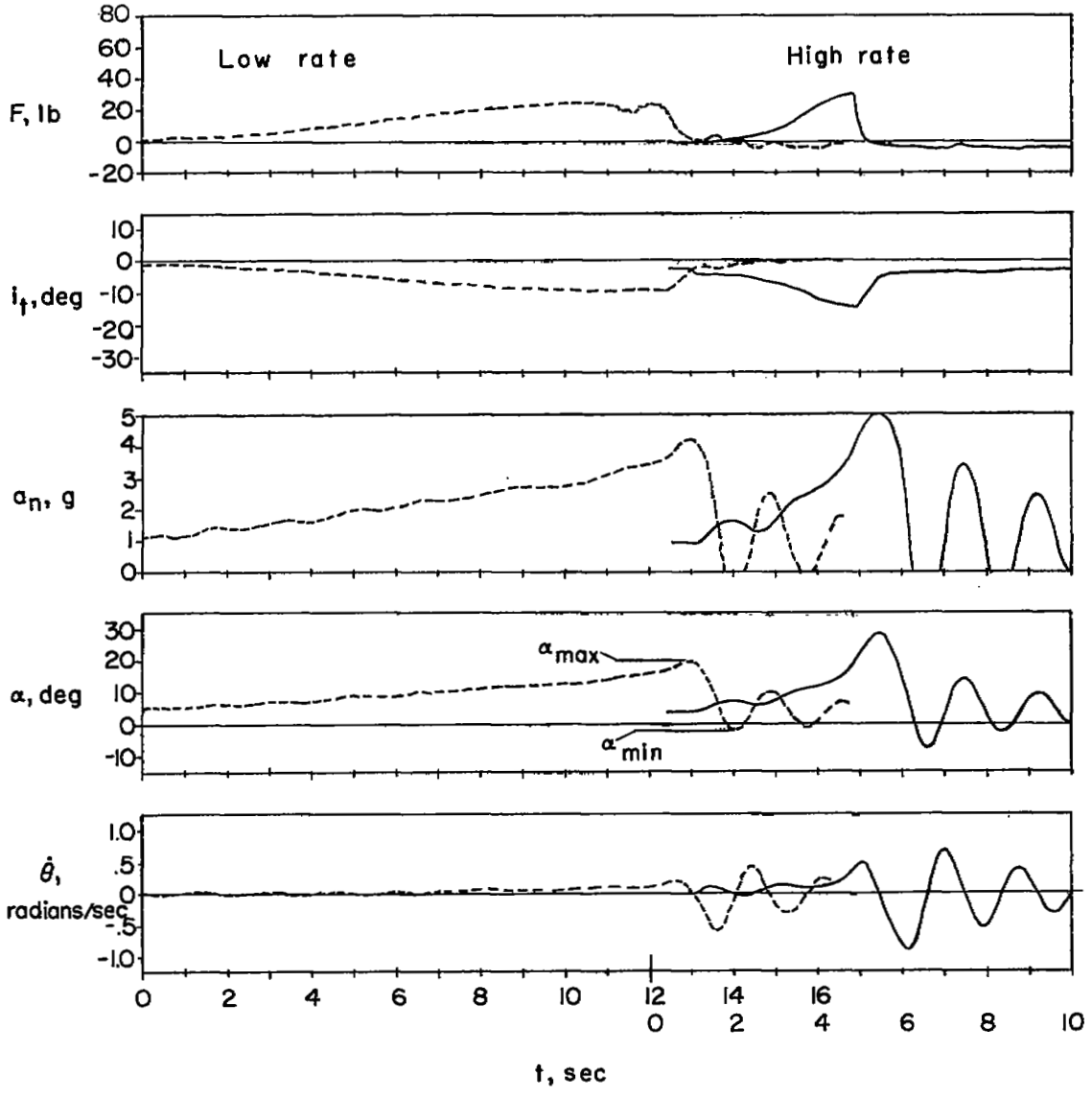

(a) M = 1.2; h_p = 50,000 feet (C_m curve A of fig. 2(b)).

Figure 4.- Typical pull-up maneuvers to determine the pitch-up characteristics of the basic configuration.

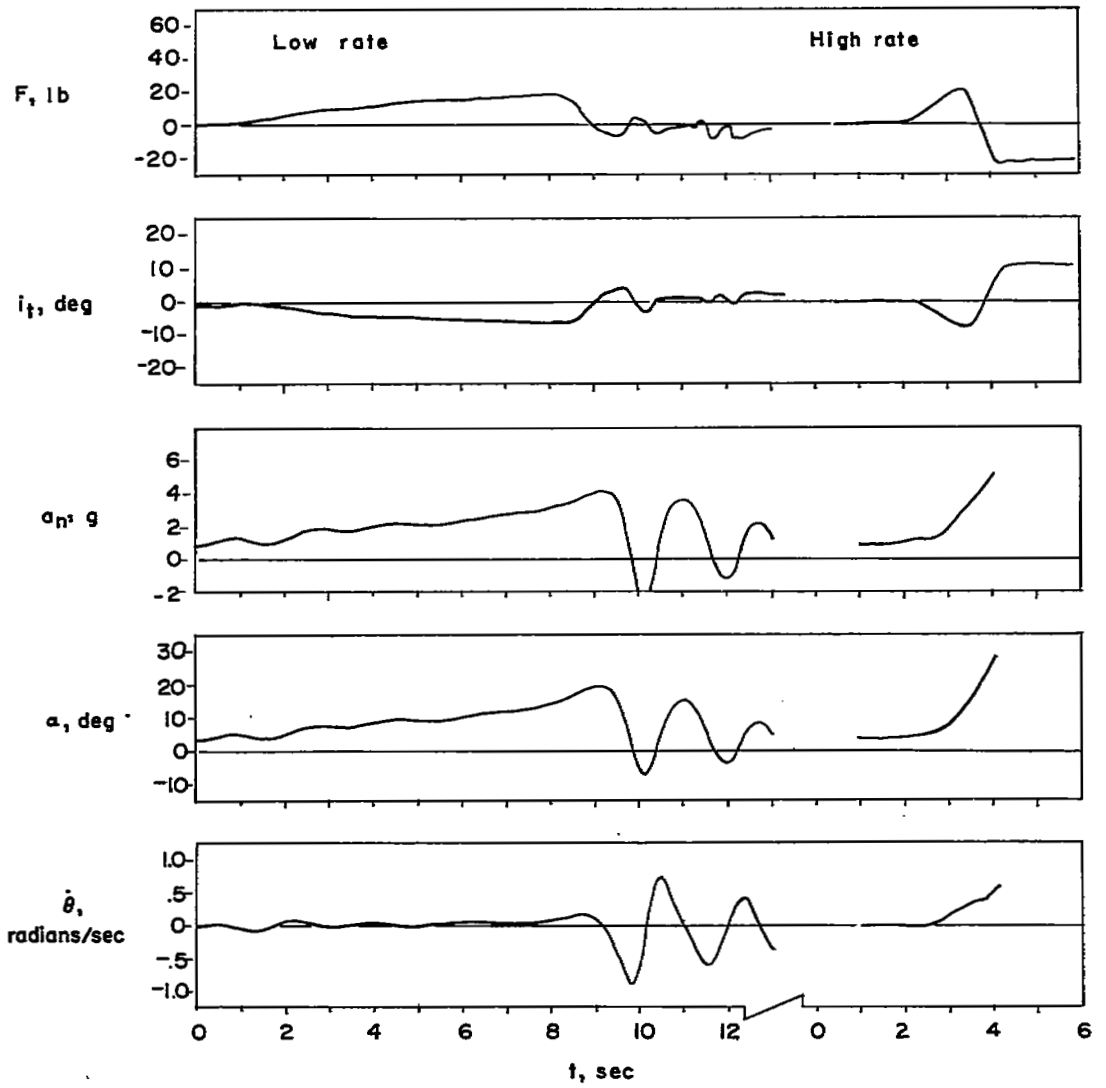

(b) M = 1.4; h_p = 50,000 feet.

Figure 4.- Concluded.

[redacted]

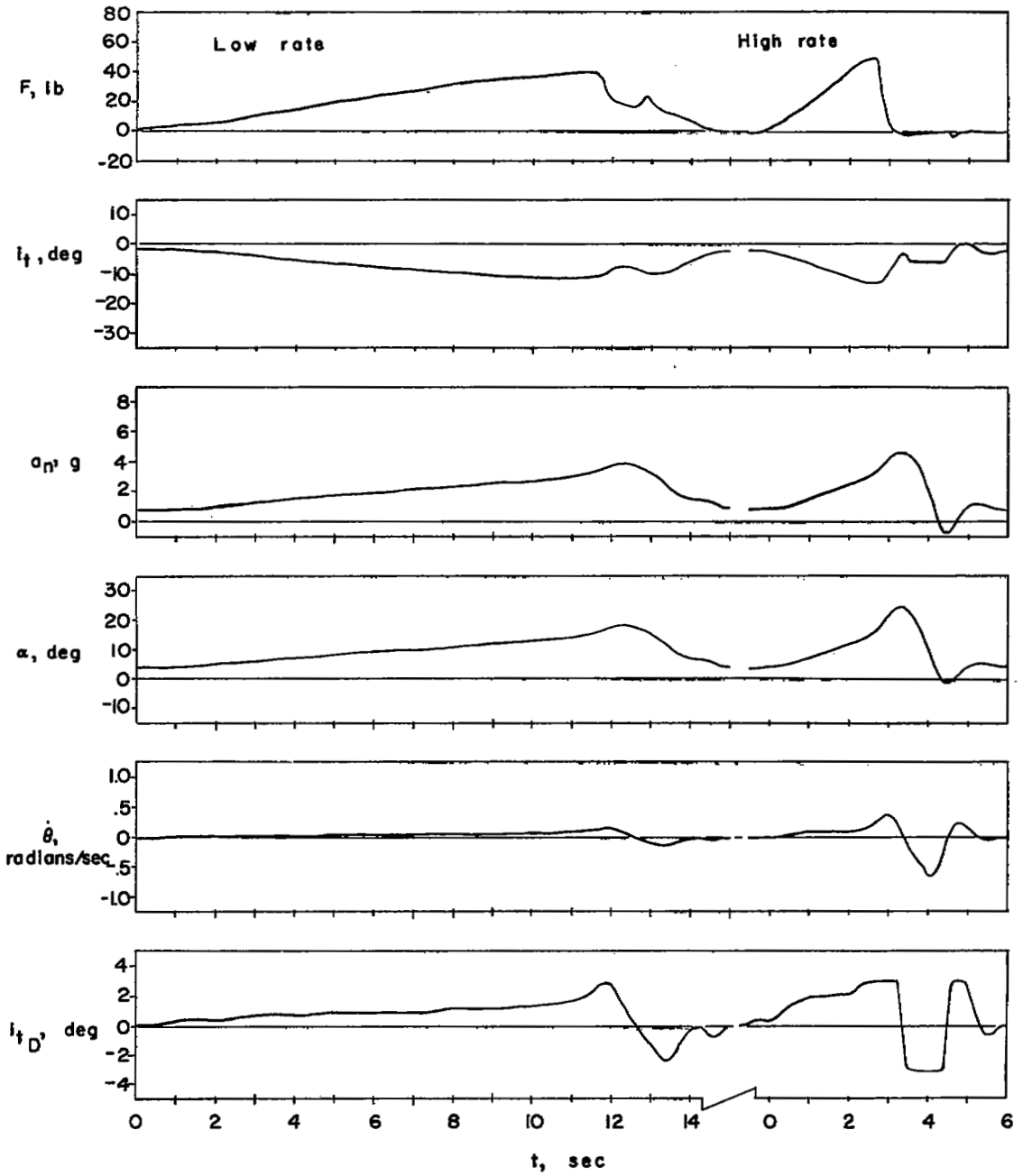

(a) M = 1.2; h_p = 50,000 feet (C_m curve A of fig. 2(b)).

Figure 5.- Typical pull-up maneuvers to determine the pitch-up characteristics of the basic configuration with pitch damper. K_D = 0.3 second; i_{t_D} = ±3°.

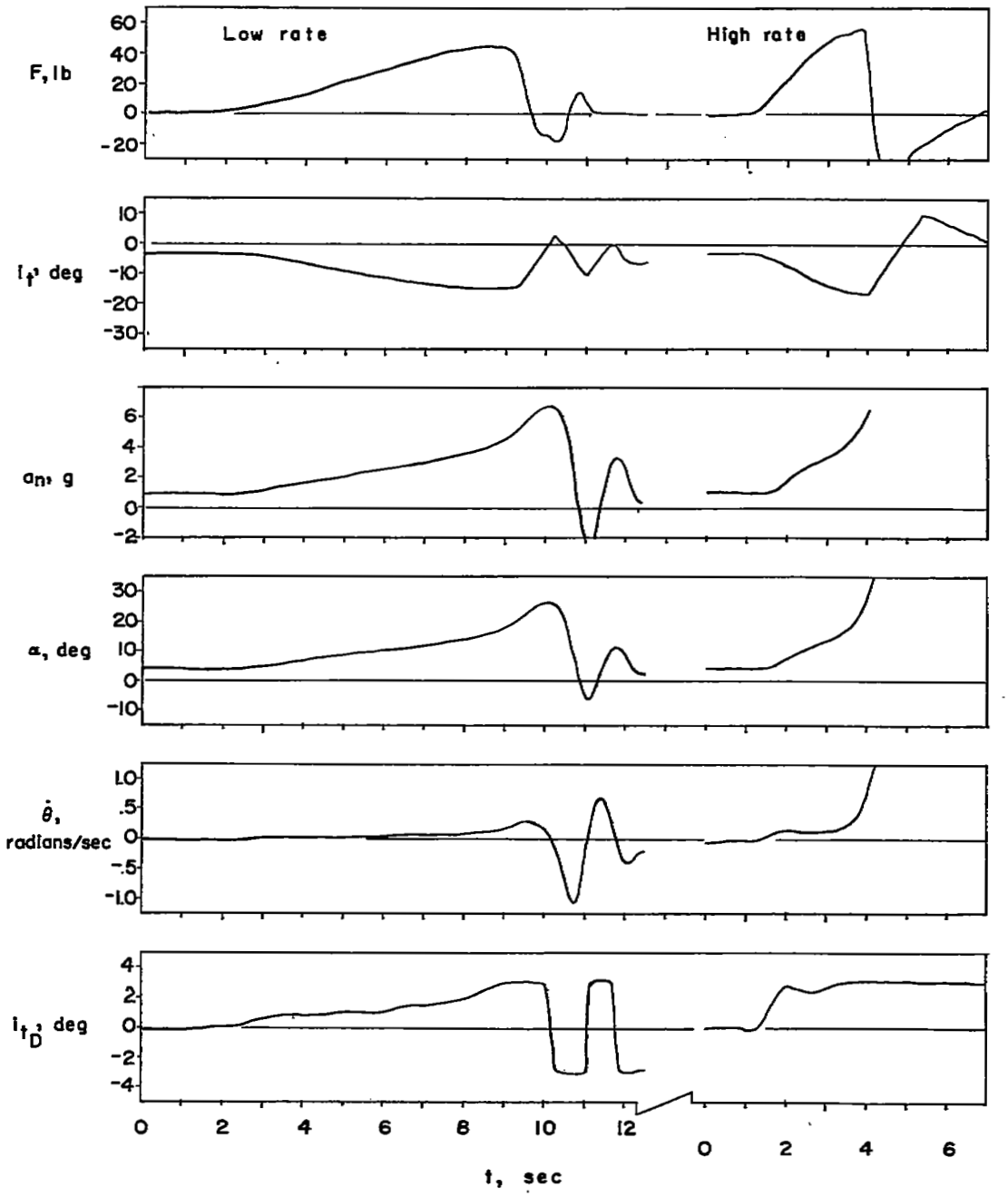

(b) M = 1.4; h_p = 50,000 feet.

Figure 5.- Concluded.

[redacted]

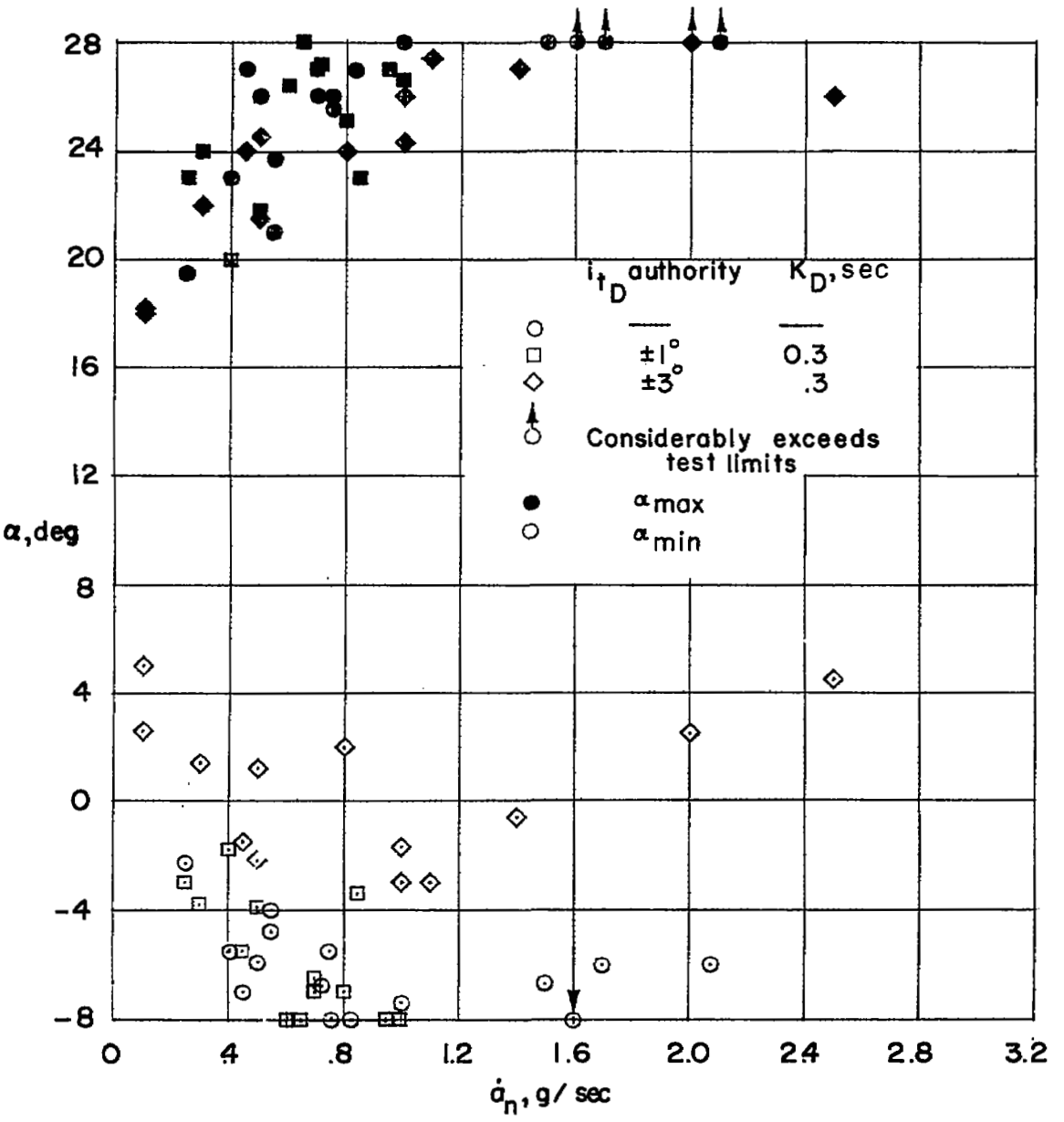

(a) M = 1.2; h_p = 50,000 feet (C_m curve A of fig. 2(b)).

Figure 6.- Summary of the angle-of-attack excursions resulting from pull-up maneuvers at various rates.

[redacted]

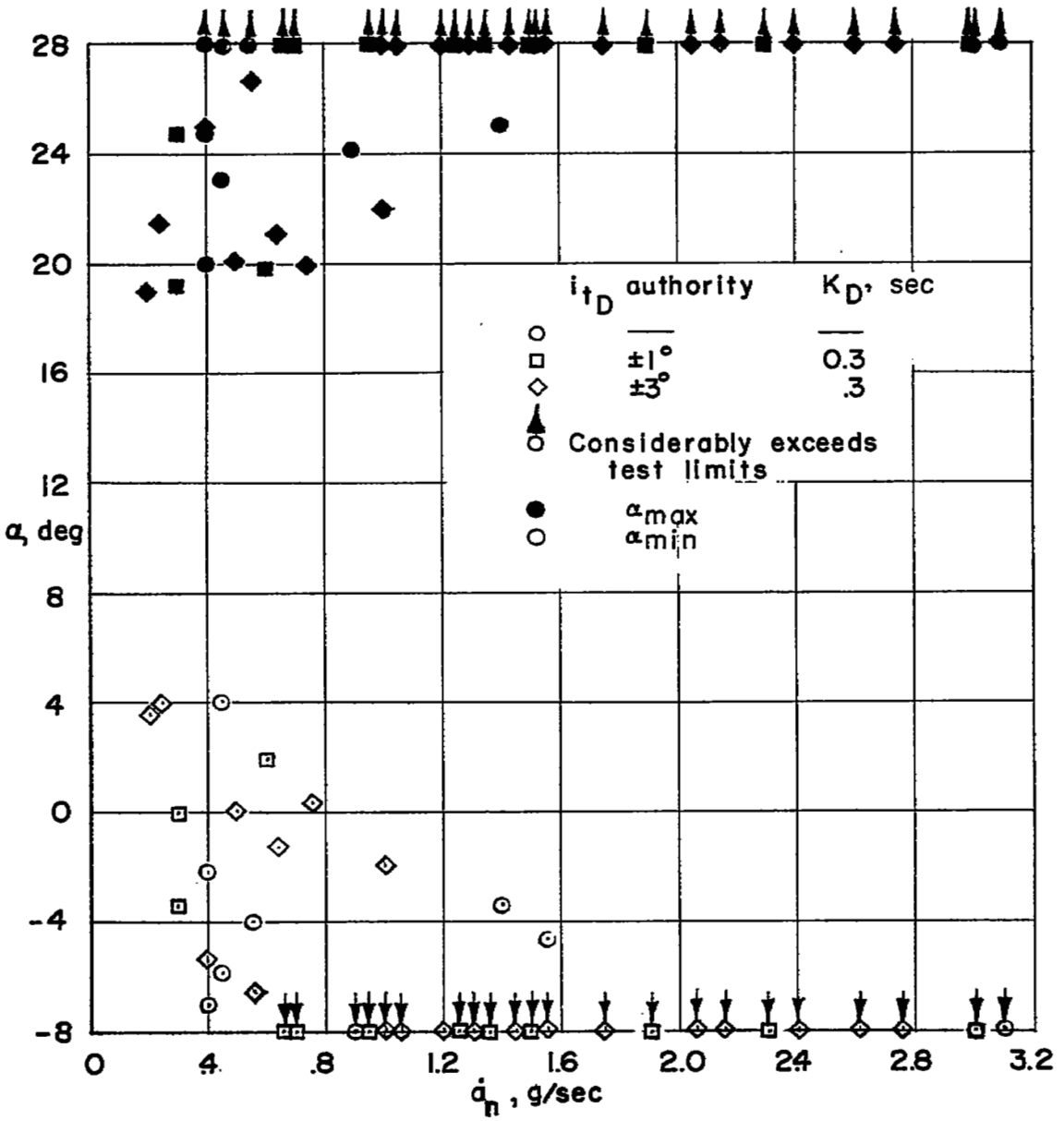

(b) M = 1.4; h_p = 50,000 feet.

Figure 6.- Concluded.

[redacted]

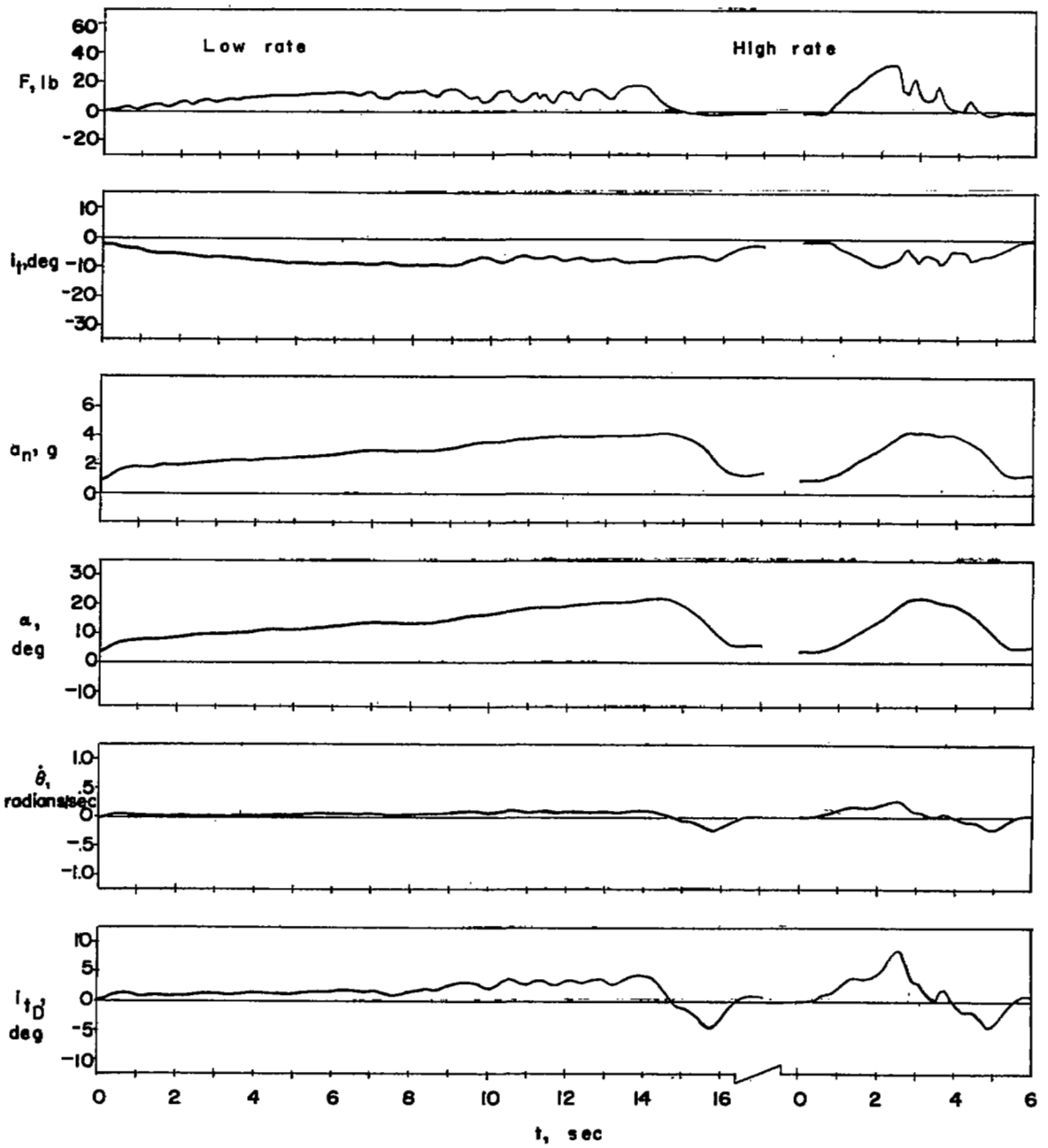

(a) M = 1.2; h_p = 50,000 feet (C_m curve A of fig. 2(b)).

Figure 7.- Typical pull-up maneuvers for basic airplane with the nonlinear pitch damper. i_{t_D} unlimited; $K_D = 0.3 + 2.5\alpha^2$.

[redacted]

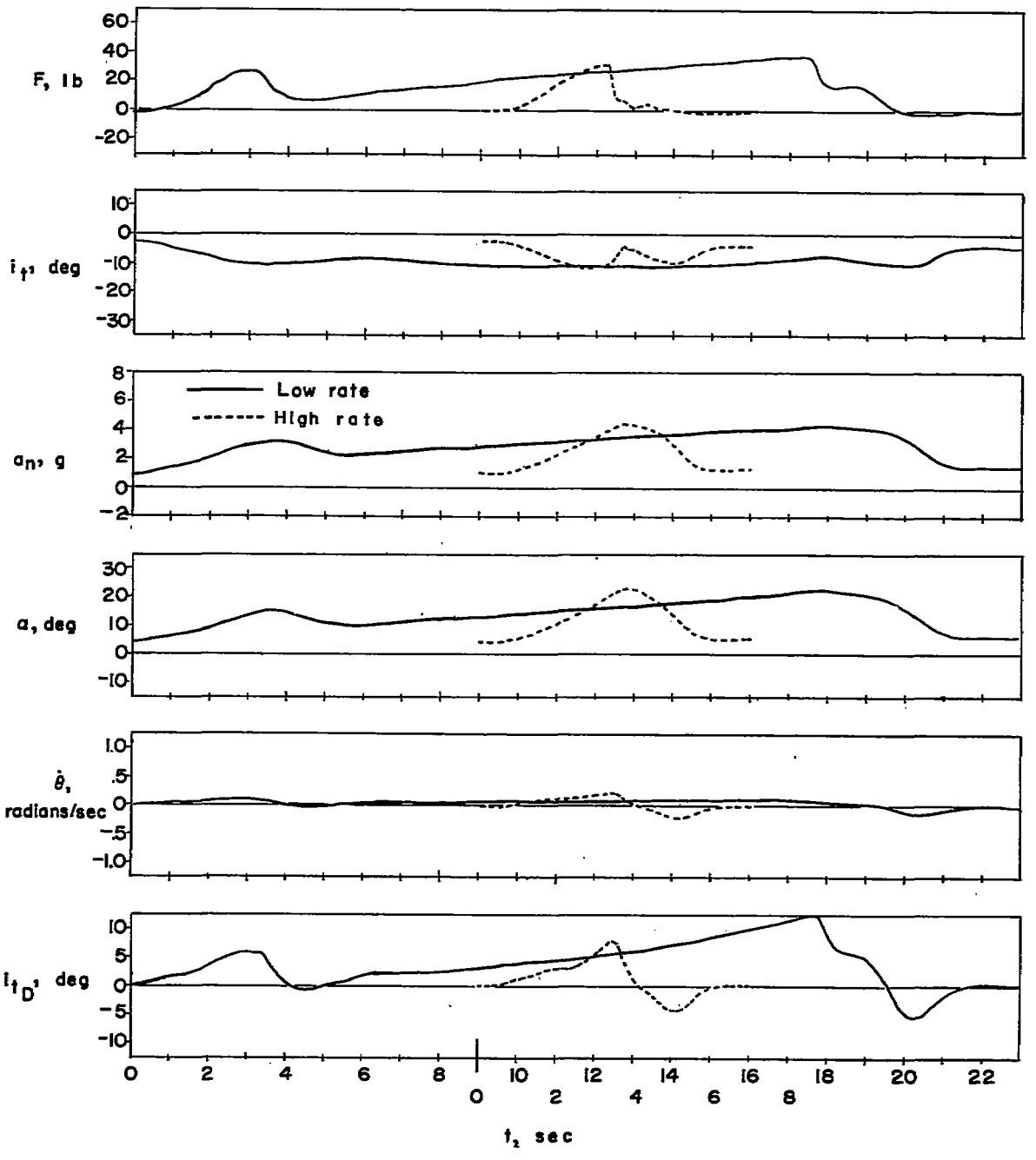

(b) M = 1.2; h_p = 50,000 feet (C_m curve B of fig. 2(b)).

Figure 7.- Concluded.

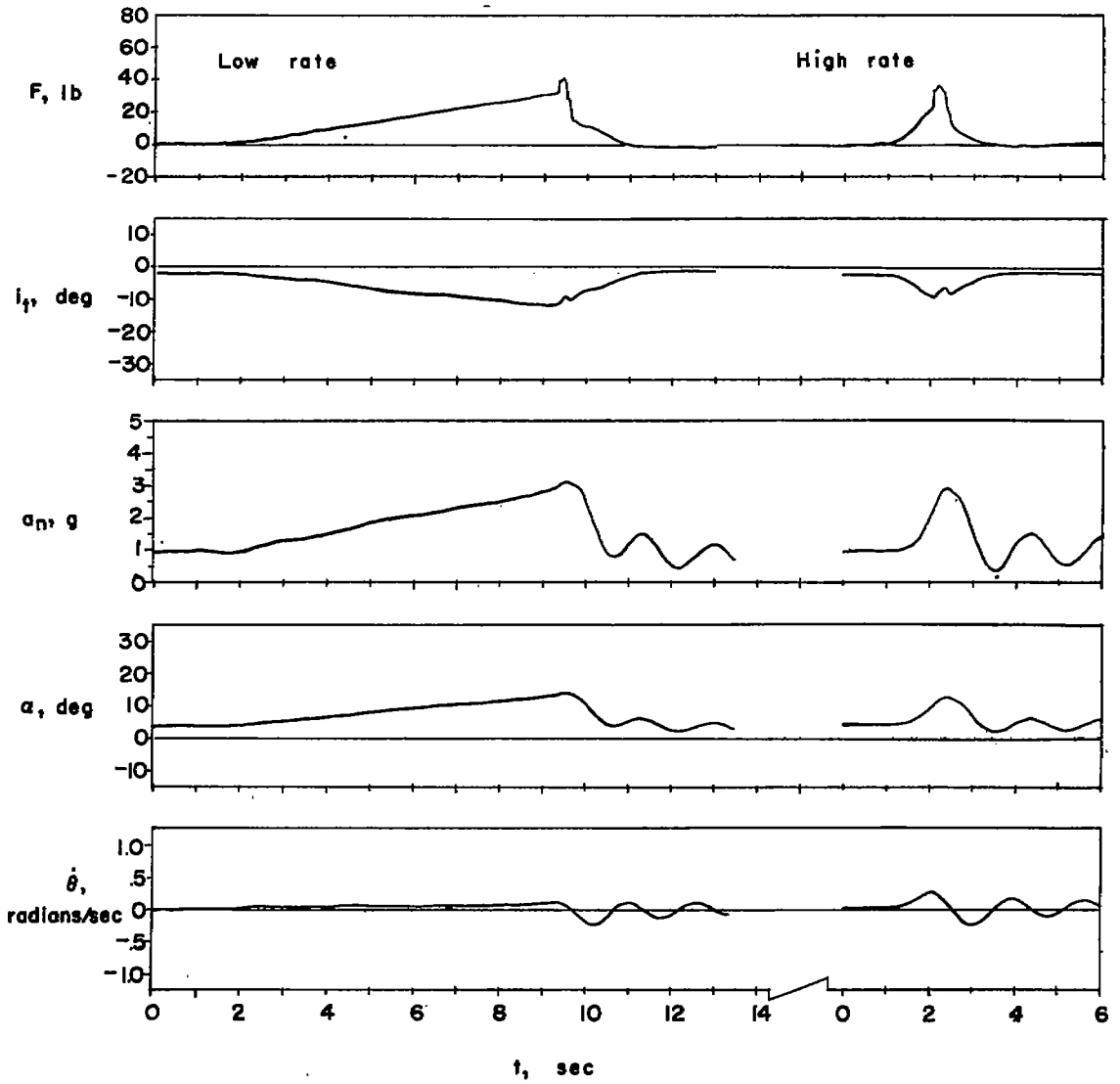

(a) Stick-pusher force, 15 pounds.

Figure 8.- Typical pull-up maneuvers with the stick pusher. Stick-pusher boundary (30-16); no pitch damper; M = 1.2; h_p = 50,000 feet (C_m curve A of fig. 2(b)).

[redacted]

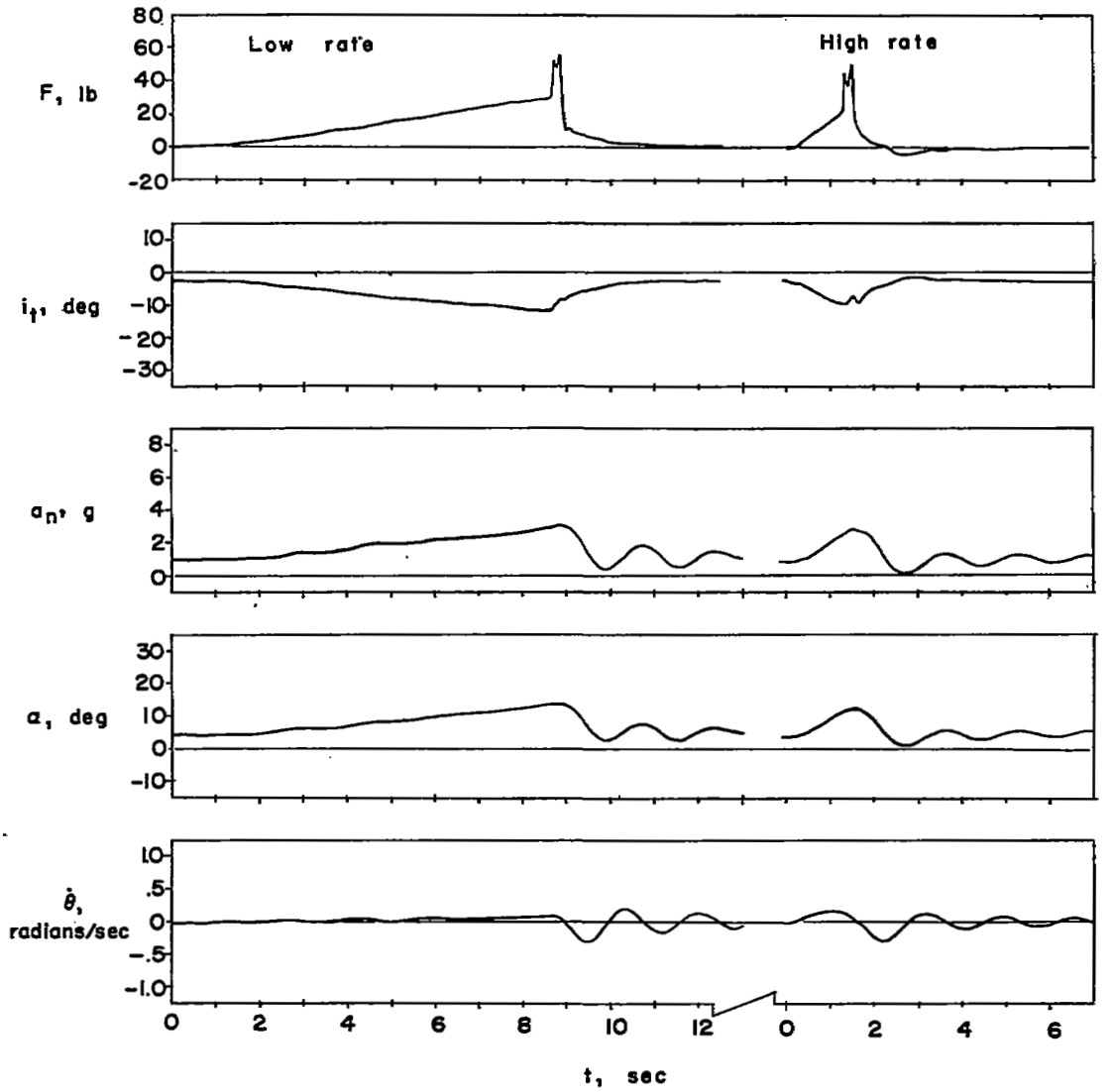

(b) Stick-pusher force, 30 pounds.

Figure 8.- Continued.

[redacted]

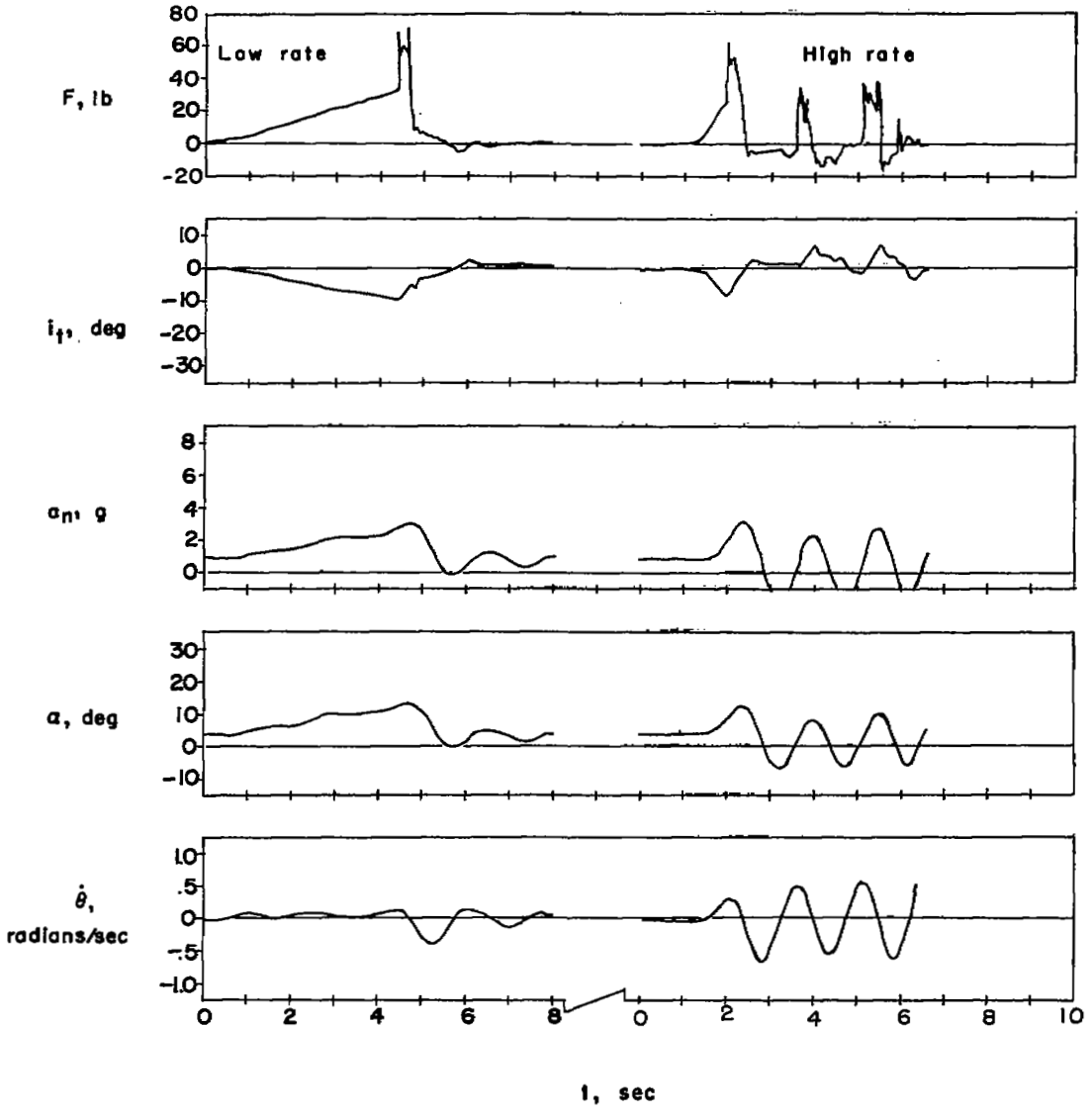

(c) Stick-pusher force, 45 pounds.

Figure 8.- Concluded.

[redacted]

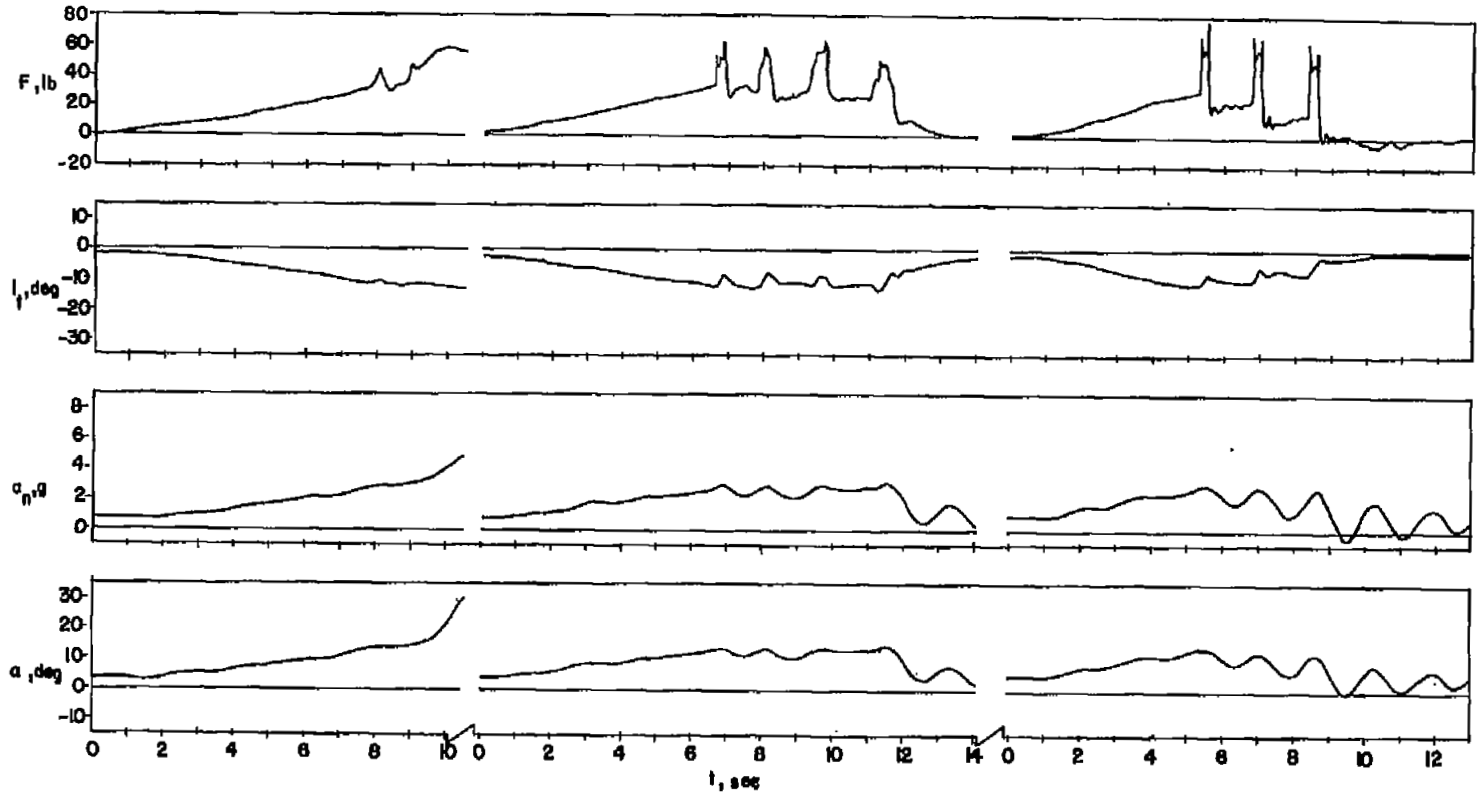

(a) Stick-pusher force, 15 pounds.

(b) Stick-pusher force, 30 pounds.

(c) Stick-pusher force, 45 pounds.

Figure 9.- Typical pull-up maneuvers during which attempts were made to override the stick-pusher. $M = 1.2$; $h_p = 50{,}000$ feet (C_m curve A of fig. 2(b)). No pitch damper. Stick-pusher boundary (30-16).

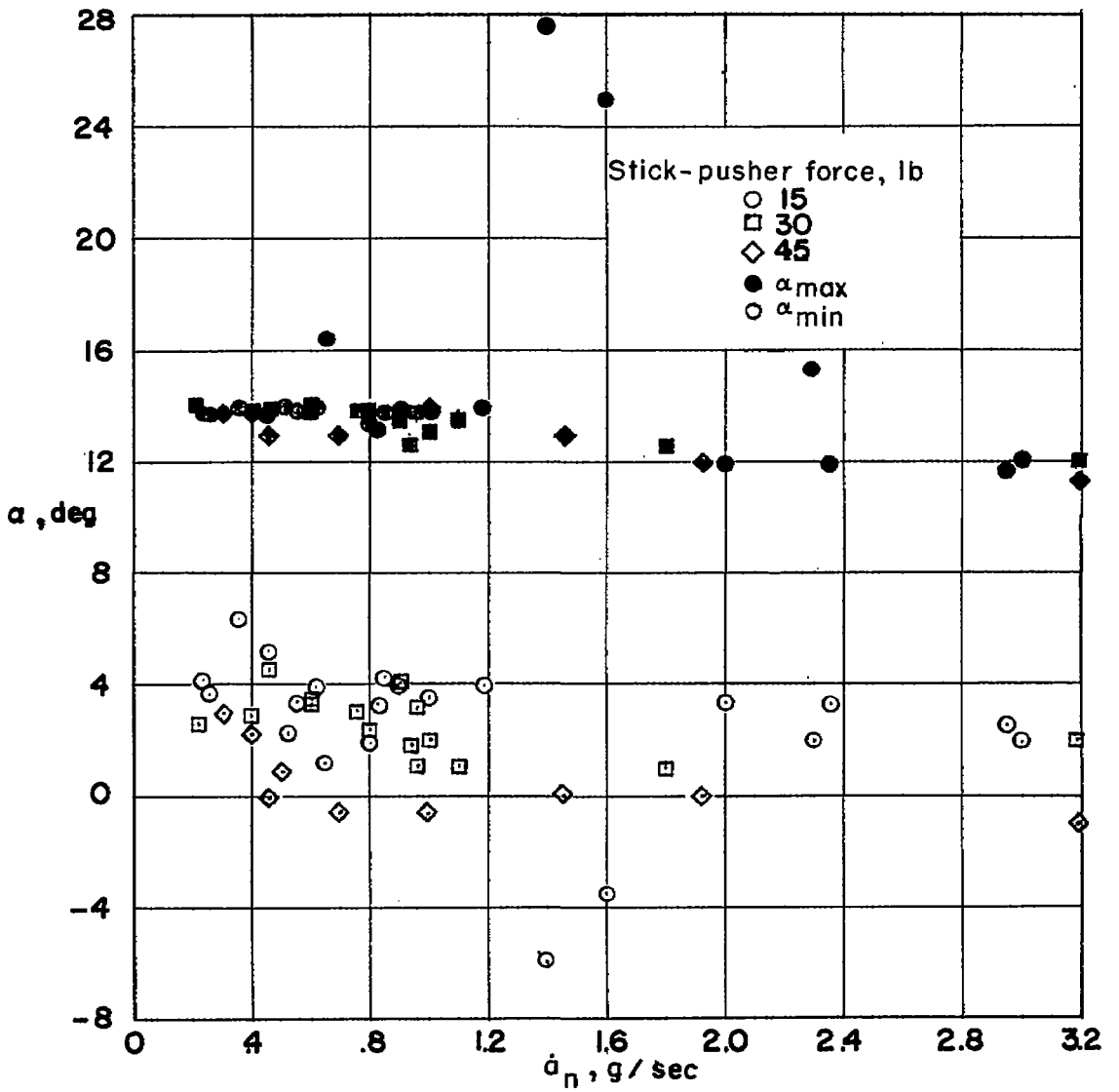

(a) No pitch damper.

Figure 10.- Angle-of-attack excursions obtained during pull-up maneuvers at various rates with three stick-pusher forces and with and without pitch damper. M = 1.2; h_p = 50,000 feet (C_m curve A of fig. 2(b)); stick-pusher boundary (30-16).

[redacted]

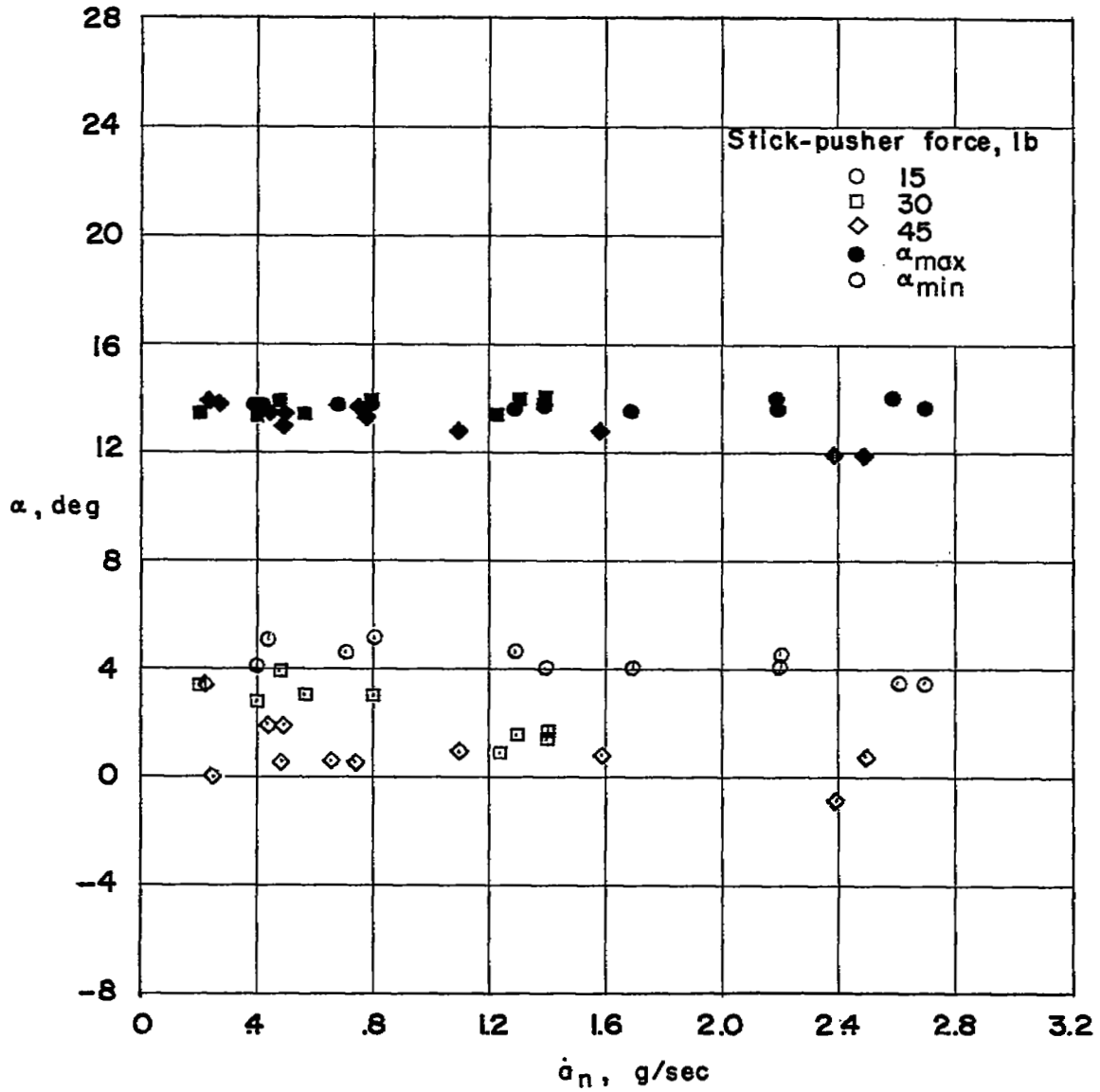

(b) $i_{t_D} = \pm 1^{\circ}$; $K_D = 0.3$ second.

Figure 10.- Continued.

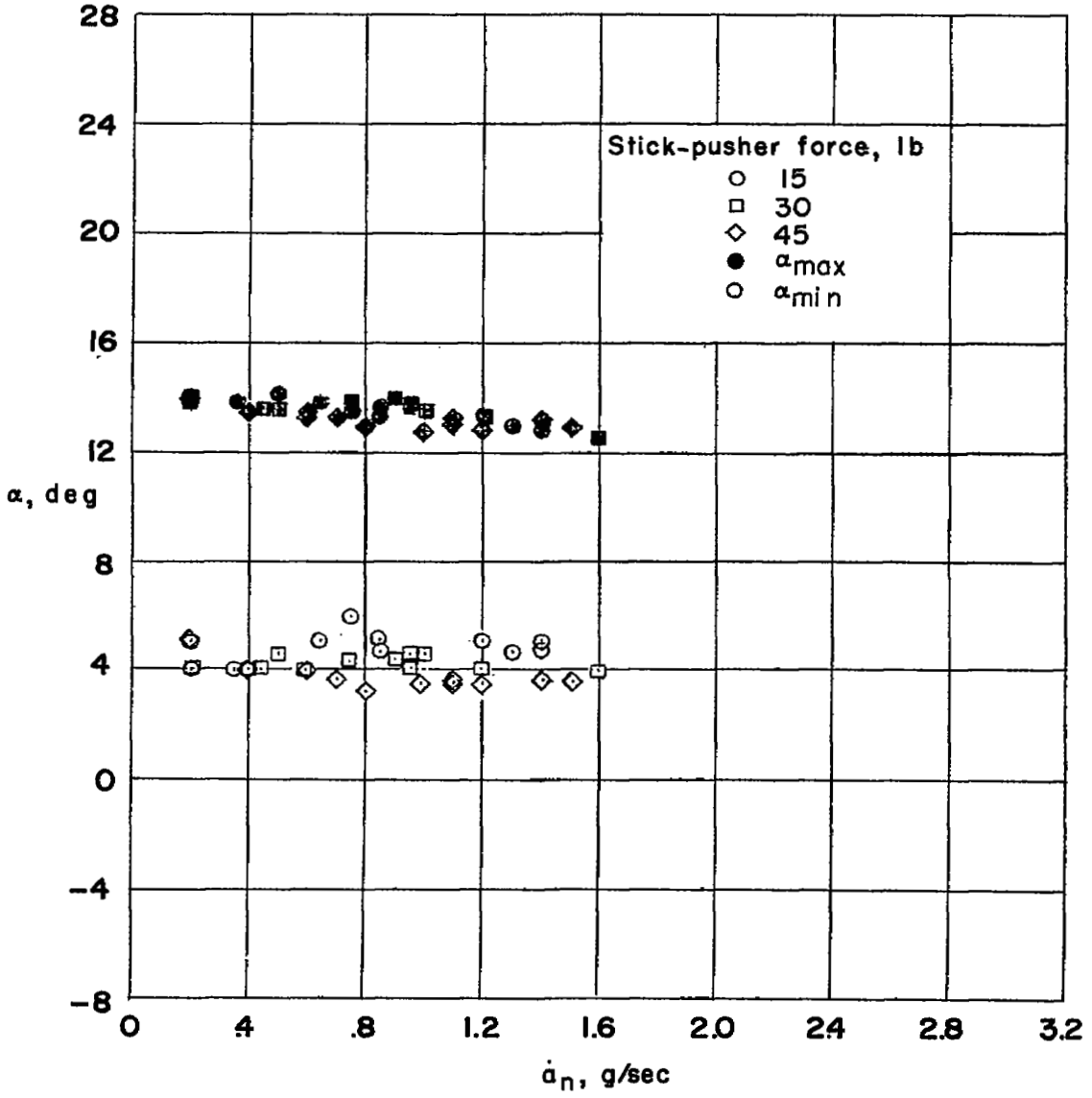

(c) $i_{t_D} = \pm 3^\circ$; $K_D = 0.3$ second.

Figure 10.- Concluded.

[redacted]

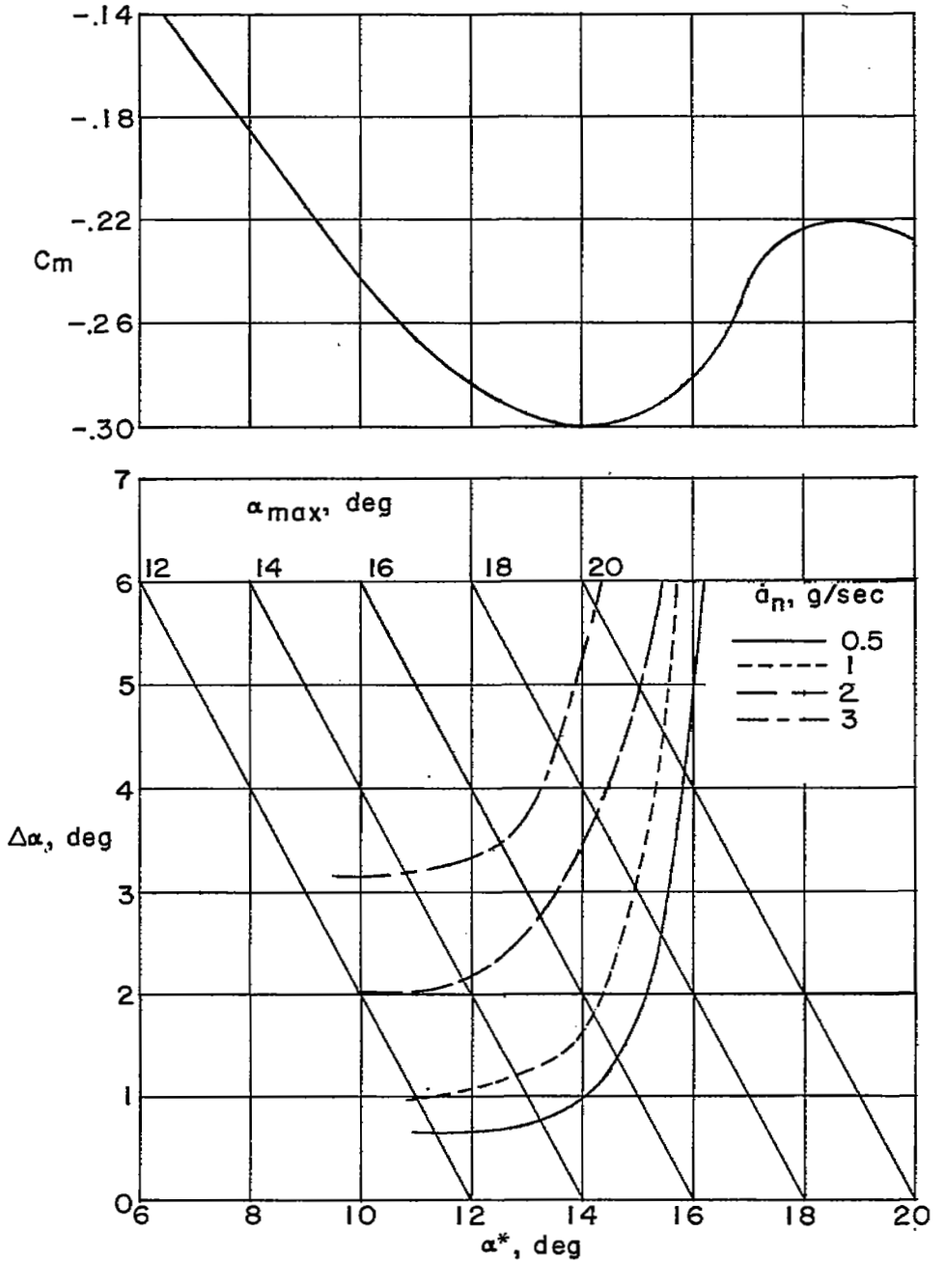

(a) M = 1.2; h_p = 50,000 feet (C_m curve A of fig. 2(b)).

Figure 11.- Effect of activation angle of attack and rate of pull-up on the overshoot α for three typical pitching-moment curves.

[redacted]

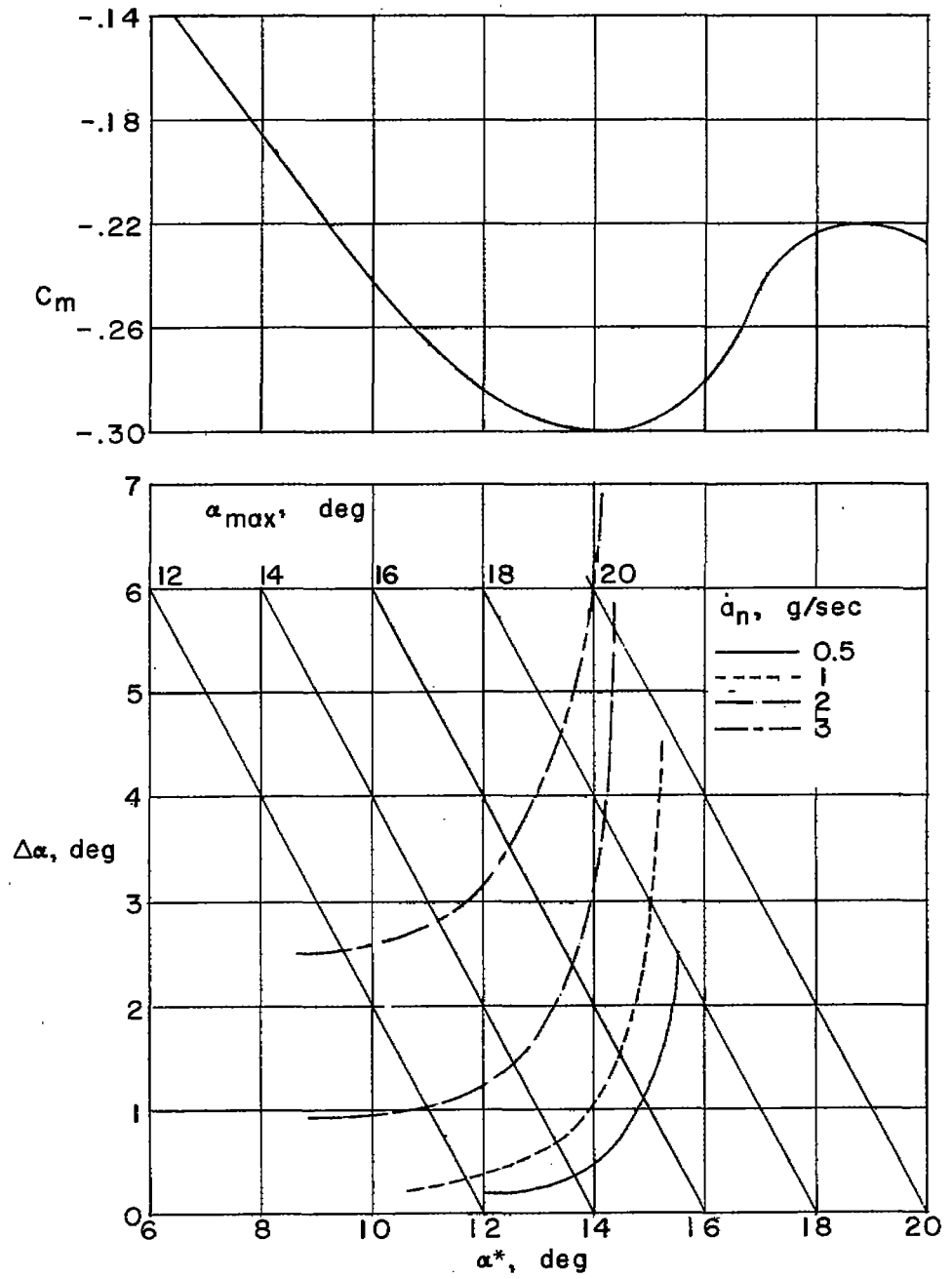

(b) M = 1.2; h_p = 40,000 feet (C_m curve A of fig. 2(b)).

Figure 11.- Continued.

[redacted]

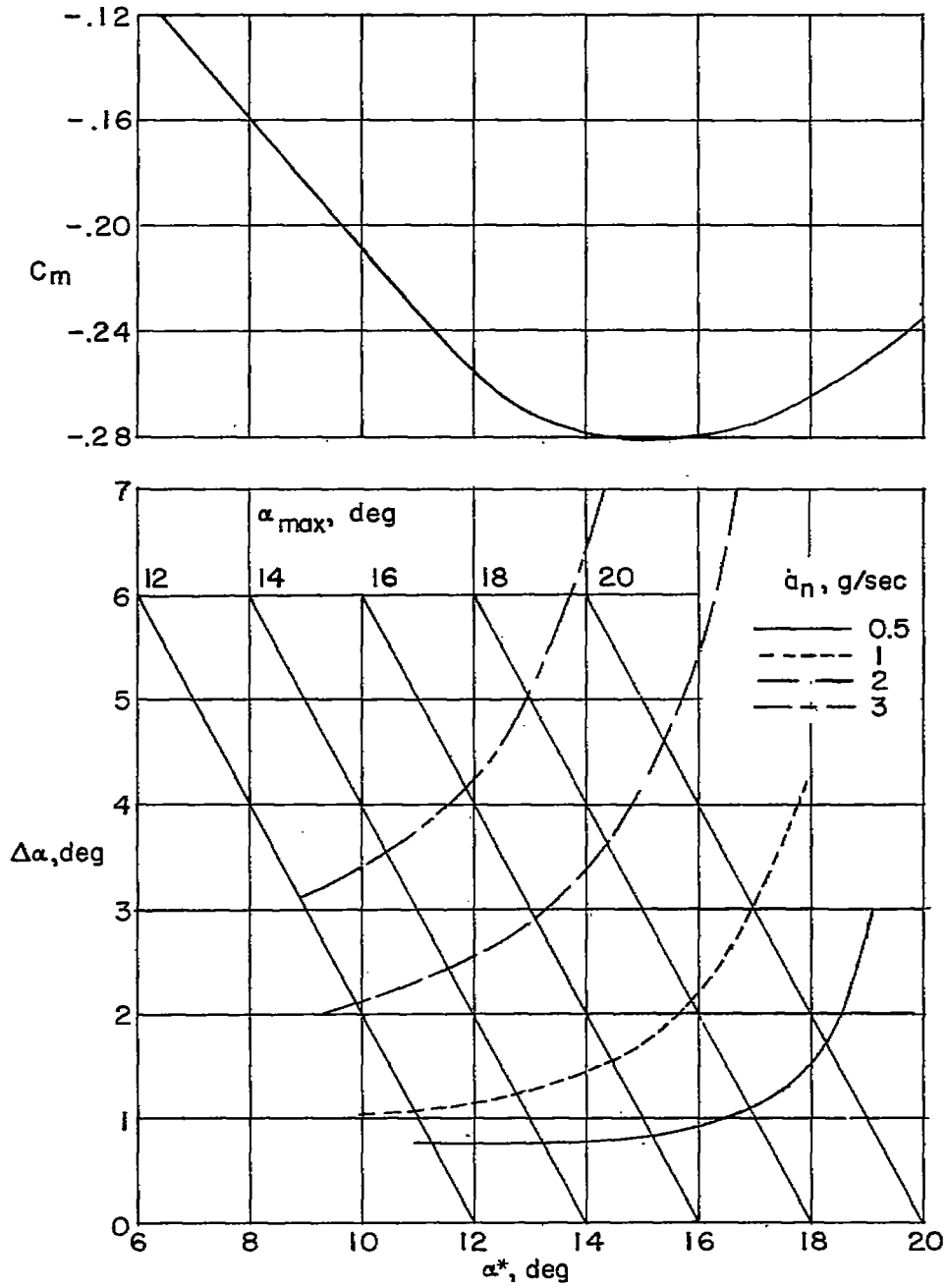

(c) M = 1.2; h_p = 50,000 feet (C_m curve B of fig. 2(b)).

Figure 11.- Continued.

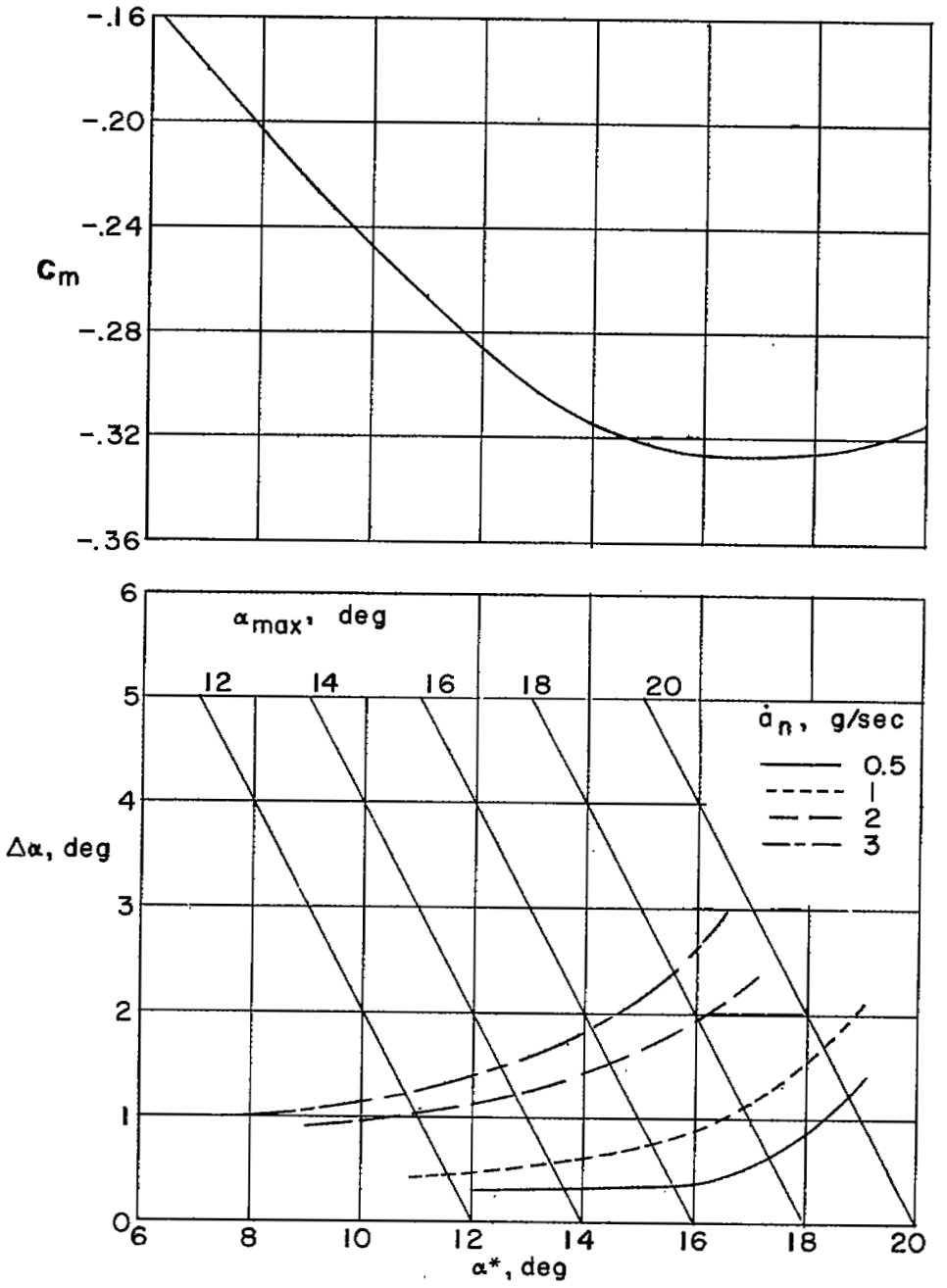

(d) M = 1.4; h_p = 40,000 feet.

Figure 11.- Concluded.

[redacted]

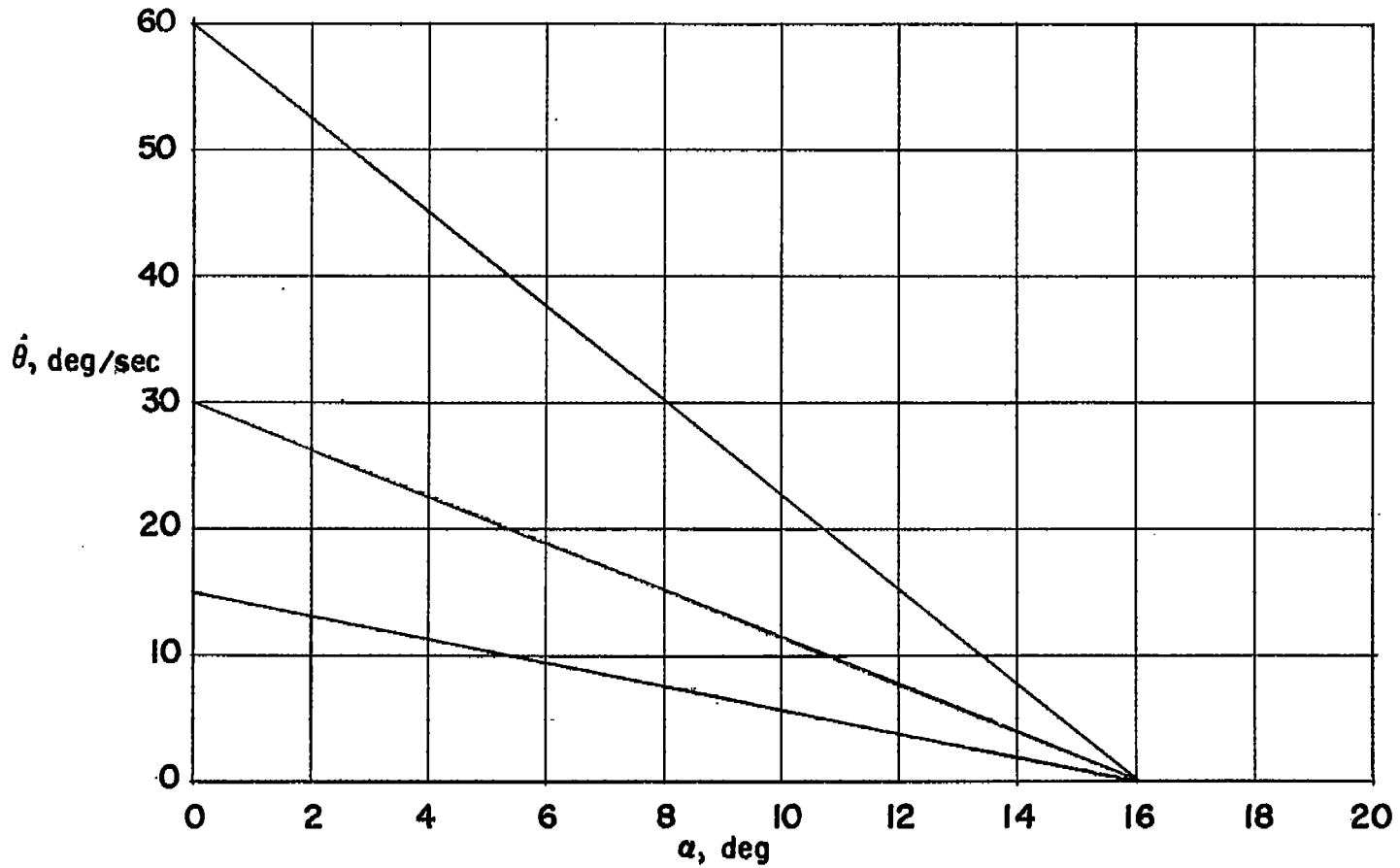

Figure 12.- Stick-pusher boundaries used in the investigation.

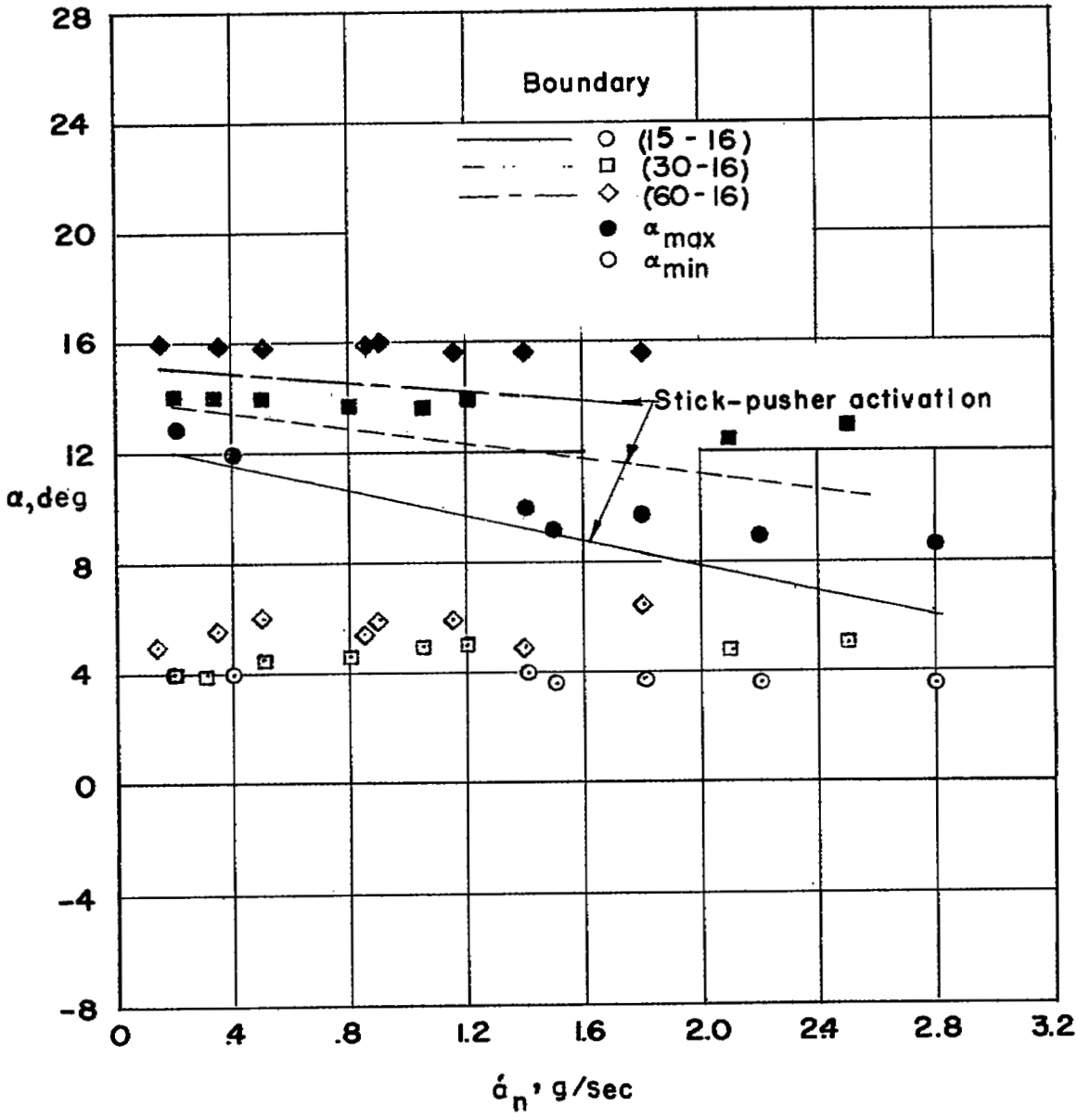

(a) M = 1.2; h_p = 50,000 feet (C_m curve A of fig. 2(b)); $i_{t_D} = \pm 3^\circ$; K_D = 0.3 second.

Figure 13.- Angle-of-attack excursions obtained during pull-up maneuvers with three stick-pusher boundaries. Stick-pusher force, 30 pounds.

[redacted]

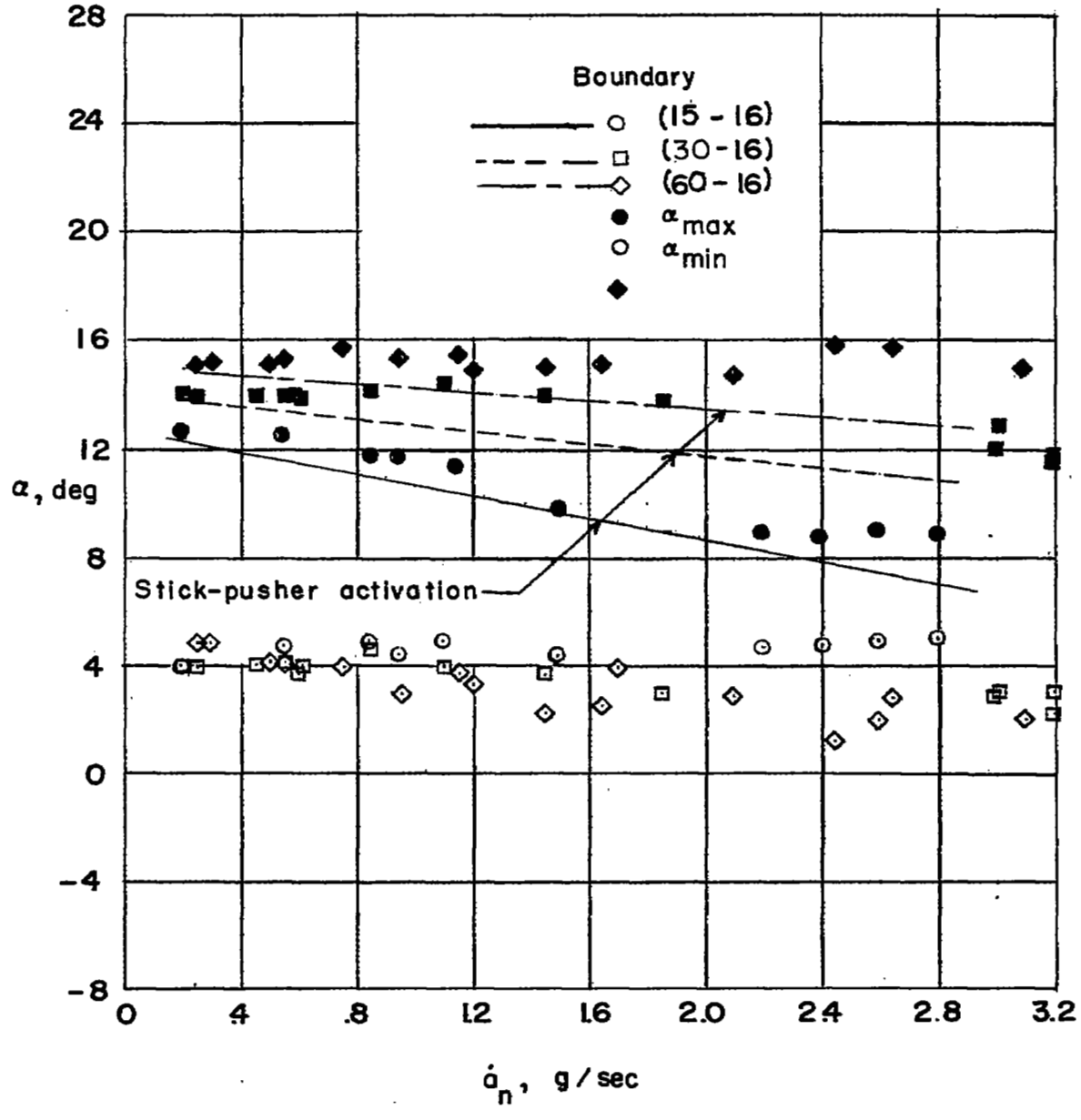

(b) M = 1.4; h_p = 50,000 feet; $i_{t_D} = \pm 3^\circ$; K_D = 0.3 second.

Figure 13.- Continued.

[redacted]

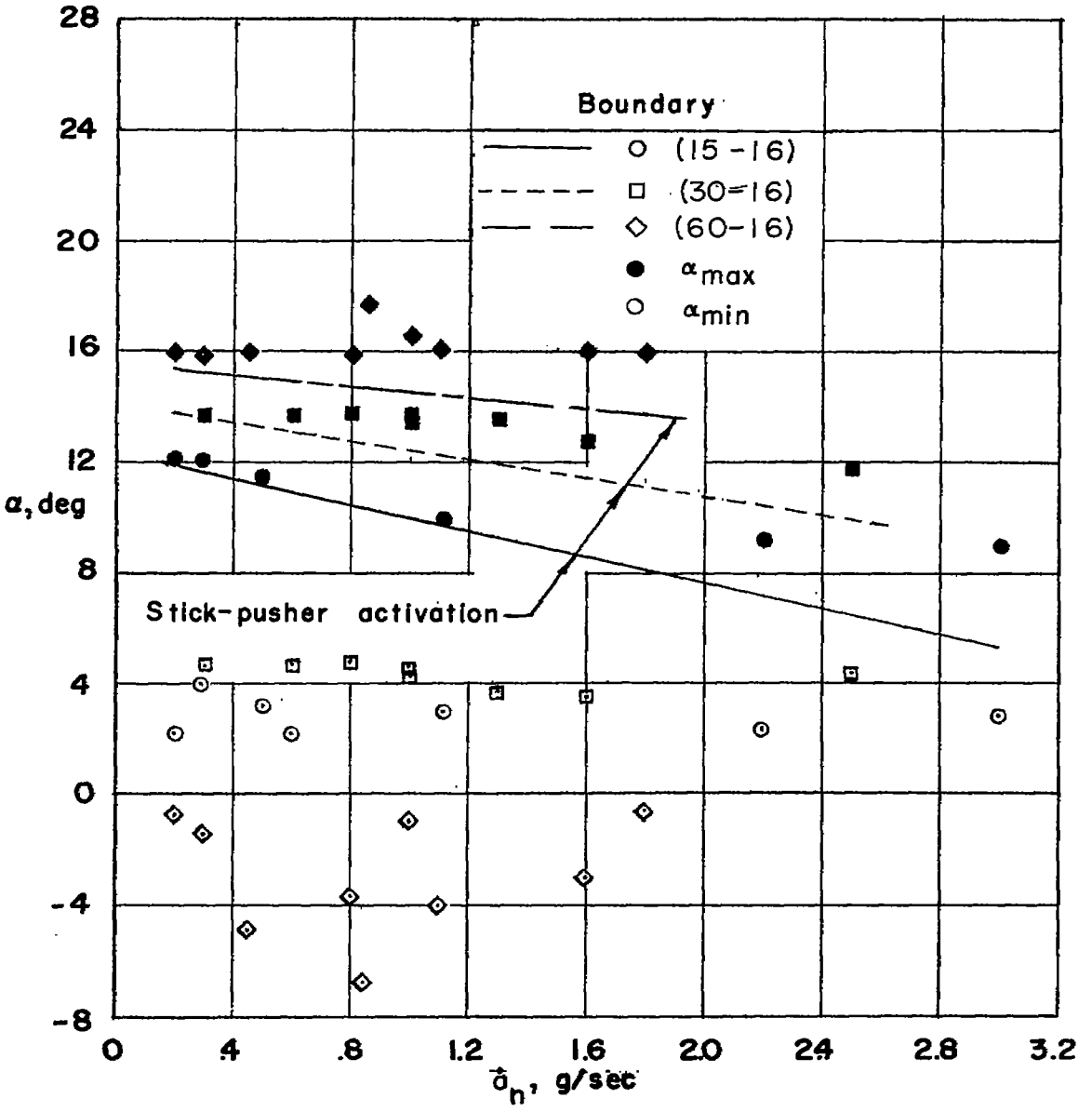

(c) M = 1.2; h_p = 50,000 feet (C_m curve A of fig. 2(b)).
No pitch damper.

Figure 13.- Concluded.

[redacted]

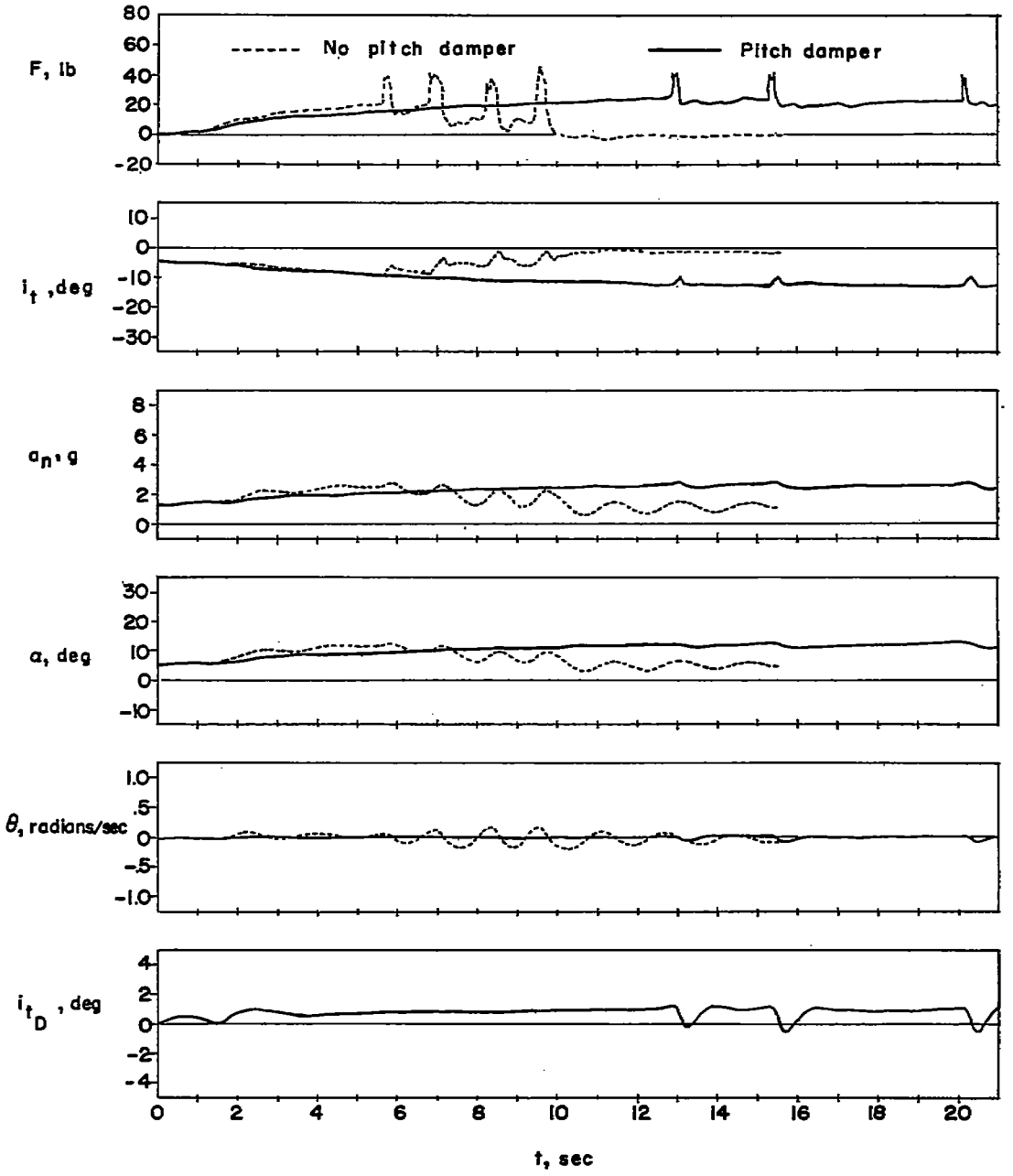

Figure 14.- The effect of pitch damping on attempts to track near the stick-pusher boundary. M = 1.2; h_p = 50,000 feet (C_m curve A of fig. 2(b)). Stick-pusher boundary (15-16); stick-pusher force, 30 pounds; $i_{t_D} = \pm 3^\circ$; K_D = 0.3 second.

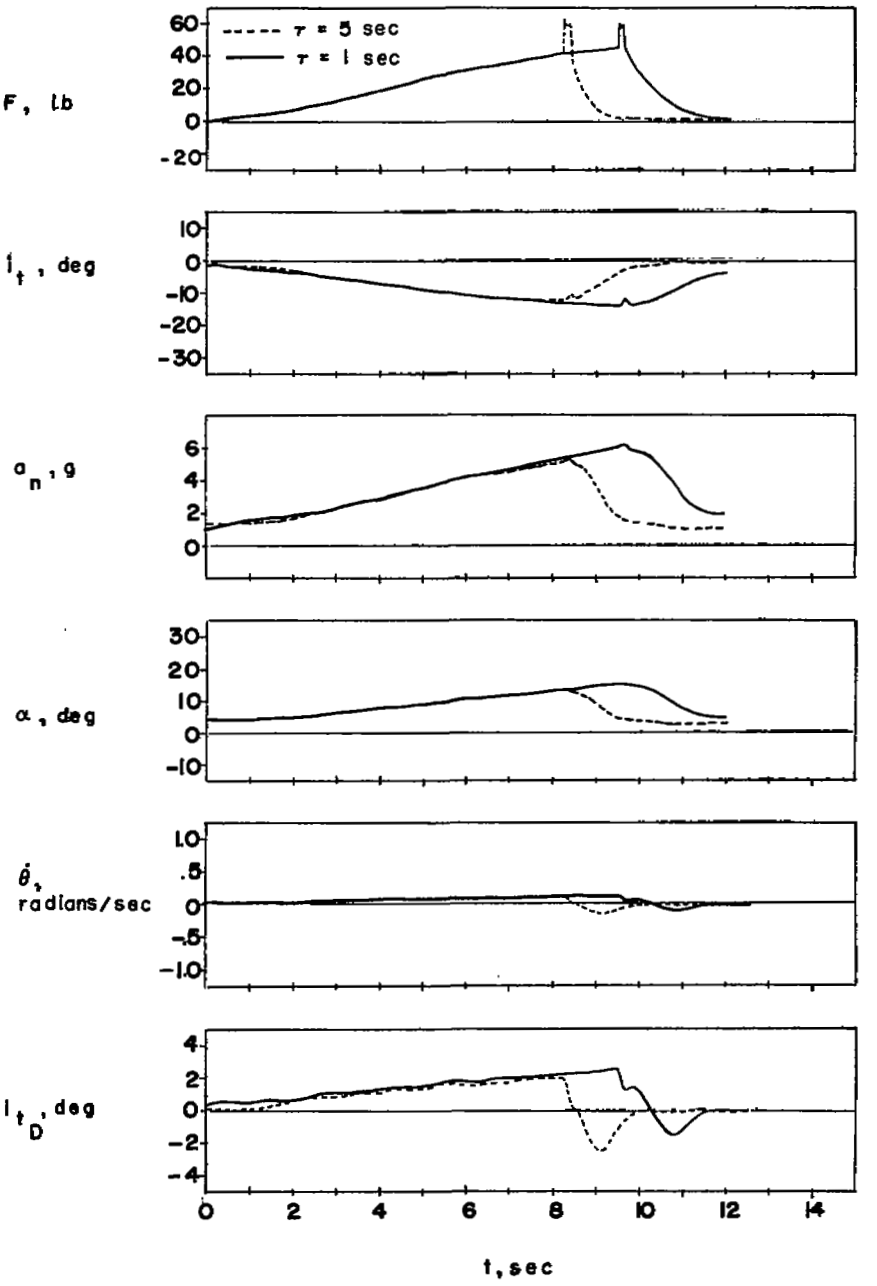

Figure 15.- Typical pull-up maneuvers with a stick pusher using washout circuit showing the effect of washout constant. M = 1.4; h_p = 40,000 feet; stick-pusher boundary (15-16); $i_{t_D} = \pm 3^\circ$; K_D = 0.3 second.

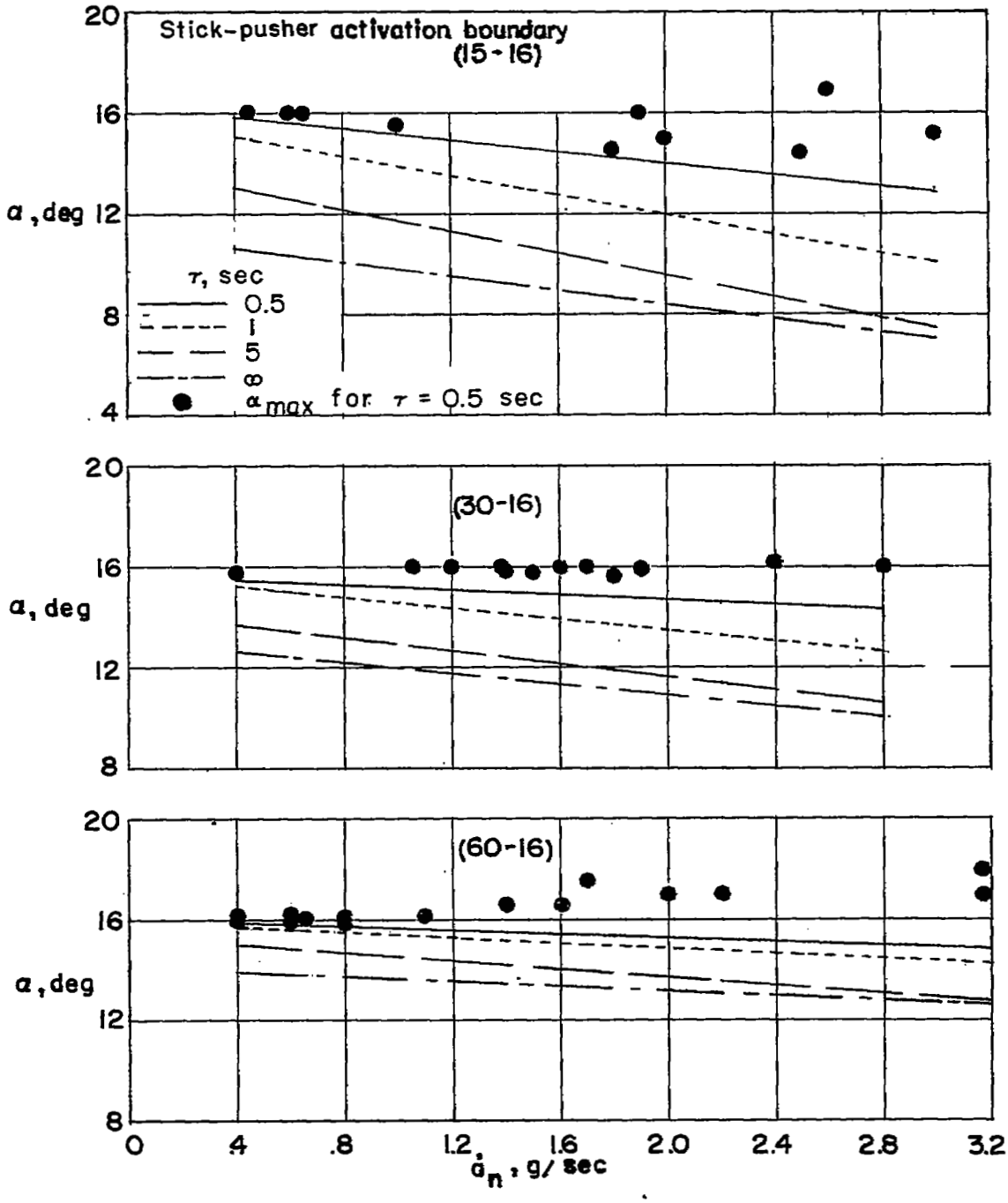

Figure 16.- Effect of washout constant on the stick-pusher activation. M = 1.4; h_p = 40,000 feet.

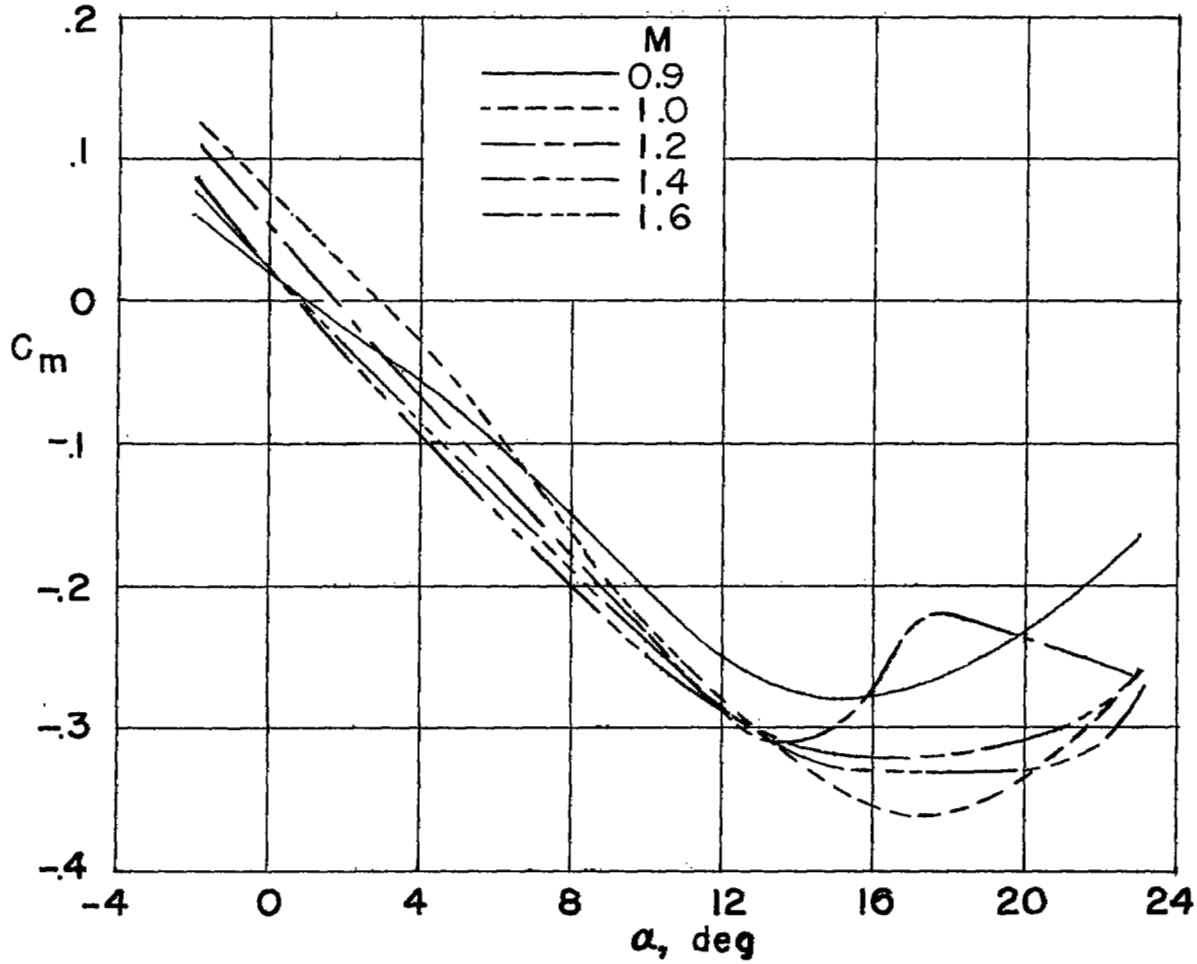

Figure 17.- Effect of Mach number on the pitching-moment characteristics.

[redacted]

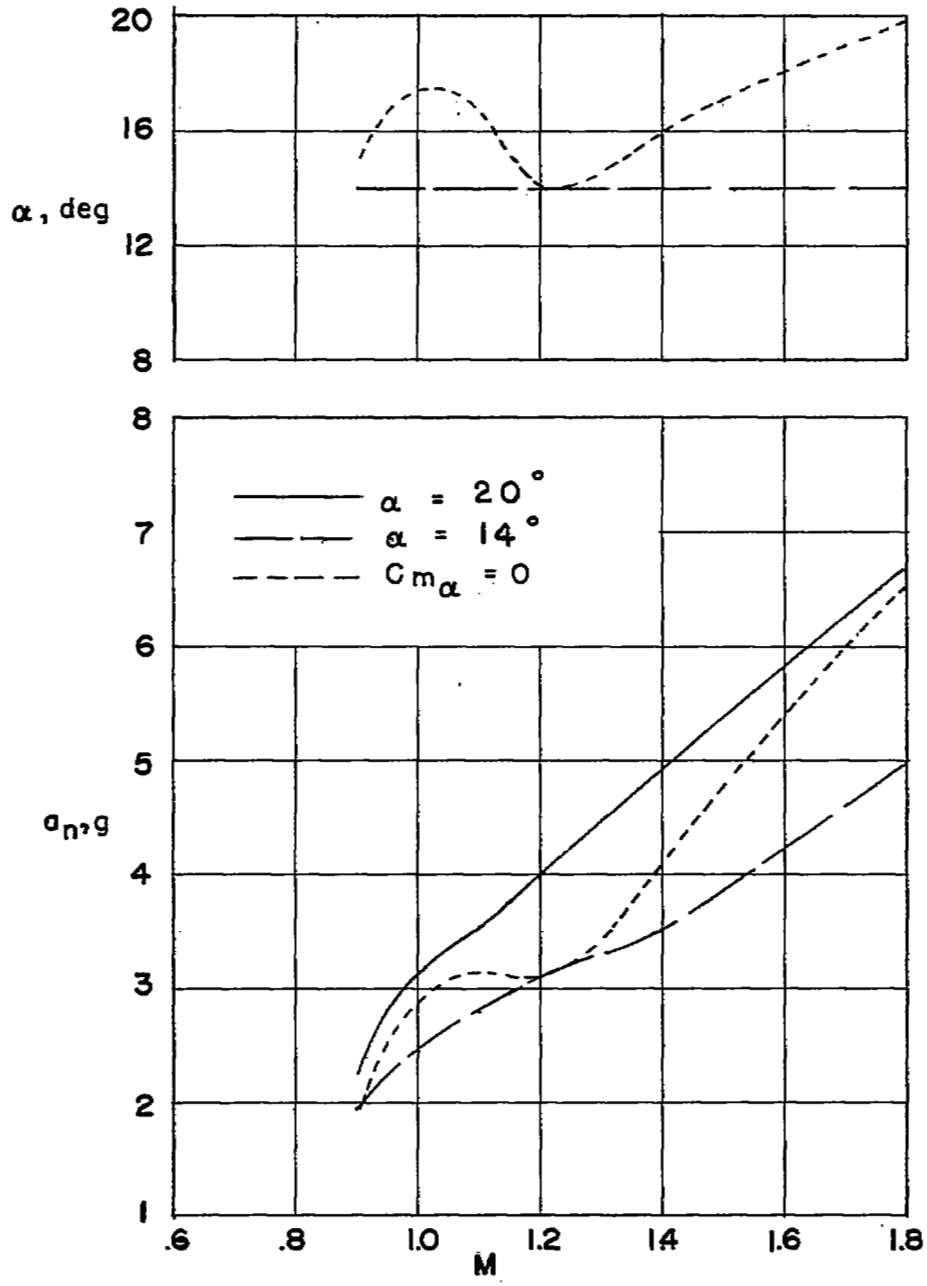

(a) h_p = 50,000 feet.

Figure 18.- Loss in attainable load factor due to angle-of-attack limiting.

[redacted]

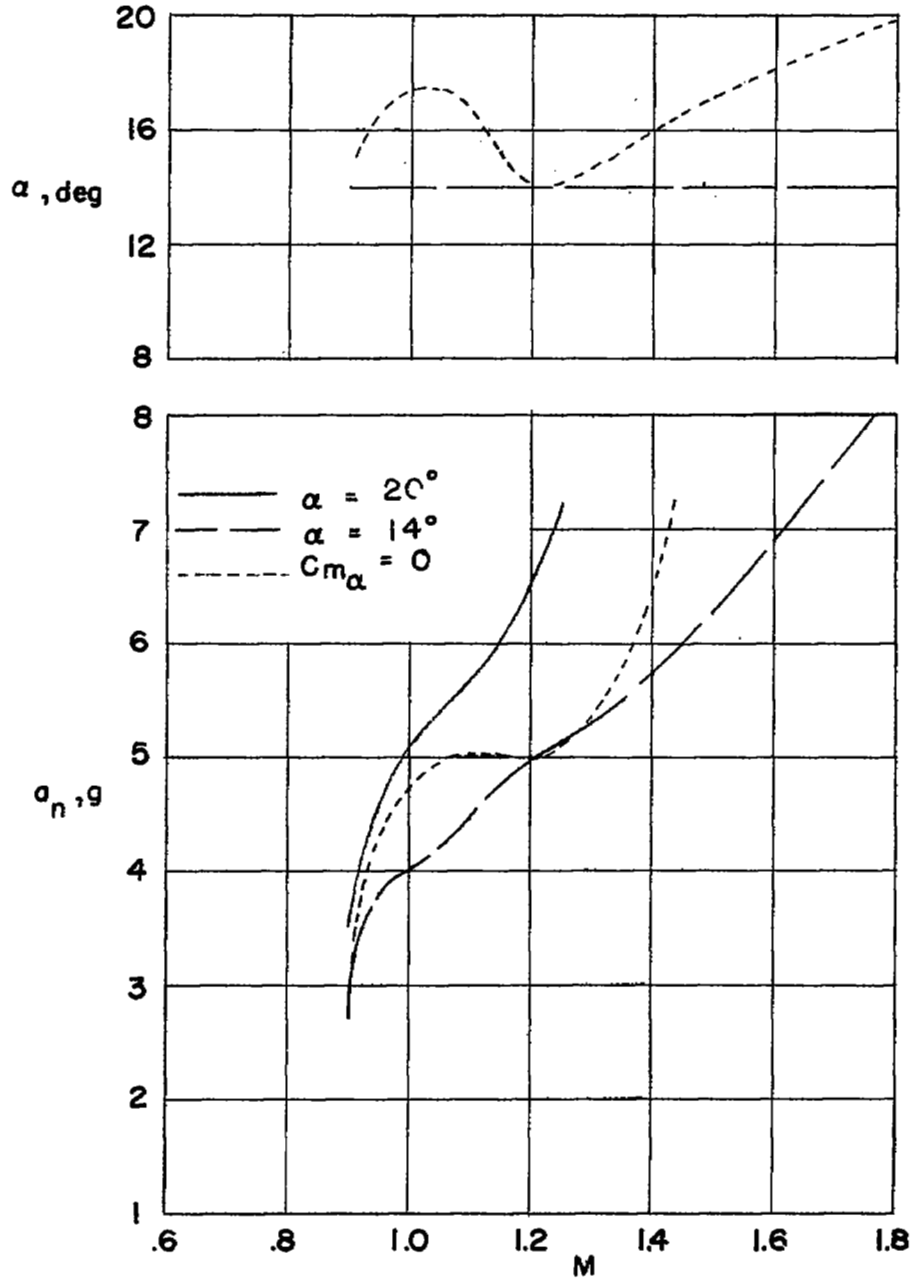

(b) h_p = 40,000 feet.

Figure 18.- Concluded.

[redacted]

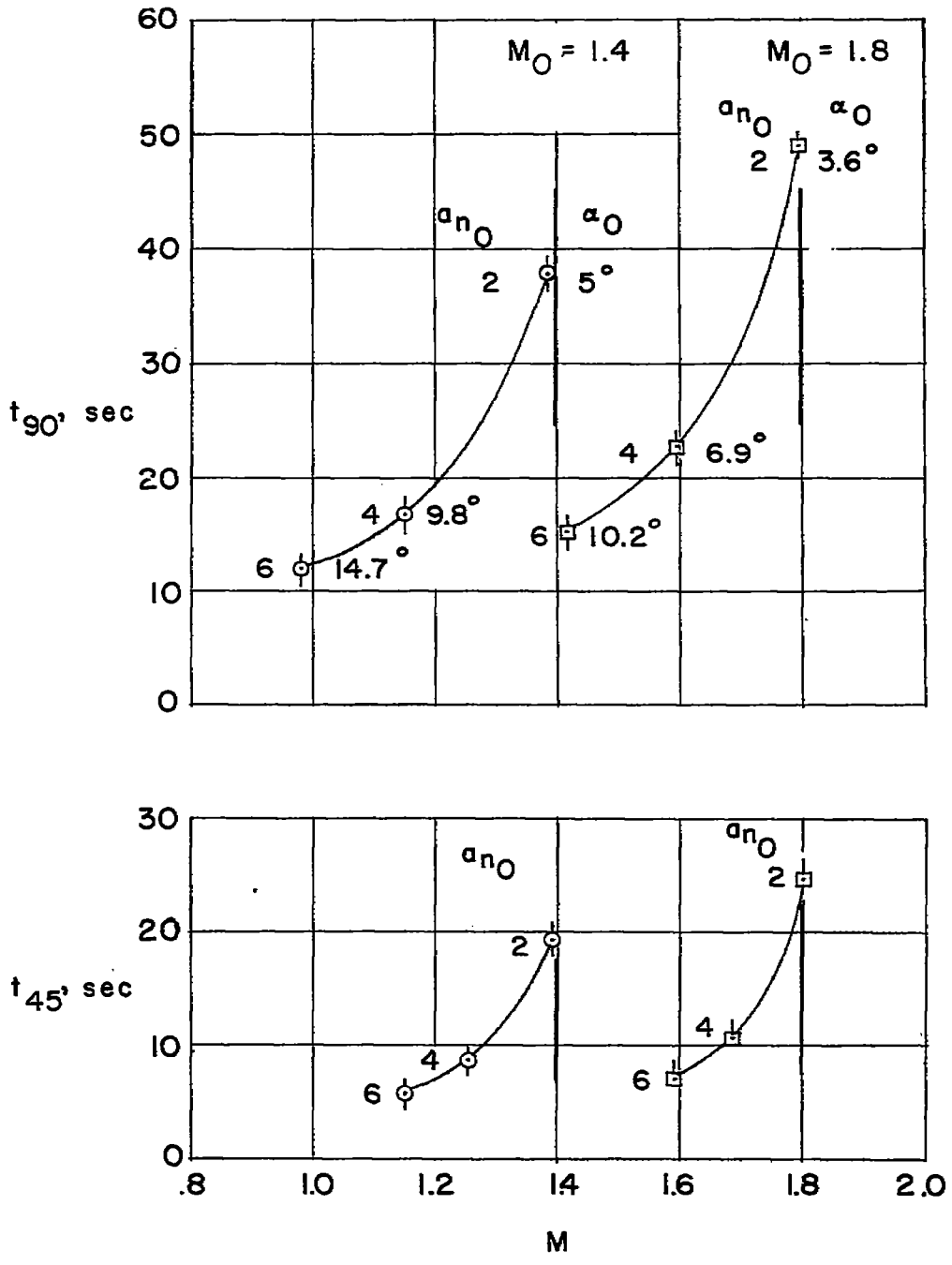

(a) h_p = 40,000 feet.

Figure 19.- An analysis of speed loss in supersonic turns.

[redacted]

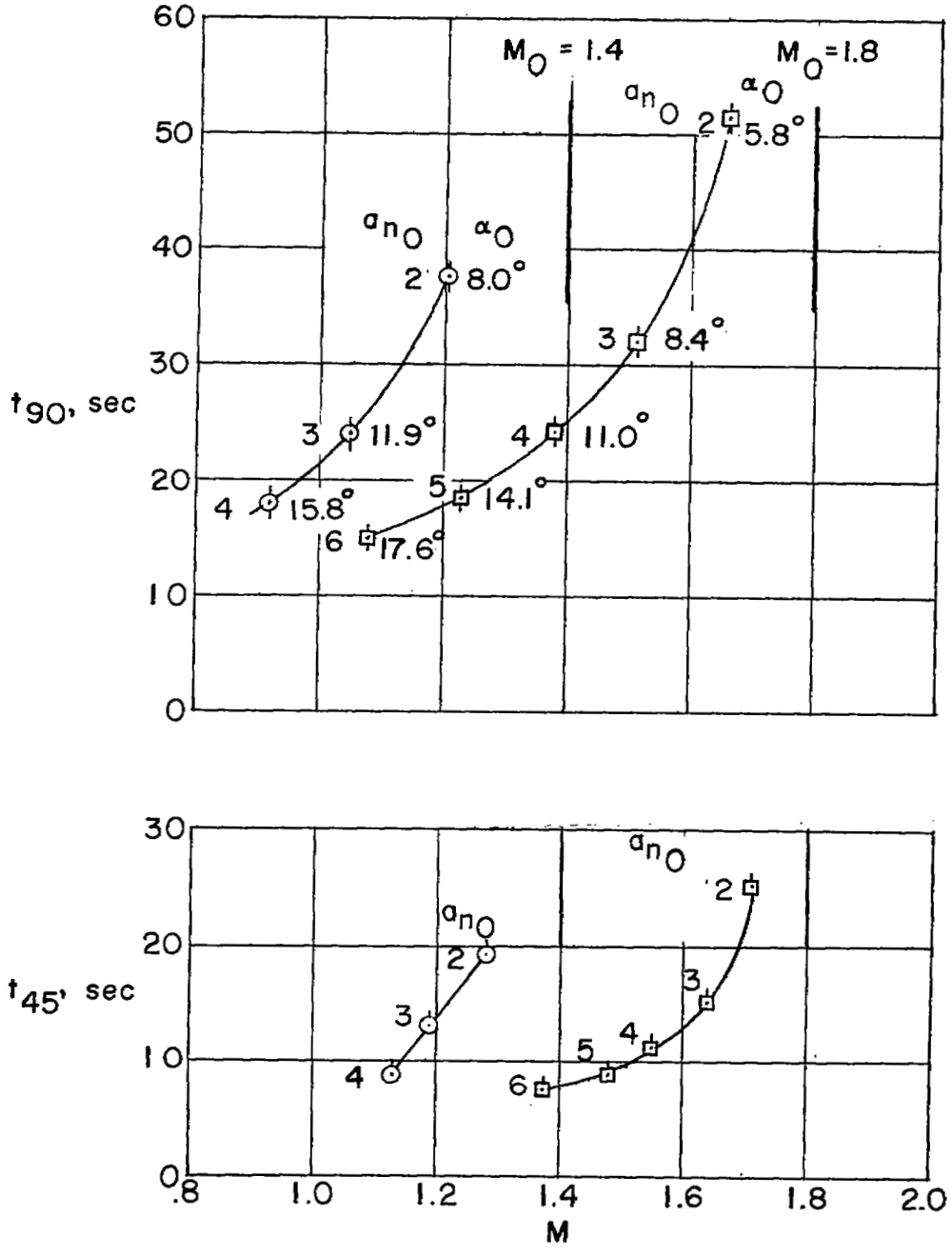

(b) h_p = 50,000 feet.

Figure 19.- Concluded.

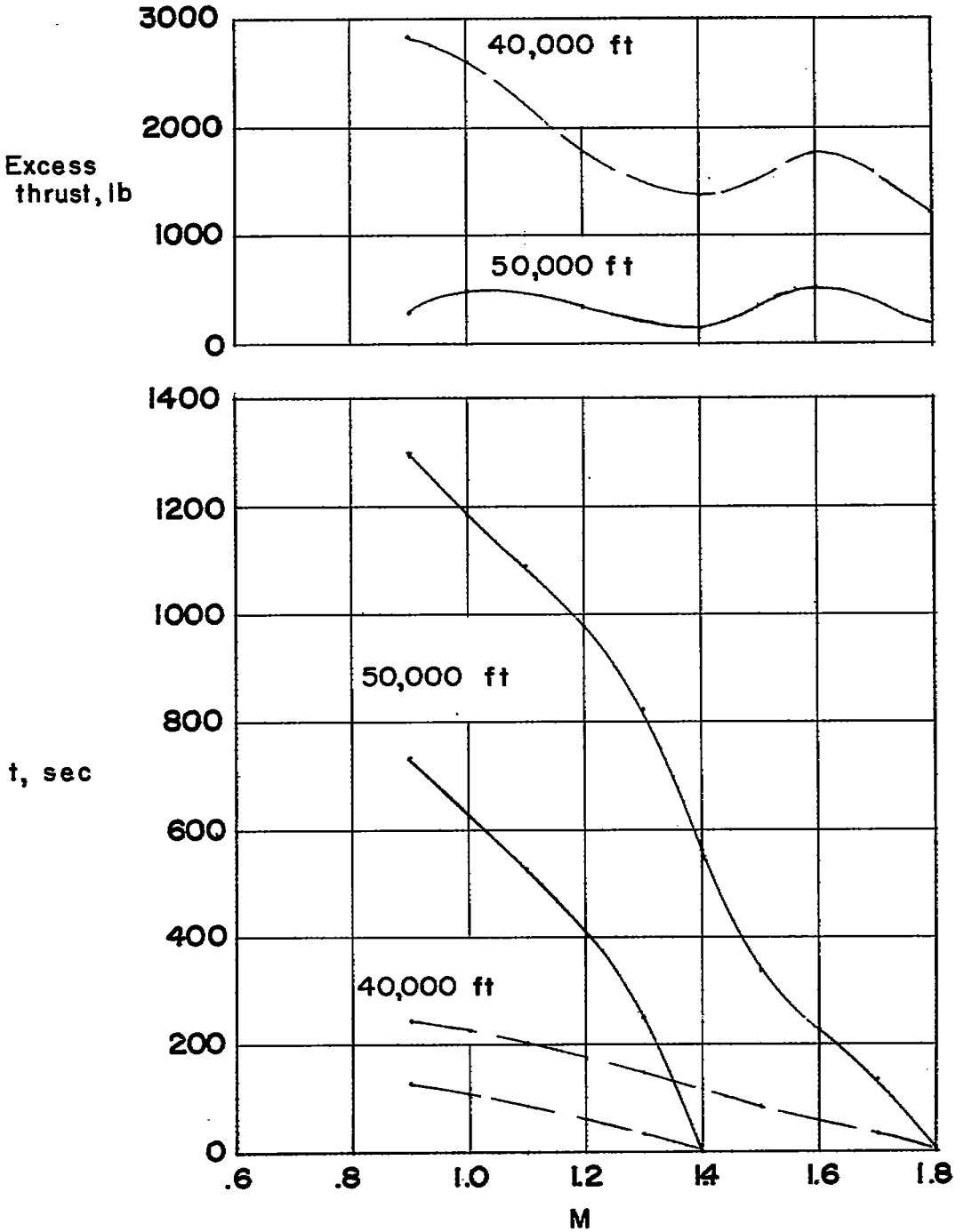

Figure 20.- Time to regain initial speed following turn maneuver.

[redacted]

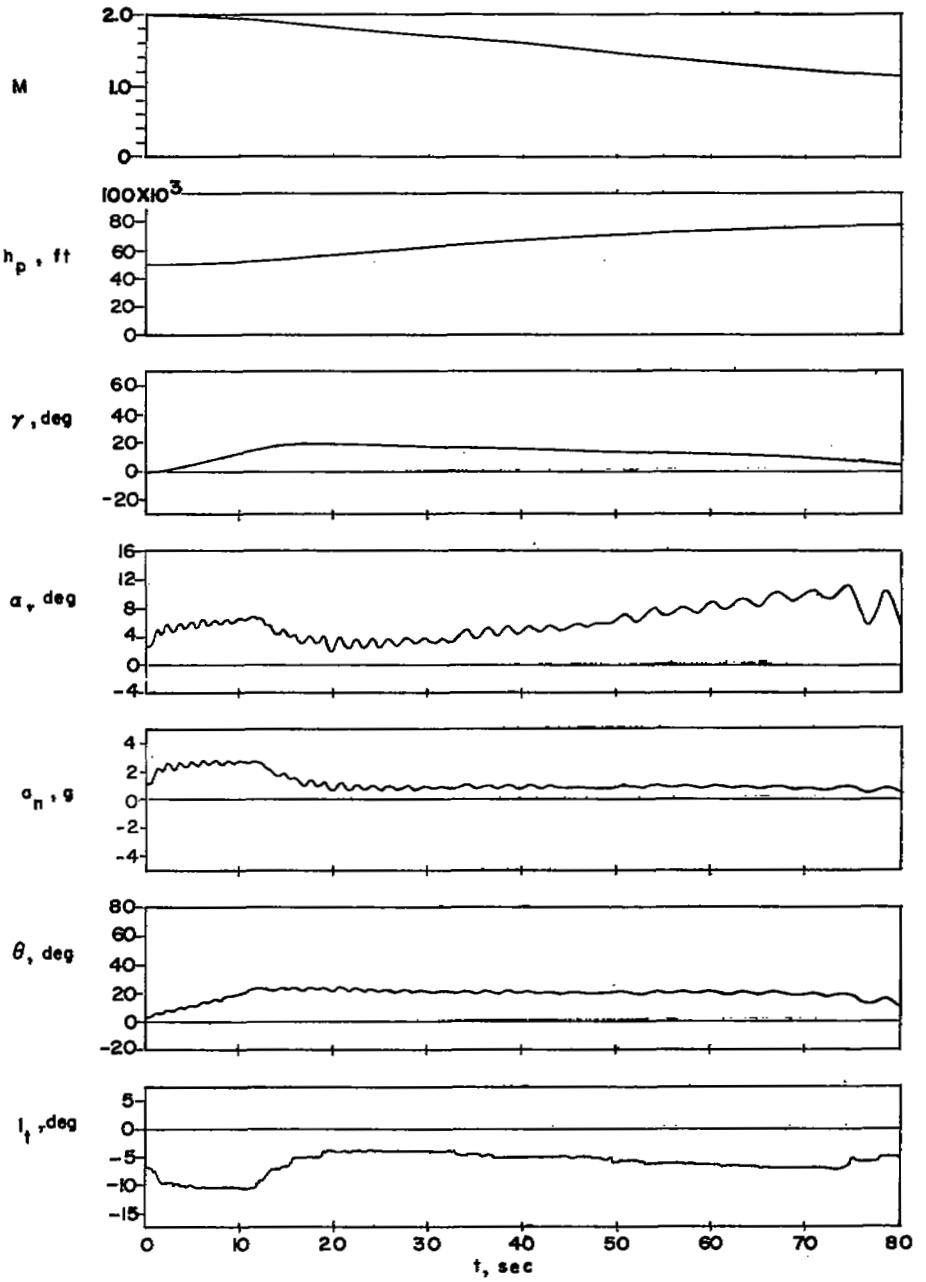

(a) No pitch damper.

Figure 21.- Typical time history of a zoom-up maneuver. a_n entry = 2.5g; $\theta = 20^\circ$.

[redacted]

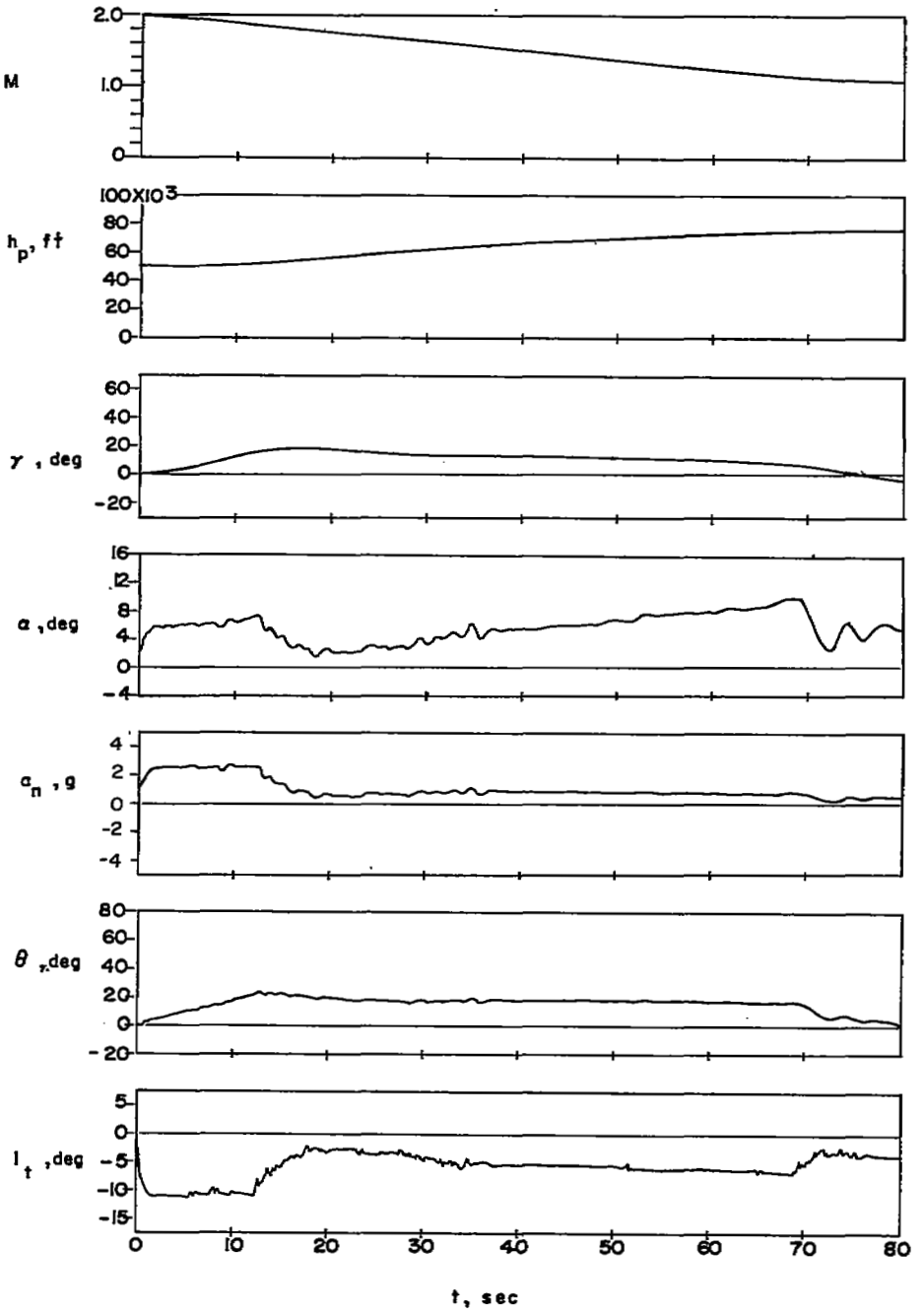

(b) With moderate-authority pitch damper.

Figure 21.- Concluded.

[redacted]

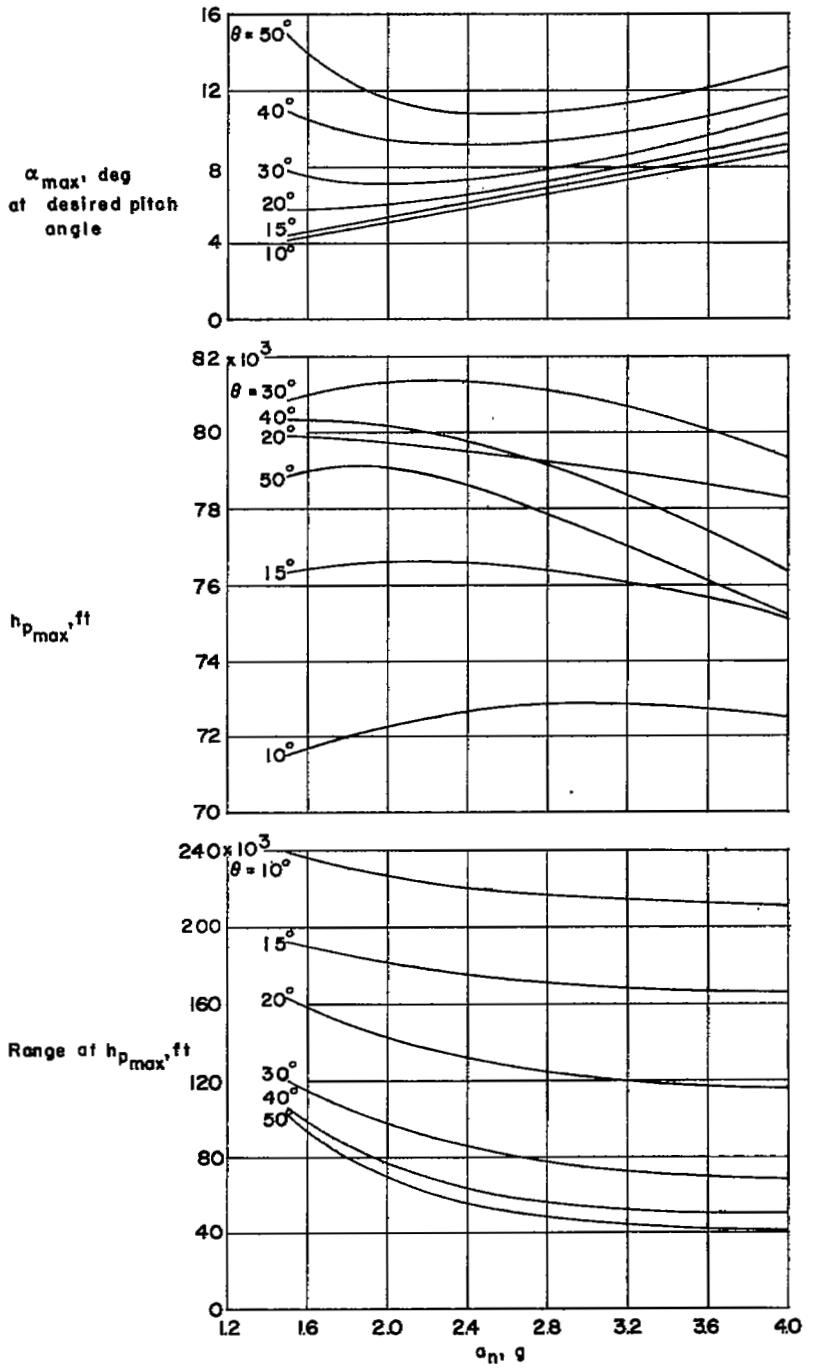

Figure 22.- Summary of the zoom characteristics. Data corrected to M final = 1.0. M_0 = 2.0; h_{p_0} = 50,000 feet.

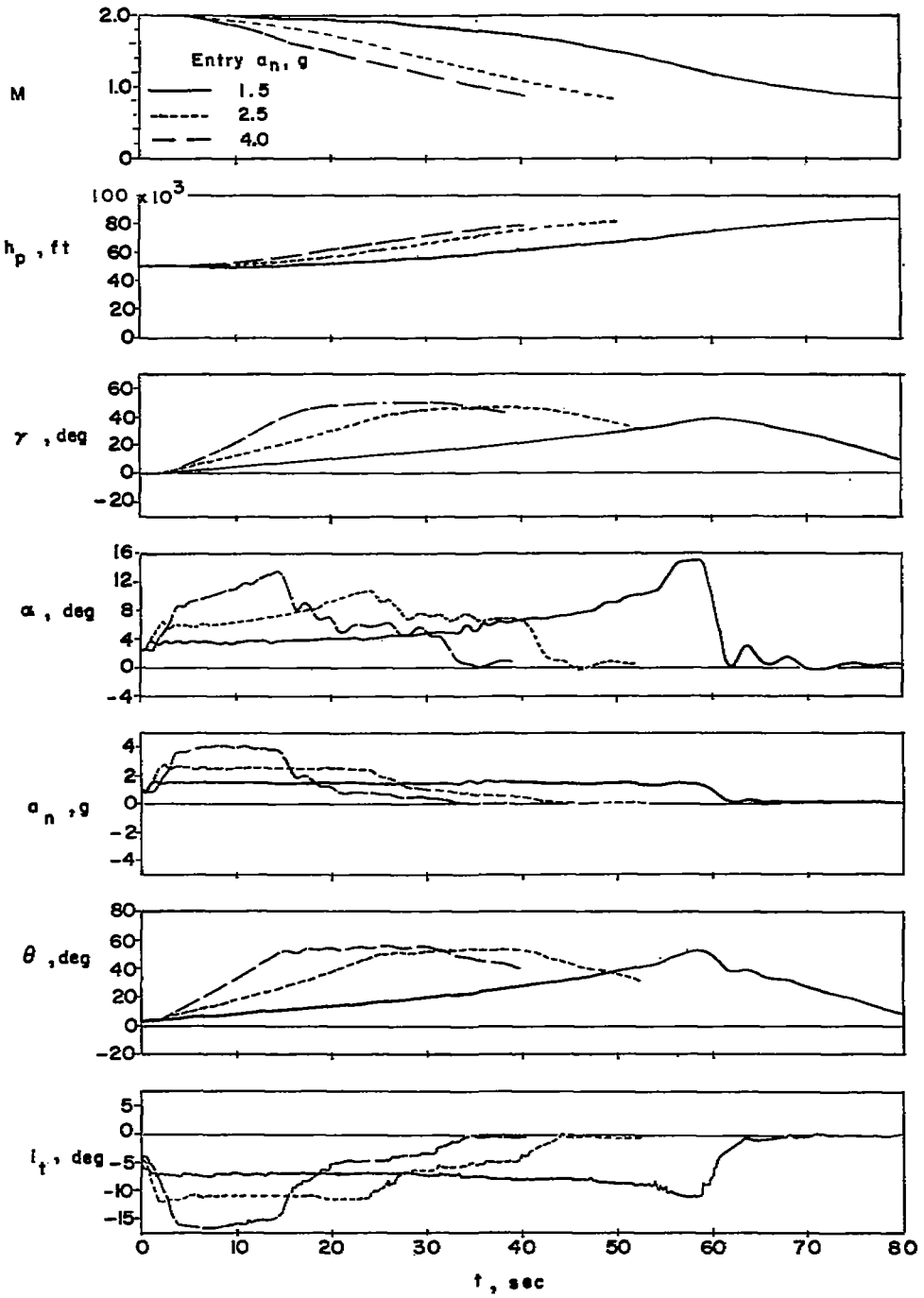

Figure 23.- Typical zoom maneuvers to maximum altitude with three entry rates. $M_0 = 2.0$; $h_{p_0} = 50{,}000$ feet; $\theta = 50^\circ$.

[redacted]

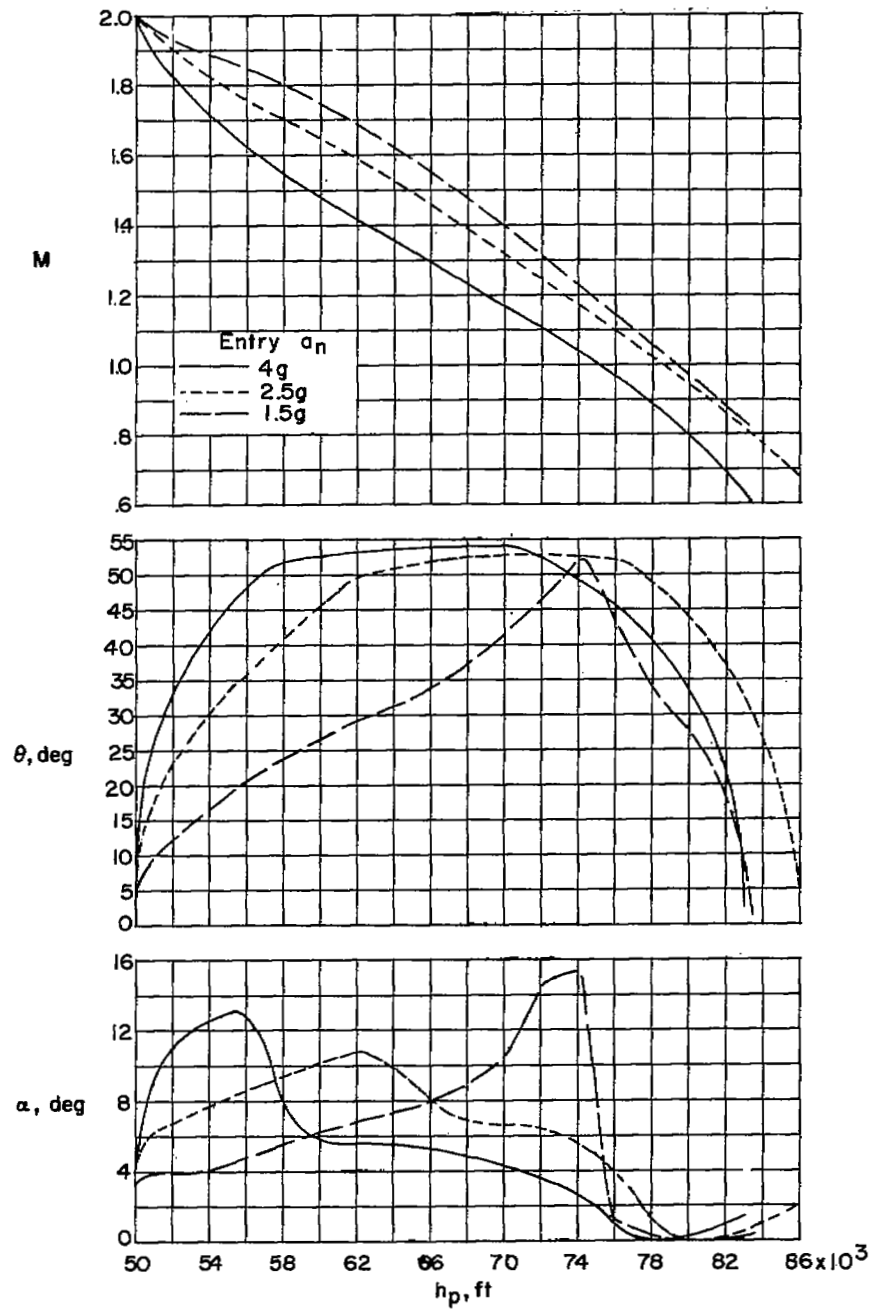

Figure 24.- Altitude history of a zoom maneuver showing the effect of entry rate on maximum angle of attack and final Mach number. $M_0 = 2.0$; $h_{p_0} = 50{,}000$ feet.

[redacted]

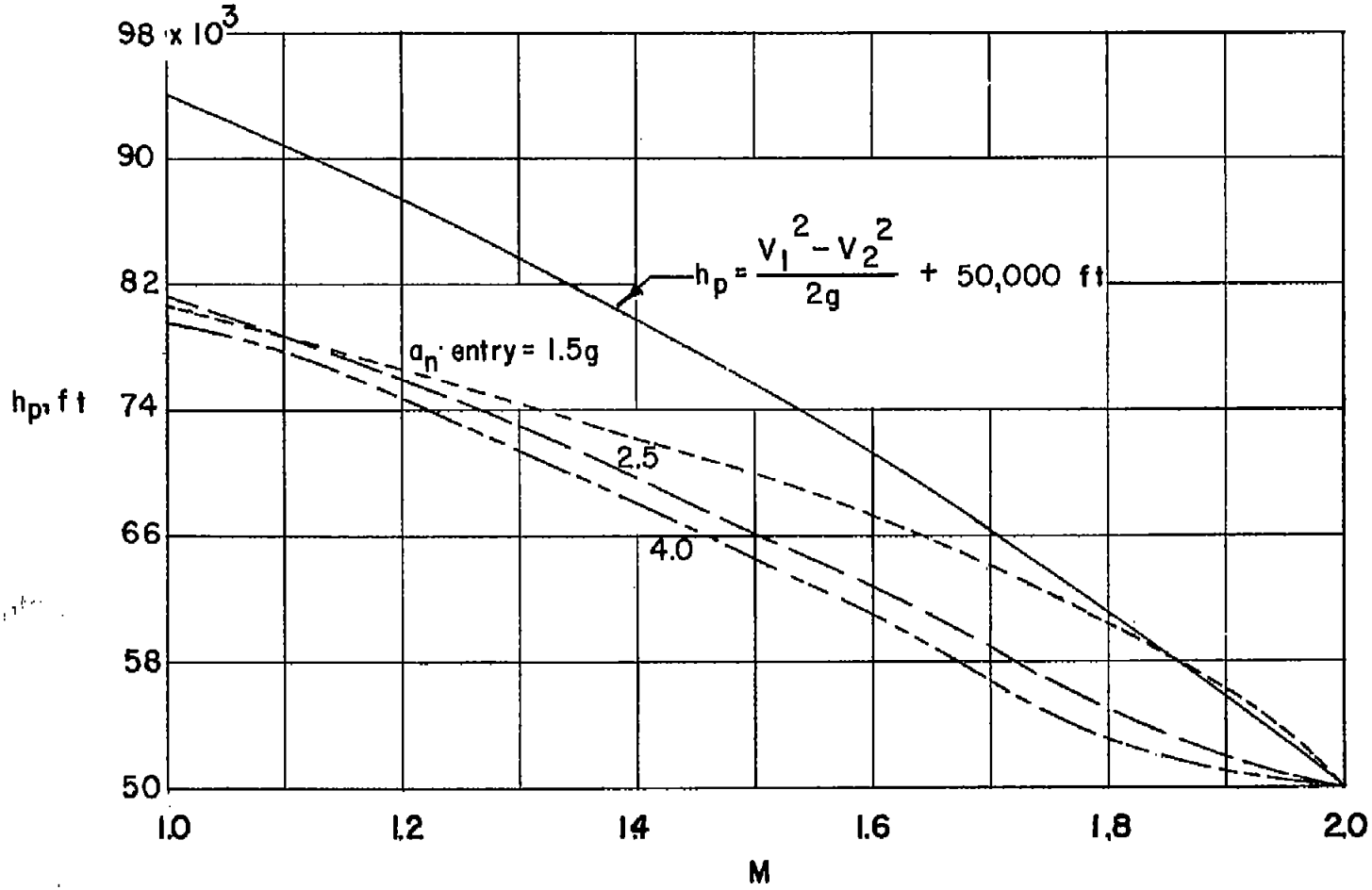

(a) $\theta = 30^\circ$.

Figure 25.- Comparison of actual altitude attained during zoom maneuvers with ideal energy conversion.

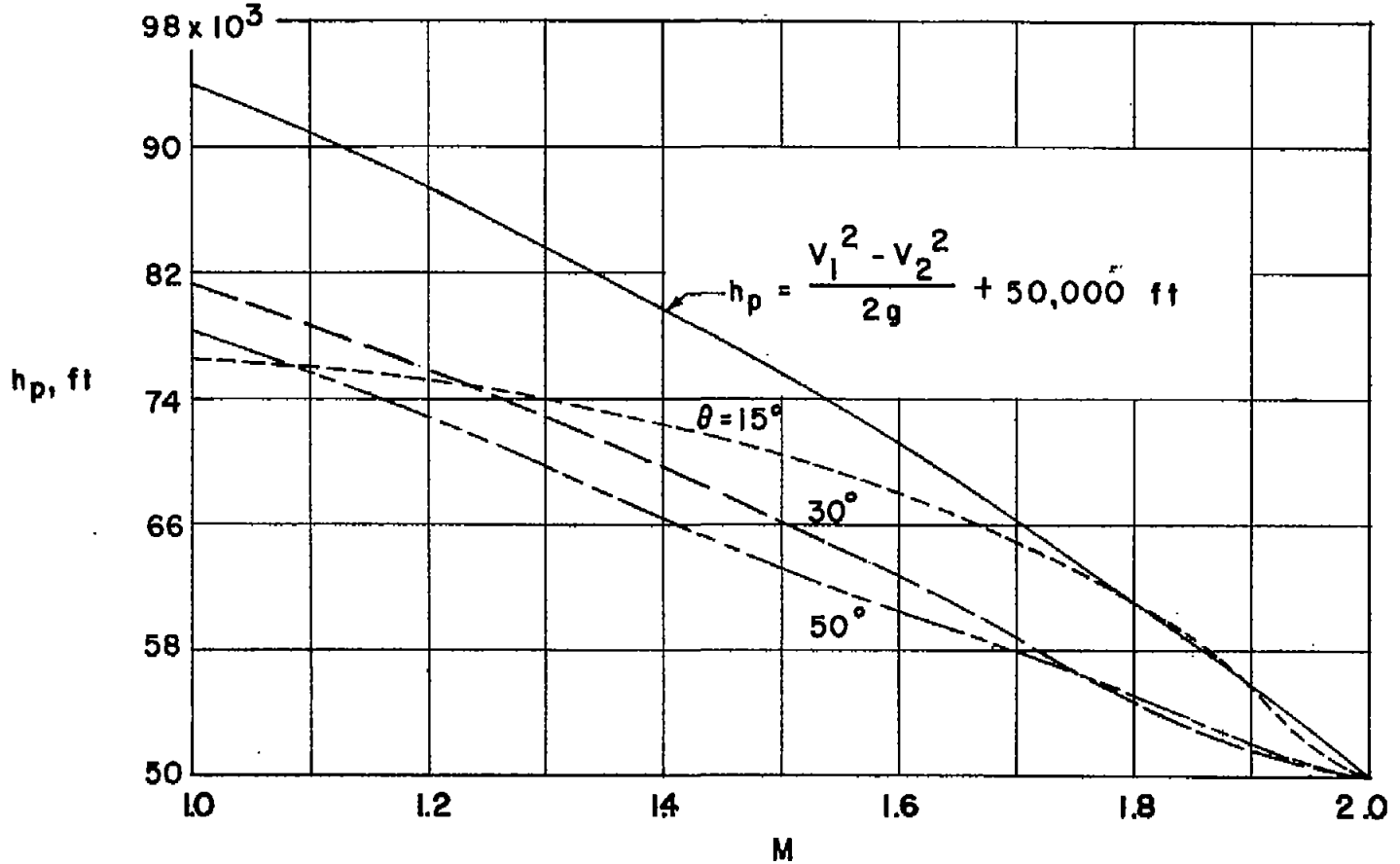

(b) a_n entry = 2.5g.

Figure 25.- Concluded.

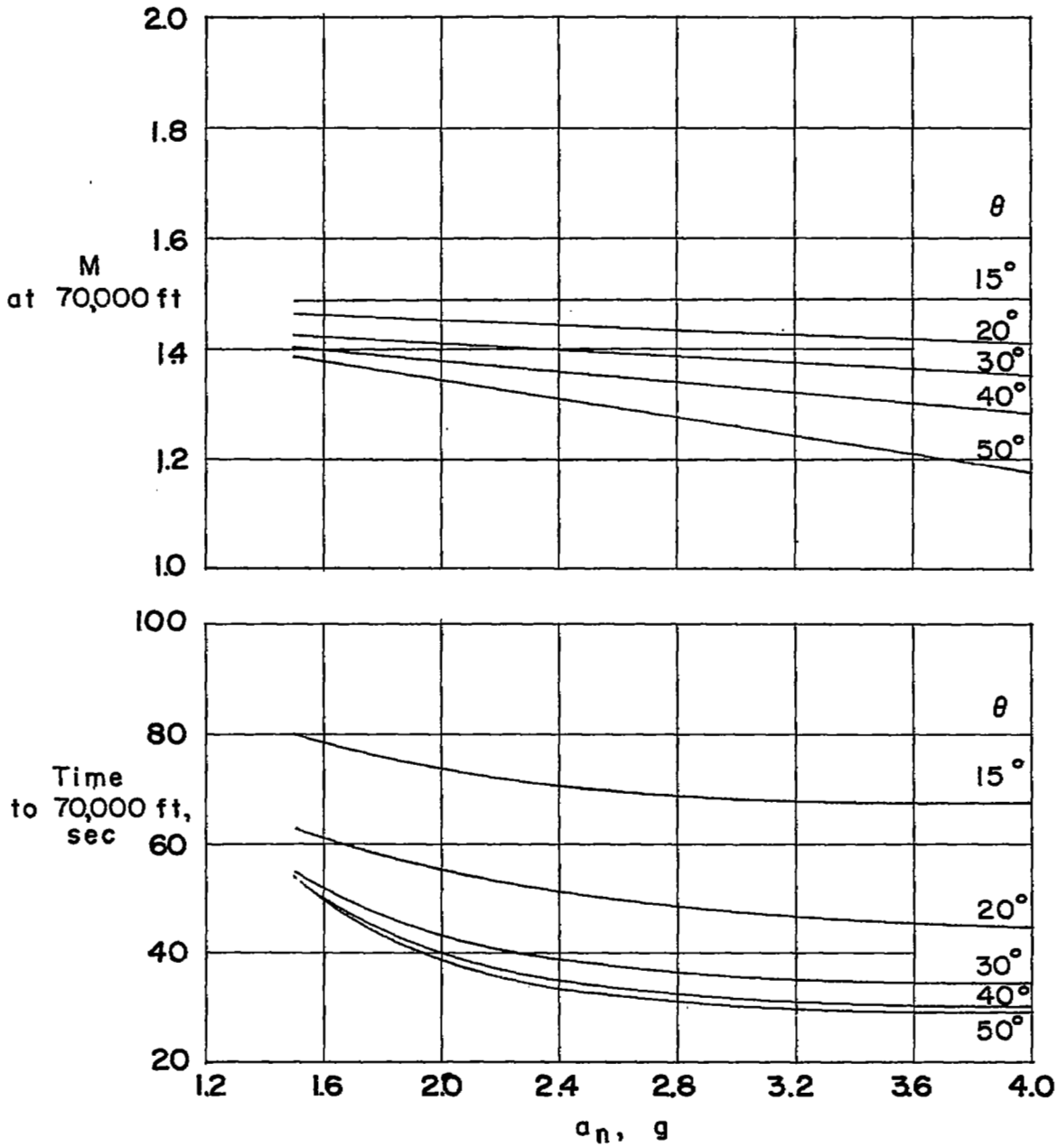

Figure 26.- Effect of entry rate and zoom angle on the speed loss and time to zoom to 70,000 feet. $M_0 = 2.0$; $h_{p_0} = 50,000$ feet.

[redacted]

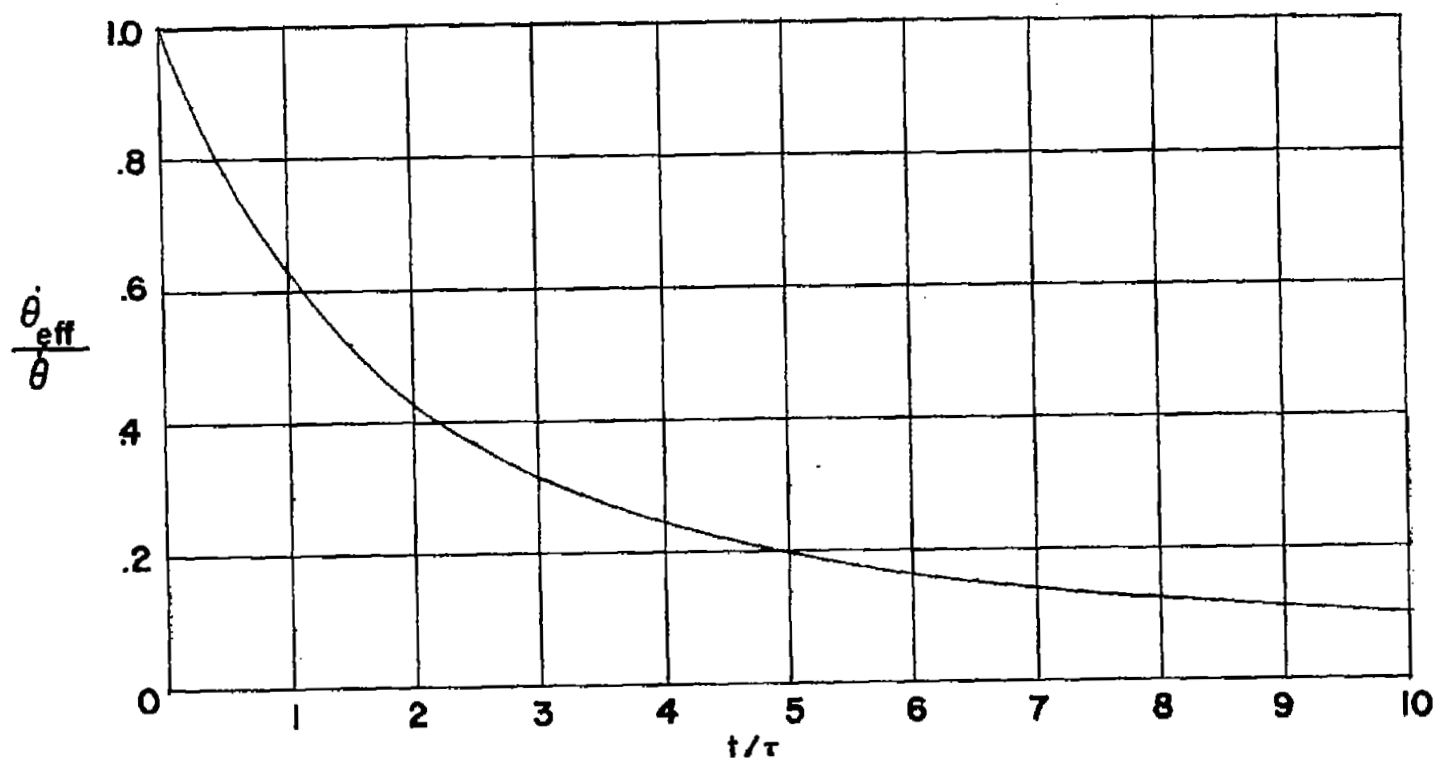

Figure 27.- Plot of the relationship, $\dot{\theta}_{eff}/\dot{\theta} = \frac{\tau\left(1 - e^{-t/\tau}\right)}{t}$, for a range of t/τ values.

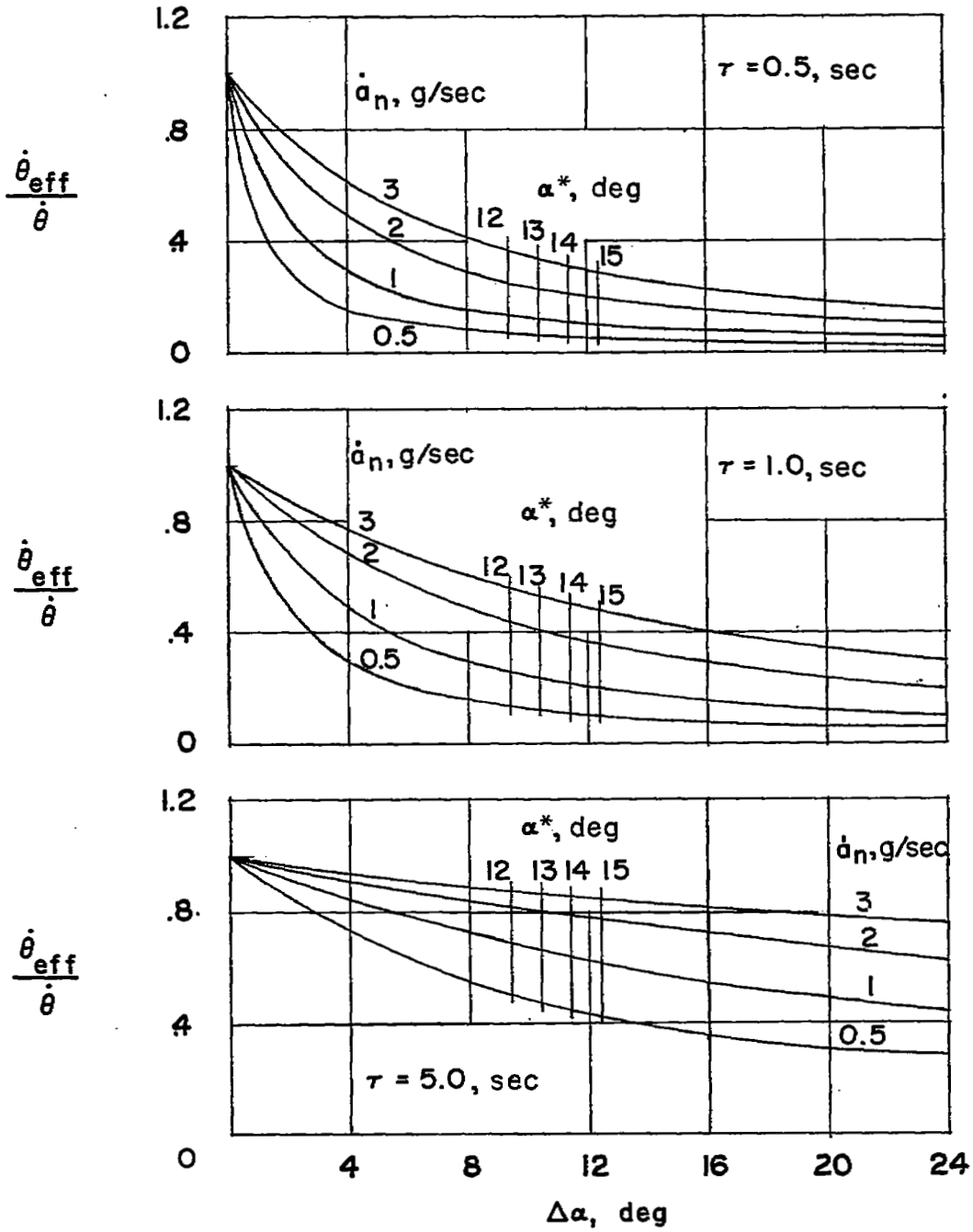

Figure 28.- Ratio of washout circuit to airplane pitching velocity during pull-ups at various rates. M = 1.4; h_p = 40,000 feet. Selected activation angles of attack shown.

[redacted]

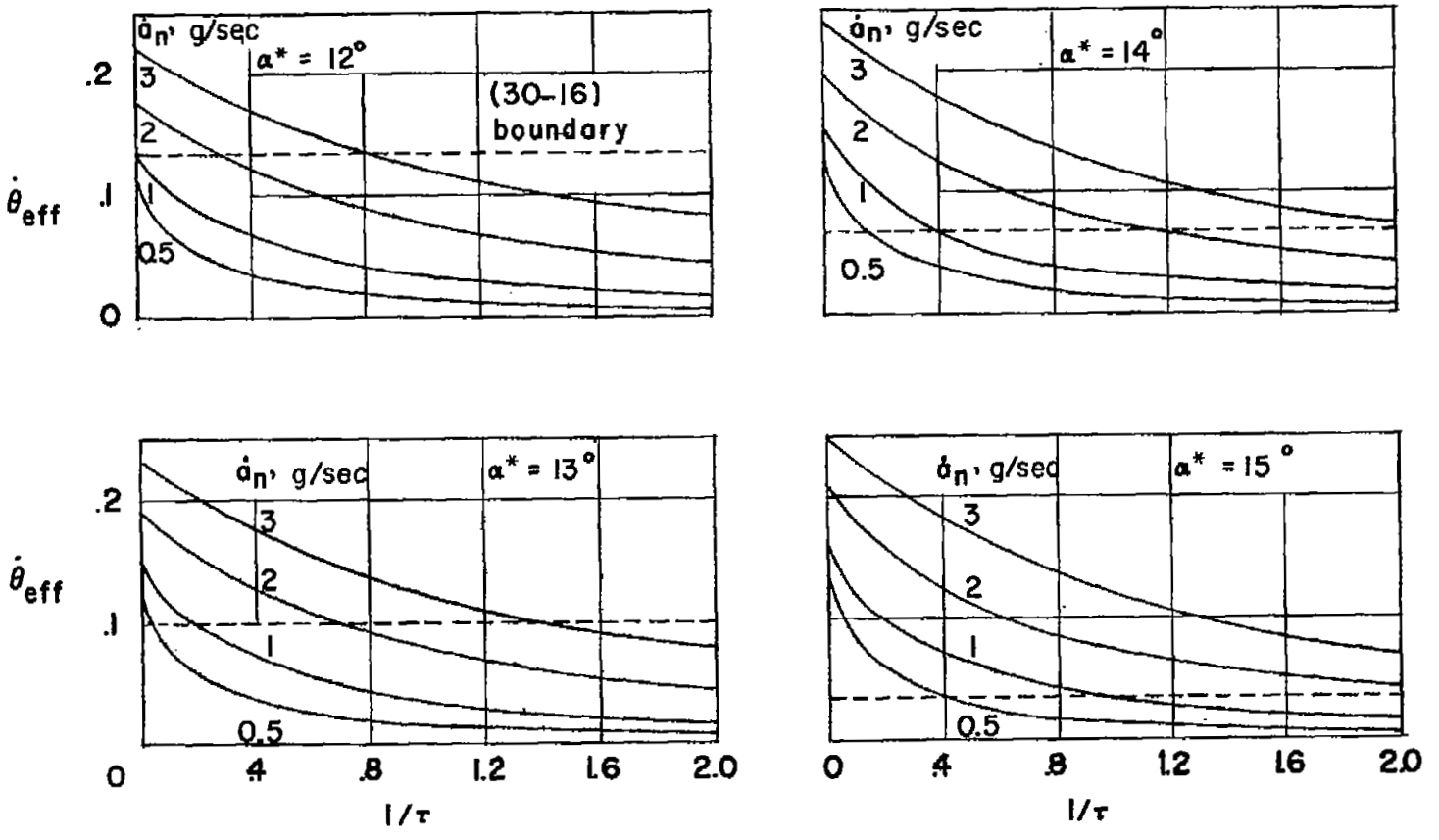

Figure 29.- Graphical method of determining $\dot{a}_n$ at which pusher activation will occur using (30-16) boundary. M = 1.4; h_p = 40,000 feet.

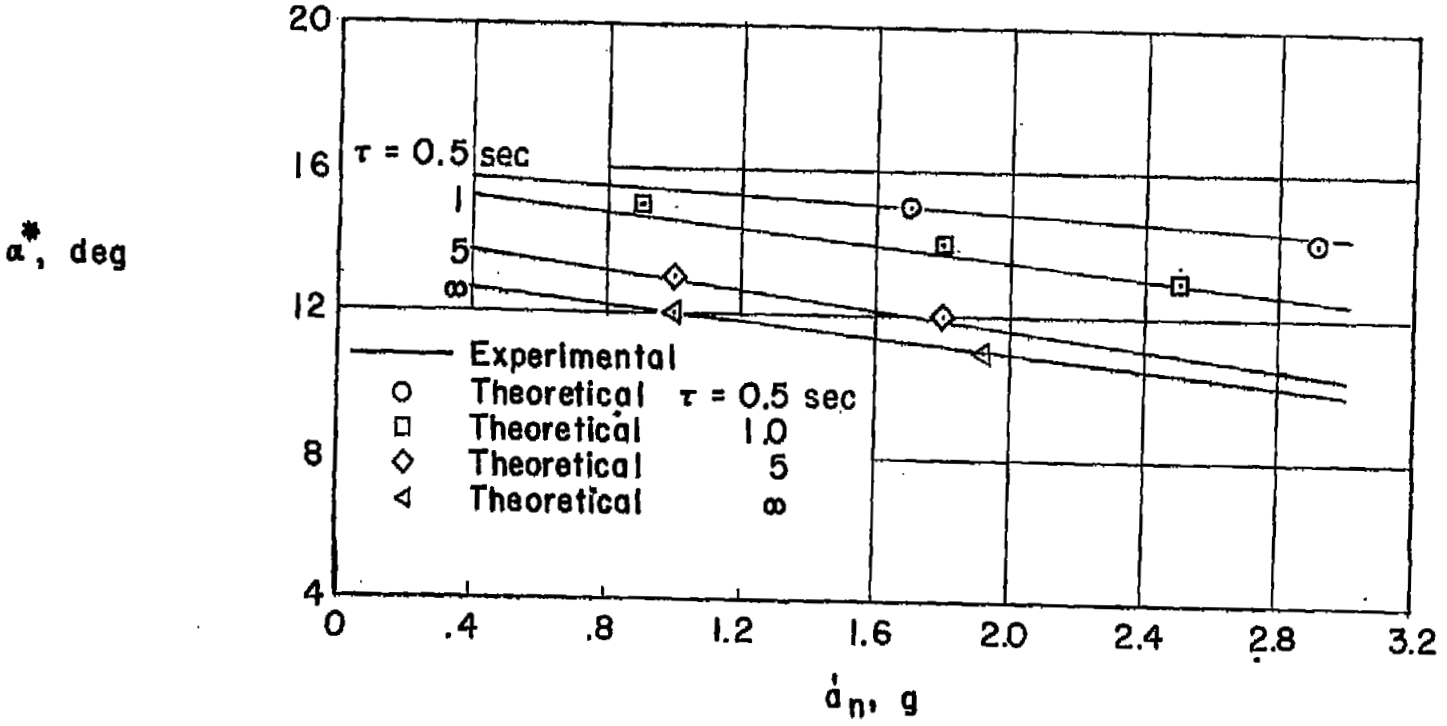

Figure 30.- Comparison of experimental and theoretical pusher activation.